FUNCTIONAL ANALYSIS OF *MaRHD3* A PREDICTED SALT RESPONSIVE GENE FROM *Musa acuminata* CV. BERANGAN IN *Arabidopsis thaliana*

WONG GWO RONG

FACULTY OF SCIENCE
UNIVERSITY OF MALAYA
KUALA LUMPUR

2019

FUNCTIONAL ANALYSIS OF *MaRHD3* A PREDICTED SALT RESPONSIVE GENE FROM *Musa acuminata* CV. BERANGAN IN *Arabidopsis thaliana*

WONG GWO RONG

DISSERTATION SUBMITTED IN FULFILMENT OF THE REQUIREMENTS FOR THE DEGREE OF MASTER OF SCIENCE

INSTITUTE OF BIOLOGICAL SCIENCES
FACULTY OF SCIENCE
UNIVERSITY OF MALAYA
KUALA LUMPUR

2019

UNIVERSITY OF MALAYA

ORIGINAL LITERARY WORK DECLARATION

Name of Candidate: **WONG GWO RONG**

Matric No: **SGR140057**

Name of Degree: **MASTER OF SCIENCE**

Title of Thesis ("this Work"):

FUNCTIONAL ANALYSIS OF *MaRHD3* A PREDICTED SALT RESPONSE GENE FROM *Musa acuminata* CV. BERANGAN IN *Arabidopsis thaliana*

Field of Study:

GENETIC AND MOLECULAR BIOLOGY

I do solemnly and sincerely declare that:

(1) I am the sole author/writer of this Work;
(2) This Work is original;
(3) Any use of any work in which copyright exists was done by way of fair dealing and for permitted purposes and any excerpt or extract from, or reference to or reproduction of any copyright work has been disclosed expressly and sufficiently and the title of the Work and its authorship have been acknowledged in this Work;
(4) I do not have any actual knowledge nor do I ought reasonably to know that the making of this work constitutes an infringement of any copyright work;
(5) I hereby assign all and every rights in the copyright to this Work to the University of Malaya ("UM"), who henceforth shall be owner of the copyright in this Work and that any reproduction or use in any form or by any means whatsoever is prohibited without the written consent of UM having been first had and obtained;
(6) I am fully aware that if in the course of making this Work I have infringed any copyright whether intentionally or otherwise, I may be subject to legal action or any other action as may be determined by UM.

Candidate's Signature Date:

Subscribed and solemnly declared before,

Witness's Signature Date:

Name:

Designation:

FUNCTIONAL ANALYSIS OF *MaRHD3* A PREDICTED SALT RESPONSE GENE FROM *Musa acuminata* CV. BERANGAN IN *Arabidopsis thaliana*

ABSTRACT

Regulation of gene expression via microRNA (miRNAs) highly influences the response of plants to abiotic stresses. In this study, expression profiling of 12 salt-responsive miRNAs and their 14 corresponding targets predicted from salt responsive banana transcriptome were validated by RT-qPCR. Among the predicted miRNA and corresponding targets, 10 miRNAs showed down-regulation and 9 miRNA-targets showed up-regulation in salt as predicted from RNAseq data. The up-regulation of these miRNA-targets indicate the involvement of these genes in banana salinity stress response mechanisms. Functional analysis of one candidate stress responsive mRNA, a target of miRNA mac-miR157m, was based on the constitutive expression of a banana cDNA, *MaRHD3* in Arabidopsis. Transgenic Arabidopsis plants expressing *MaRHD3* had roots with enhanced branching and more root hairs when challenged with drought stress. The MaRHD3 plants had higher biomass accumulation (2.6-fold), higher relative water content (2.4-fold), higher chlorophyll content (2.5-fold) and an increase in activity of reactive oxygen species (ROS) scavenging enzymes; SOD (1.6-fold), CAT (4-fold), GR (3-fold), POD (1.74-fold) and APX (1.9-fold) with reduced transpiration rates compared to control plants. The analysis of oxidative damage indicated lower cell membrane damage in transgenic lines compared to control plants. These findings, together with data showing higher expression of ABF-3 (6.8-fold) and higher levels of ABA in drought-stressed transgenic MaRHD3 expressing plants, support the involvement of the ABA signal pathway and ROS scavenging enzyme systems in MaRHD3 mediated drought tolerance.

Keywords: Banana, Abiotic stress, miRNA target, G protein, Ectopic expression

ANALISIS FUNGSI *MaRHD3* YANG DIRAMALKAN RESPONSIF GARAM DARIPADA *Musa acuminata* CV. BERANGAN DALAM *Arabidopsis thaliana*

ABSTRAK

Regulasi expresi gen melalui mikroRNA (miRNA) mempengaruhi tindak balas daripada tumbuhan terhadap tekanan abiotik. Dalam kajian ini, pengekrspresian 12 miRNA dan 14 sasarannya yang diramalkan daripada transkriptom pisang atas respons garam disahkan dengan RT-qPCR. Di antara miRNA yang diramalkan dan sasarannya, 10 miRNA menunjukkan penurunan regulasi dan 9 sasarannya menunjukkan peningkatan regulasi miRNA atas respons garam seperti yang diramalkan dalam data RNAseq. Peningkatan regulasi sasaran ini menunjukkan penglibatan gen dalam mekanisme tindak balas stres dalam pisang. Analisis fungsi salah satu daripada mRNA responsif stres, yang merupakan sasaran kepada miRNA mac-miR157m didasarkan pada ekspresi konstitutif cDNA pisang, *MaRHD3* dalam Arabidopsis. Arabidopsis transgenik yang mengekspresikan *MaRHD3* mempunyai akar yang lebih bercabang dan numbor akar yang lebih banyak apabila dicabar dengan tekanan kemarau. Tumbuhan mengekspresikan *MaRHD3* mempunyai biojisim yang lebih tinggi (2.6 kali ganda), kandungan air relatif yang lebih tinggi (2.4 kali ganda), kandungan klorofil yang lebih tinggi (2.5 kali ganda) dan peningkatan aktiviti enzim pemusnahan spesies oksigen reaktif (ROS); SOD (1.6 kali ganda), CAT (4 kali ganda), GR (3 kali ganda), POD (1.74 kali ganda) dan APX (1.9 kali ganda) dengan kadar transpirasi yang rendah berbanding dengan tumbuhan kawalan. Analisis kerosakan oksidatif menunjukkan nilai kerosakan membran sel yang lebih rendah dalam transgenik berbanding dengan tumbuhan kawalan. Penemuan ini, selari dengan data ekspresi *ABF-3* (6.8-fold) dan ABA tahap yang lebih tinggi daripada tumbuhan transgenik yang mengekspresikan *MaRHD3*, ini menyokong penglibatan

mekanisme ABA dan sistem enzim pemusnahan ROS dalam toleransi kemarau yang dimediasi oleh *MaRHD3*.

Kata Kunci: Pisang, stres abiotik, sasaran miRNA, protein G, ekspresi ektopik

ACKNOWLEDGEMENTS

This research and thesis become a reality with the kind support from the University of Malaya Research Grant UMRG: RP005B-13BIO and CEBAR Research University grants RU006-2017 and RU015-2016. I also would like to acknowledge Skim Biasiswa Universiti Malaya (SBUM) for the scholarship, that financially supported for 18 months throughout my study.

I would like to express my deepest appreciation to my supervisor, Professor. Dr. Jennifer Ann Harikrishna for her guidance, insightful comments, and considerable motivation, to complete my study. Without her cogent and illuminating instruction, this thesis would not have reached its present form. I wish to express my gratitude to Dr. Purabi Mazumdar, Postdoctoral Research Fellow, CEBAR, who helped me in experimental designing, technical advice and also in manuscript writing in this project. I would like to acknowledge the assistance of Ms. Lau Su-Ee, Research Officer, CEBAR in biochemical analysis and in administrative issues.

Besides, I also would like to take this opportunity to thanks present and past members of BGM, HIR, CEBAR, and PBF, Dr. Ranga Gudimella, Dr. Lee Wan Sin, Dr. Fauziah Abu Bakar, Dr. Ho Hui Li, Khai Swan, Marina Mokhtar, Tyson, Mazni Omar, Jasdeep Kaur, Xue Li, Dr. Rezaul Karim, Dr. Teo Chee How and Dr. Pooja Singh for being supportive lab-members in providing a friendly working environment during my study.

Last but not least, special thanks to my beloved family, especially to my late father, Wong Yeet Fu, always being supportive in my life. Not to forget, to my mother, Lee Yoke Ching and brother, Wong Gwo Shyan for their love and support in all circumstances.

TABLE OF CONTENTS

LIST OF FIGURES

LIST OF TABLES

LIST OF SYMBOLS AND ABBREVIATIONS

bp	:	Base pair
ºC	:	Celcius
Ca^{2+}	:	Calcium ions
d	:	Day
ε^{M}	:	Extinction coefficient
K^{+}	:	Potassium ions
kb	:	Kilobase
L	:	Litre
M	:	Molar
Mbp	:	Mega base pair
mg	:	Milligram
min	:	Minute
mL	:	Millilitre
mM	:	Millimolar
mm	:	Millimetre
µg	:	Microgram
µL	:	Microlitre
µM	:	Micromolar
µmol	:	Micromole
ng	:	Nanogram
nm	:	Nanometre
$O_2^{\bullet-}$	:	Superoxide anions
OD	:	Optical density
OH•	:	Hydroxyl radical
%	:	Percentage

P	:	Probability
s	:	Second
V	:	Voltage
v/v	:	Volume per volume
W	:	Watt
w/v	:	Weight per volume
ABA	:	Abscisic acid
APX	:	Ascorbate peroxidase
CAT	:	Catalase
cDNA	:	Complementary deoxy ribonucleic acid
CDS	:	Coding DNA sequence
Chl a	:	Chlorophyll a
Chl b	:	Chlorophyll b
CI	:	Chloroform Isoamyl
CTAB	:	Cetyltrimethylammonium bromide
DAB	:	3, 3'- diaminobenzidine tetrahydrochloride
ddH_20	:	Sterile distilled water
DEPC	:	Diethyl dicarbonate
DMF	:	N, N-dimethylformamide
DNA	:	Deoxy ribonucleic acid
dNTPs	:	Deoxyribonucleotide triphosphate
DW	:	Dry weight
EV	:	Empty Vector (pCAMBIA1304)
FW	:	Fresh weight
gDNA	:	Genomic DNA
GFP	:	Green Fluorescent Protein

GR	:	Glutathione reductase
GTP	:	Guanosine triphosphate
GUS	:	β-Glucuronidase
H_2O_2	:	Hydrogen peroxide
LB	:	Luria bertani
MDA	:	Malondialdehyde
miRNAs	:	Micro-ribonucleic acid
mRNAs	:	Messenger ribonucleic acid
NaCl	:	Sodium chloride
NaOH	:	Sodium Hydroxide
NAPDH	:	Nicotinamide adenine dinucleotide phosphate
NBT	:	Nitro Blue Tetrazolium
PCI	:	Phenol Chloroform Isoamyl
PCR	:	Polymerase chain reaction
PEG	:	Polyethylene glycol
POD	:	Guaiacol peroxidase
RH	:	Relative humidity
RHD3	:	Root Hair Defective 3
RNA	:	Ribonucleic acid
ROS	:	Reactive Oxygen Species
rpm	:	Revolutions per minute
RT-qPCR	:	Quantitative real time PCR
siRNAs	:	Small interfering ribonucleic acid
SOD	:	Superoxide dismutase
Spp.	:	Species
SPSS	:	Statistical package for social sciences

SSC	:	Saline-sodium citrate
TBA	:	Thiobarbituric acid
TCA	:	Trichloroacetic acid
Tris-HCl	:	Trisaminomethane hydrochloride
UV	:	Ultraviolet
WT	:	Wild type

LIST OF APPENDICES

CHAPTER 1: INTRODUCTION

Over the last century, the global population has exponentially increased. This may reach a human population of 9 billion by 2050 and 11 billion by 2100 which will increase the demand for food, feed and energy (United Nations, 2017), therefore, there is a need to improve crop yields. Crop plants are highly influenced by environmental conditions. The primary causes of low yield crop production are the shortage of land and water and increase of abiotic stresses due to climate change. Among the abiotic stresses, soil salinity and drought are the major threats to agricultural production. Drought and salinity interfere with water uptake and salinity additionally causes ion toxicity.

The decline of agricultural productivity due to abiotic stress is worsened by climate change. The effects of climate change on agriculture were clearly showed by the several episodes of drought followed by flooding in Malaysia since 2014 ("Dry, muddy, very windy," 2014; "Malaysia, Seasonal Flooding" 2017). Such combination of high rainfall and flooding increasing salinization of soil due to deposition of salts from seawater especially in the east coast of Peninsular Malaysia. Agricultural crops grown in coastal regions, especially banana production, are negatively affected in such stress conditions.

Owing to a shallow root system, banana is highly vulnerable to abiotic stress conditions, particularly, flooding, salinity and drought. The losses recorded in banana due to water scarcity are up to 65% of fruit yield per year (Sreedharan et al., 2013) and up to 30% per year in high saline-sodic conditions (Jeyabaskaran et al., 2000).

Studies of plant root systems have shown longer roots with more root hairs to provide better protection against water deficit conditions (Paez-Garcia et al., 2015). Root hairs constitute vital parts of root systems and their density, extension, and patterns are strongly influenced by environmental conditions. Root patterns also determine the plant

survivability in stress conditions. Hence, changes in root architecture in terms of length and number of root hairs in banana may provide better tolerance to drought and salt stresses. However, no systematic study has reported functional analysis of banana genes responsible for root traits in response to abiotic stresses.

Abiotic stress responses in plants are mediated at a molecular level and recent studies have shown micro RNA (miRNA) to be important in this response for plant survivability (Shriram et al., 2016). Micro RNAs differentially expressed during various abiotic stress responses and their negative regulation of target gene expression appears to be a major protective mechanism in plants at the transcriptional and post-transcriptional levels. The up-regulation of target gene expression in such stress conditions could be an indication of their functional role as part of protective responses in plant. A mac-miR157m target, banana *Root Hair Defective 3* (*MaRHD3*) was identified to be stress responsive in salt stress treated banana roots based on transcriptome data (Lee et al., 2015). The orthologues of *MaRHD3* have been reported to regulate cell enlargement and root hair morphogenesis in Arabidopsis (Galway et al., 1997; Wang et al., 1997) and lateral root branching in poplar (Xu et al., 2012). However, no association with abiotic stress tolerance had been reported. Thus, this thesis was based on a hypothesis that overexpressing *MaRHD3* in a model plant would improve abiotic stress tolerance. The study of this hypothesis was expected to produce valuable information for supporting the development of abiotic stress tolerant varieties of banana for sustainable agriculture.

The main objectives of this study were:

1. To quantify expression of selected *Musa* specific miRNAs and their target mRNA in response to salinity stress
2. To characterize a selected miRNA mac-miR157m-target, *MaRHD*3, through bioinformatics and functional analysis
3. To generate and characterise the phenotypes of transgenic Arabidopsis lines (T_3 generation) over-expressing *MaRHD3*

CHAPTER 2: LITERATURE REVIEW

2.1 History, taxonomy and nutritional value of banana

Bananas (Musa spp.), are herbaceous monocotyledon plants of order *Zingiberales*. Member of the order *Zingiberales* are grouped into two groups which are 'banana group' and 'ginger group' which was made up of eight families that are different in terms of fertile stamen number (Prince & Kriss, 2002). These eight families include *Marantaceae*, *Cannaceae*, *Zingiberaceae*, *Costaceae*, *Heliconiaceae*, *Lowiaceae*, *Strelitziaceae* and *Musaceae*. Banana belongs to the *Musaceae* family with a unique pseudostem made up from leaf sheaths that sprout from the rhizome.

Musaceae, the family of banana plants, consists of 3 genera which are *Musa*, *Ensete*, and *Musella*. *Musaceae* species majority belong to the genus *Musa* which has a distribution range coincides with different tropical Southeast Asian hotspots (Sundaland, Philippines, Wallacea, and Indo-Burma) (Janssens et al., 2016). *Ensete* is distributed mostly in Madagascar, tropical Africa and Asia (Champion, 1967; Väre & Häkkinen, 2011). Whereas, *Musella* is a monospecific genus which is native to southern Sichuan (Hong et al., 2011) and northern Yunnan (Wu, 2000).

Up to date, almost all modern edible-fruited cultivars from the genus *Musa* are allopolyploid triploids with a genome constitution of AAA (dessert banana), AAB (some of which are referred to as plantains) and ABB (cooking banana/plantains) which originated from two-diploid species originating from two seed-producing ancestors, *Musa acuminata* (genome designated as "AA") and/or *Musa balbisiana* (genome designated as "BB") (Venkataramana et al., 2015). They are commonly found in both tropical and subtropical countries (Xu et al., 2014). The *M. acuminata* was probably in Papua New Guinea around 8000 before the "Common Era" which mainly comes under the region

between Malaysia and Indonesia whereas, *M. balbisiana* was reported to be originated from Southeast Asia (De buck & Swennen, 2016).

Banana fruit are enriched with carbohydrates (95%), vitamins A, C and B6 (FAO, 2016) and have a low fat (1-2%) content. In the past, banana fruits were recommended in treatments by doctors such as for obesity (Gasster, 1963), coeliac disease (Seelig, 1969), infantile diarrhoea (Koszler, 1959). In addition, more recent studies show that banana also helps in preventing and reducing the risk of cardiovascular diseases, high blood pressure, arthritis, ulcer and kidney disorders (Agin & Jegtvig, 2009). These properties of banana, made the choice of fruit for millions of people around the world.

2.2 Socio-economic importance of banana

Annual production of banana more than 145 million metric tons in over 130 countries along with an economic value of 44.1 billion dollars (De Buck & Swennen, 2016), ranked them as the world's fourth ranking food crop among maize, rice, wheat, cassava and potatoes (Calberto et al., 2015). Banana significantly contributes to food safety and security for millions of people in developing countries (Olaoye & Ade-Omowaye, 2011) and is the most popular fruit in industrialized countries (D'Hont et al., 2012).

In term of worldwide production, bananas increased steadily from 76.25 million tonnes in 1991 to 148 million tonnes in 2016, with an increase of 93.44% in production for the past 26 years (Figure 2.1) (FAOSTAT, 2018). Similar increase pattern was observed for world gross production value of bananas for the past 26 years (Figure 2.2), bananas in the year of 2016 was achieved at 67,644 million USD compared to the most important food crop such as rice (337,078 million USD), maize (239,998 million USD), wheat (167,896 million USD), cassava (39,012 million USD), potatoes (111,056 million USD), sorghum

(10,567 million USD), millet (6,901 million USD) and sweet potatoes (26,459.33 million USD) (FAOSTAT, 2018). This indicates that the world banana production trends increasing significantly as staples and export commodity year-to-year.

Bananas are cultivated worldwide, only 15% from the worldwide production of bananas is exported among countries and the remaining 85% of bananas are cultivated by small farmers for consumption and/or trade in locally and regionally (De Buck & Swennen, 2016). In Malaysia, National Agricultural Policy 3 (1998-2010) and National Agrofood Policy (2011-2020) identified banana as one of the potential fruits influence Malaysia's export markets. Bananas are enormously popular among the farmers to use as staple crop because banana plants are perennial crop and production does not depend on seasonal as well as rapid fruit harvest time of 9 to 18 months (Samson, 1986). As a commodity, bananas have the great socio-economic potential to small-scale farmers especially in the developing countries by providing the main source of income, food and job security as well as one of the key contributors to the economies of many developing countries (Obaga & Mwaura, 2018).

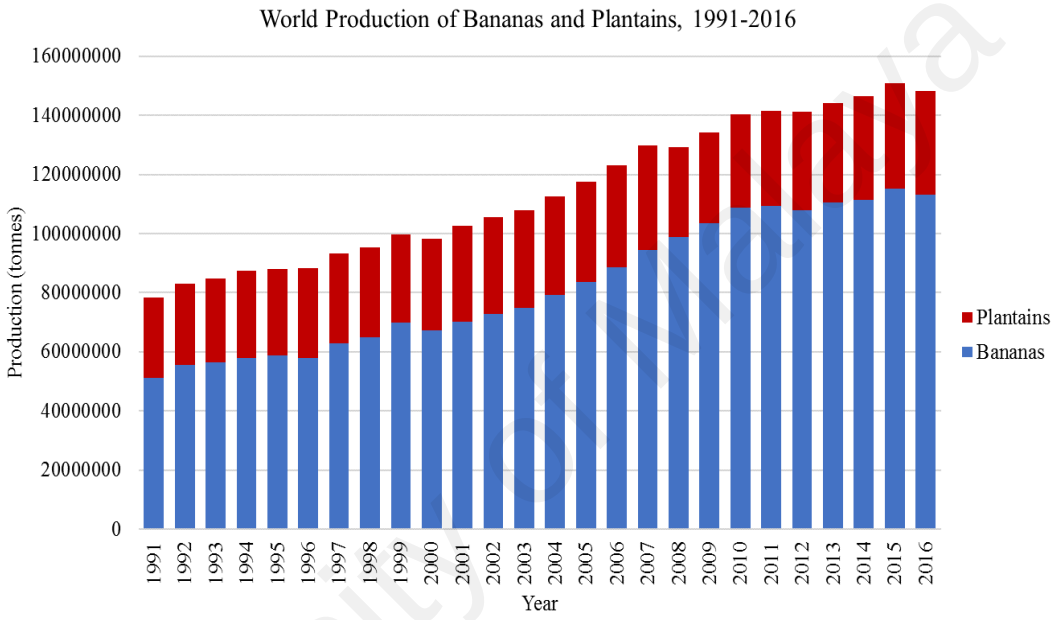

Figure 2.1: World production of bananas and plantains from the year 1991 to 2016. Based on data from FAOSTAT (2018, accessed from http://faostat.fao.org/), 'bananas' is defined as *Musa sapientum*, *M. cavendishii* or *M. nana* (raw eaten banana), 'Plantains' is defined as *Musa paradisiaca* (cooking banana). FAOSTAT is an online tool that provides time-series and cross-sectional statistic of varies data in food and agriculture for over 150 countries and is fully compliant with the principles of good practice governing international statistics. The data showed steadily increase of world production of bananas and plantains over the past 25 years.

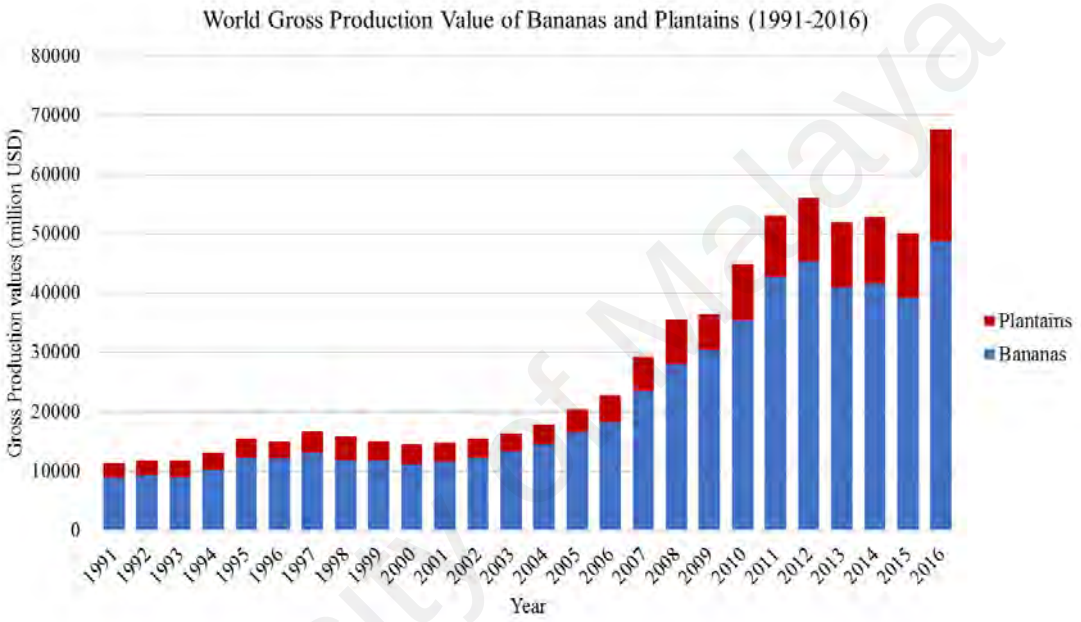

Figure 2.2: World gross production value of bananas and plantains from the year 1991 to 2016. Based on data from FAOSTAT (2018, accessed from http://faostat.fao.org/), 'bananas' is defined as *Musa sapientum, M. cavendishii or M. nana* (raw eaten banana), 'Plantains' is defined as *Musa paradisiaca* (cooking banana). FAOSTAT is an online tool that provides time-series and cross-sectional statistic of varies data in food and agriculture for over 150 countries and is fully compliant with the principles of good practice governing international statistics. The data showed a general increase of world gross production value of bananas and plantains over the past 25 years. The decrease of world gross production value of bananas was shown between the year of 2012 to 2015.

2.3 Abiotic stress and its impact on banana cultivation

Abiotic stresses are non-biological stress such as salinity, drought, flood, and extremes of temperature, which adversely affect crop growth, development, productivity and yield (Lamaoui et al., 2018). The emergence of abiotic stresses is often triggered by erratic climate conditions such as irregular temperatures, the absence of rain, high precipitation intensities or high radiation intensities (Calanca, 2017). Problems caused by high salinity are common in arid and semi-arid areas (Qadir et al., 2014) and irrigation is one of the important causes of secondary salinization (Shrivastava & Kumar, 2015). Salinity limits the productivity of crop plant by reducing average yields for most crops by 50% (Carillo et al., 2011). An estimated worldwide 20% of cultivated lands has been severely damaged by salts (Shrivastava & Kumar, 2015) and an estimated 1.5 million hectares are taken out of production each year due to high salinity levels in the soil (Munns & Tester, 2008). Increased soil salinity also results from deposition of salts from irrigation water, coastal flooding and high evapotranspiration rates. Soils are considered saline when the electrical conductivity (EC) in the root zone exceeds 4 dSm^{-1} (approximately equivalent to 40 mM NaCl). Different plant species show different levels of tolerance to saline soil. Most crop plants, including rice, maize and banana are glycophytes, which show minimal tolerance towards saline soil with values of greater than 100 mM NaCl (EC < 10 dSm^{-1}) (Assaha et al., 2017). Bananas are generally salt sensitive especially *Musa acuminata*. The salt stress leads to poor plant growth by inducing ion toxicity and causes cell injury in the transpiring organs. In bananas, fruit development was highly influenced by salt including fruit length, fruit pulp, peel weight, volume and density (Ravi & Vaganan, 2016)

In addition to salinity, drought and heat are also major threats to agricultural productivity and weaken global food security (Lamaoui et al., 2018). The current issue of atmospheric warming, has been recorded as an average increase of at least 0.2°C per

decade and this rate is accelerating (Easterling & Wehner, 2009). Drought exposure limits current crop growth and productivity more than any other abiotic stress. For example, global wheat production was simulated to decline by 6% for each degree Celsius rise in temperature (Asseng et al., 2015). In banana, drought is gaining importance in the face of changing climate (Ravi et al., 2013). Since bananas are a semi-perennial fruit crop, they are susceptible to drought stress any time in the crop cycle when there is a shortage of rainfall or in arid climates (Ravi & Vaganan, 2016). In fact, owing to the shallow root system and high leaf area index, banana is particularly prone to soil water stress (Ravi et al., 2013). Reduction of yield in important crops has been widely reported with examples in maize (40%), wheat (21%) (Daryanto et al., 2016), cowpea (34-68%) (Farooq et al., 2017) and banana (65-87%) (Ravi & Vaganan, 2016).

2.4 Role of micro RNA in abiotic stress

MiRNA have been reported to regulate abiotic stress responses in plants (reviewed in Khraiwesh et al., 2012; Zhang et al., 2013). MiRNAs are non-coding small endogenous RNAs of 21 to 24 nucleotides in length and are well known for their function as regulators of plant development with a major role in the post-transcriptional gene silencing pathway based on sequence-specific binding to their messenger RNA (mRNA) targets (Mallory & Vaucheret, 2004). MiRNAs are important intermediaries in plant salinity responses in which down-regulate target gene expression by mRNA cleavage or repressing the mRNA translation (Xie et al., 2017). Double-stranded RNA is cleaved into 21 to 24 nt siRNAs by RNAse III enzymes belonging to the DICER family (DCL proteins in the plant).

Several reports have shown that miRNAs regulate target gene expression under various abiotic stress conditions. Experimental demonstration of a miRNA target, by

overexpressing miRNVL5 corresponding target GhCHR from cotton conferred better tolerance to salt stress by reducing Na^+ accumulation in plants and improved primary root growth and biomass in Arabidopsis. However, ectopic expression of miRNVL5 showed hypersensitivity to salt stress in Arabidopsis (Gao et al., 2016). In another report, overexpression of OsmiR393, which targets auxin receptor genes OsTIR1 and OsAFB2, showed the transgenic plants to be hypersensitive to salt and auxin (Xia et al., 2012). In a similar study, overexpression of homolog ZmAFB2 showed the transgenic tobacco to have enhanced salt tolerance (Yang et al., 2013). In addition, overexpression of banana miRNA156 caused the transgenic banana to have stunted growth with reduced height, root length and number of roots (Ghag et al., 2015). Micro RNA156 is highly conserved and expressed during the juvenile stage of plant growth. The miRNA156 targets include *Squamosal promoter binding protein-like* (*SPL*) family transcription factors, which are involved in plant development (Huijser & Schmid, 2011), plant fertility (Xing et al., 2010), and flowering pattern (Yu et al., 2010). Altered expression either of miRNAs or their targets during abiotic conditions were proposed to have potential applications for genetic improvement of plants (Zhang, 2015). Examples of stress-tolerant transgenic plants produced by expressing miRNAs and miRNA targets is shown in Table 2.1.

Table 2.1: Expression of stress-responsive miRNA towards abiotic stress tolerance in Arabidopsis and crop plants

miRNA	**Origin of gene**	**Target gene**	**Transgenic plant (host)**	**Expression strategy**	**Responses**	**References**
miR156	*Oryza sativa*	*SPL*	*Oryza sativa*	Overexpression of OsmiR156k	Reduced cold tolerance	Cui et al., 2015
miR172	*Glycine max*	AP2 like *TFs*	Arabidopsis	Overexpression of gma-miR172c	Enhanced water deficit and salt tolerance	Li et al., 2015
miR319	*Oryza sativa*	*PCF5*, *PCF8*	*Oryza sativa*	RNAi	Enhanced cold tolerance	Yang et al., 2013
miR319	*Oryza sativa*	*TCP*	*Agrostis stolonifera*	Overexpression of osa-miR319a	Enhanced salt and drought stress tolerance	Zhou et al., 2013
miR393	*Oryza sativa*	*AFB2*, *TIR1*	*Agrostis stolonifera*	Overexpression of Osa-miR393a	Enhanced salt and drought stress tolerance	Zhao et al., 2018
miR390	*Oryza sativa*	*SRK*	*Oryza sativa*	Overexpression of miR90	Reduced Cd tolerance	Ding et al., 2016
miR394a	*Glycine max*	F-box protein	Arabidopsis	Overexpression of gma-miR394a	Enhanced drought tolerance	Ni et al., 2012
miR394a	Arabidopsis	*LCR*	Arabidopsis	Overexpression of gma-miR394a/LCR mutant	Enhanced cold tolerance	Song et al., 2016

Table 2.1: continued

miR395	Arabidopsis	*BnSultr*, *BnAPS*	*Brassica napus*	Overexpression of miR395	Shorten/ no surface trichomes	Huang et al., 2010
miR396	*Oryza satina*	*Plant growth-related gene*	*Arabidopsis, Oryza sativa*	Overexpression of osa-MIR396c	Sensitive to salt and alkali stress	Gao et al., 2010
miR398	Arabidopsis	*CSD1*, *CSD2*, *CSS*	Arabidopsis	CSD1, CCS, CSD2 mutant	Enhanced thermo tolerance	Guan et al., 2013
miR399	Arabidopsis	*IPS-1*	*Solenum lycopersicum*	Overexpression of Ath-miR399d	Enhanced phosphorus toxicity and low temperature tolerance	Gao et al., 2015
miR408	Arabidopsis	Copper related gene	*Cicer arietinum*	Overexpression of Athpre-miR408	Enhanced drought tolerance	Hajyzadeh et al., 2015
miR408	*Triticum aestivum*	Phosphorus related gene	*Solenum lycopersicum*	Overexpression of TaemiR408	Enhanced salt stress Pi starvation tolerance	Bai et al., 2018

Adapted from Shriram et al., 2016 with the addition of a few recent studies. *SPL, Squamosa promoter binding protein-like; AP, Apetala; TFs, Transcription factors; TCP, Teosinte Branched Cycloidea and PCF family; PCF, Proliferating cell factors; SRK, Stress responsive leucine rich repeat receptor like kinases; LCR, Leaf curling responsiveness; CSD, Copper/Zinc superoxide dismutase; CCS, Copper Chaperon of CSD; IPS, IFN-β Promoter stimulator; BnSultr, Brassica napus sulfate transporters; BnAPS, B. napus ATP sulfurylases; AFB2, F-box auxin receptors, TIR1, Protein transport inhibitor response.*

2.5 Morphological and biochemical responses of the plant to abiotic stress

As sessile organisms, plants have adopted a series of responses to counteract abiotic stresses at the physiological, morphological and biochemical levels, allowing them to endure the abiotic stress conditions in non-adapted plant genotypes (Bielach et al., 2017). Salinity and drought stresses are the first perceived by the root system and inhibit plant growth. Salinity and drought stress can be exhibited as a physiological dehydration at the cellular level (Vinocur & Altman, 2005). In order to adapt to such conditions, morphological and physiological adjustment are the initial phase, including changes in root system (Sicher et al., 2012), reduced stomatal number, stomatal conductance and decreased leaf area to minimize water loss from the plants (Goufo et al., 2017). In fact, early responses to salinity and drought stress are similar, except that salinity stress has the additional effects of toxicity due to ionic components (Bartels & Sunkar, 2005).

During the early stages of both drought and salinity stresses, the function of plants root for water absorption is compromised, thus many of the resulting changes in cellular and metabolic processes are shared and interconnected for both types of stress (Bartels & Sunkar, 2005). During the second stage, it is mostly the ionic component from salinity stress which causes the inhibition of plant growth (Bartels & Sunkar, 2005). Optimum root systems are vital for plant growth, since roots serve as an interface between plants and the soil (Vamerali et al., 2003). Well-proliferated root systems are better for plants to adapt under stressful conditions, allowing them to penetrate deeper layers of the soil to acquire sufficient nutrients and water for survival (Franco et al., 2011). The changes in the root system are different for each type of stress. Under salinity conditions, roots were observed to have shorter lateral roots and primary roots (reviewed in Acosta-Motos et al., 2017), but under drought conditions, roots were observed to have increased number and longer roots (reviewed in Goufo et al., 2017). Besides, plants also trigger similar

protective mechanisms under both stresses by inducing ABA for regulation of stomatal closure (Goufo et al., 2017). This regulation affects the photosynthetic ability of plants by reducing CO_2 intake and fixation, thus favouring the production of Reactive Oxygen Species (ROS) and promotes oxidative damage, which will eventually lead to plant chlorosis and necrosis (Arbona et al., 2017). ROS including hydrogen peroxide (H_2O_2), superoxide anions ($O_2^{\bullet-}$) and hydroxyl radicals (OH•) are by-products from physiological responses under abiotic stress conditions, and this is regulated by an antioxidant defence system (You & Chan, 2015). Therefore, plants induced antioxidant compounds such as ROS scavenging enzymes, for example Superoxide dismutase (SOD), Catalase (CAT), Peroxidase (POD), Ascorbate peroxidase (APX) and Glutathione reductase (GR) as well as an involvement of ABA-mediated pathways, as an adaptive mechanism to water loss and oxidative stress under abiotic stress (Pandey et al., 2017). ABA is the most important phytohormone involved in regulation of tolerance to abiotic stresses such as drought and salinity (Lata & Prasad, 2011). The role of ABA as central mediator under drought stress includes regulation of stomatal (Goufo et al., 2017), ABA-mediated gene expression (Cho et al., 2011), and physiological responses (Sah et al., 2016). ABA plays an important role in modulating root architecture including lateral roots and root length (Sah et al., 2016). Moreover, the ratio of root growth to shoot growth is higher with the presence of ABA (Saab et al., 1990). A similar study showed that ABA accumulation maintains maize primary root elongation by restricting the production of ethylene (Spollen et al., 2000). The increased concentration of ABA in maize, helps in root elongation, allowing the plant to cope with stress. ABA is also important in promoting stomatal closure by regulating guard cell-specific protein kinase to reduce water loss during stress conditions (Li & Assmann, 1996) a process mediated by G protein signalling, to regulate ion channels during stress (Zhang et al., 2008; Chakravorty et al., 2011).

2.6 Root hair defective 3 (RHD3) as a candidate gene for abiotic stress tolerance

Root hairs are tubular extensions of the epidermis and are the main surface area for uptake of water and nutrients for a plant. Root hairs are also important for microorganism-root interactions that give fitness to plants (Lan et al., 2013). Root hair defective 3 (RHD3), a large GTP-binding protein, is involved in the regulation of cell expansion throughout both root epidermis and root tip development in Arabidopsis, as reported by Wang et al. (1997). Up to date, three isoforms of RHD3 have been reported in Arabidopsis and were found to be analogous with the mammalian atlastin GTPases, which are involved in shaping endoplasmic reticulum tubules (Hu et al., 2003). Arabidopsis RHD3 contains two motifs conserved in GTP-binding proteins which are GXXXXGKS and DXXG but lacks a third motif (N/TKXD) found in other GTP-binding proteins (Wang et al., 1997). GTP-binding proteins are involved in a range of vital cellular processes, including signal transduction, intracellular trafficking, cytoskeleton organization, and protein synthesis (reviewed by Xu et al., 2012). Point mutation of RHD3 altered cell size, but not cell number, in all organs of Arabidopsis (Wang et al., 1997). The RHD3 mutants showed abnormality in vacuole enlargement and vesicle distribution in root hairs (Galway et al., 1997) exhibiting a short and wavy root hair phenotype (Wang et al., 1997). RHD3 was found to be involved in transport between the endoplasmic reticulum and Golgi apparatus by using a GFP-based assay (Zheng et al., 2004). Chen et al., (2011) proposed that Arabidopsis RHD3 helps in the generation of the tubular endoplasmic reticulum network and is required for normal distribution and motility of the Golgi apparatus. Xu et al. (2012) reported that overexpression of RHD3 in Populus showed the formation of only a single prominent adventitious root with well-developed lateral roots, characteristic abnormalities in the root tips, and longer and more plentiful root hairs.

2.7 *Arabidopsis thaliana* as a model plant system and application

Arabidopsis thaliana, commonly known as *Thale cress*, is a small dicot plant and a member of the *Brassicaceae* family. This family includes various economically important crops such as mustard, cabbage, broccoli, turnip, and radish, but Arabidopsis has no major agronomic significance (Sharma et al., 2014). Although Arabidopsis was long thought to have the smallest genome of all flowering plants (Leutwiler et al., 1984), the smallest plant genomes are now known to belong to plants of the genus *Genlisea*, order *Lamiales*, with *Genlisea tuberosa*, a carnivorous plant which has an approximately 61 Mbp genome size (Fleischmann et al., 2014). In spite of this, Arabidopsis was the first plant to have its genome sequenced and has been the center of attention for intense genetic, biochemical, molecular biology and physiological study for several years (Meinke et al., 1998). The small, fully-sequenced and annotated genome, availability of complete genetic and physical maps of all 5 chromosomes and short life cycle (6 weeks, from germination to seed maturation) (Meinke et al. 1998), make it an organism of choice for laboratory study over other plants. The life cycle stages of Arabidopsis include seed germination, rosette formation, bolting, flowering and seed maturation. The founder for using Arabidopsis as model plant for research is Friedrich Laibach (Koornneef & Meinke, 2010). Arabidopsis offers further advantages of easy and rapid genetic transformation by *Agrobacterium tumefaciens*-mediated transformation (Valvekens et al., 1988), limited space requirements and easy adaptability to greenhouse or indoor growth chamber environments (Somerville & Koornneef, 2002)

Besides, by using Arabidopsis as model plants also provide wide range of application for example as a platform for protein production (Nykiforuk & Boothe, 2012), cross-kingdom research (Bakar et al., 2015) and tripartite interactions among plants (plant-nematode-endophyte) for fundamental study (Martinuz et al., 2015).

CHAPTER 3: MATERIALS AND METHODS

3.1 Plant materials and sample treatments and growth conditions

3.1.1 Growth conditions for *Musa acuminata* cv Berangan

Clonal, tissue culture-derived *Musa acuminata* cv Berangan (AAA triploid genome) banana plantlets were obtained from Felda Agricultural Services Sdn Bhd (FASSB) company (Negeri Sembilan, Malaysia). One-month-old tissue culture-derived banana plantlets were transferred to Murashige & Skoog (MS) basal medium (Murashige & Skoog, 1962) supplemented with 300 mM NaCl for 48 h. After 48h, roots were collected for RNA extraction. Samples were kept at -80ºC prior to use for validation of 12 miRNAs and 14 predicted miRNA-1target mRNAs by RT-qPCR and for the isolation of *MaRHD3* cDNA for constitutive expression in Arabidopsis.

3.1.2 Growth conditions for *Arabidopsis thaliana*

Arabidopsis ecotype Columbia (Col-0) was used in this study. Seeds were surface sterilized with 0.05 % (µL/mL) of Tween 20 for 5 min followed by soaking in 70% ethanol for 3 min then rinsed with sterile water for 5 times and stratified by placing seeds in sterile distilled water at 4°C for 3 days. The sterilized seeds were placed on a sterilized potting soil mixture for germination. A mixture of organic soil and mushroom compost in the ratio of 3:1 was used for growing Arabidopsis. Soil and pots were autoclaved before use. Two weeks after germination, Arabidopsis seedlings were transferred to individual pots containing the same potting soil mixture and grown at 22 ± 1ºC with 60 ± 5% relative humidity and a 16-h/8-h light/dark in a controlled-environment at growth room D, Plant Biotech Facility, CEBAR, University of Malaya. Arabidopsis seedlings were allowed to grow up to the inflorescence stage (at about six weeks) and were used for floral dip transformation following the method of Davis et al. (2009).

3.2 Bioinformatics analysis of MaRHD3

The *MaRHD3* gene sequence was extracted from the banana genome (http://banana-genome-hub.southgreen.fr/blast) using BLAST with the CDS of *MaRHD*3 as a query. Putative protein sequences were predicted with the ExPASy translate tool (Gasteiger et al., 2005). Sequence alignment was performed using ClustalW (http://www.ebi.ac.uk/clustalw/). MEGA 7.0 (Kumar et al., 2016) was used for phylogenetic analysis of the predicted MaRHD3 amino acid sequence with orthologous RHD3 sequences. Subcellular localization of MaRHD3 was predicted using PSORT (https://www.genscript.com/psort.html) (Nakai & Kanehisa, 1991).

3.3 Isolation and cloning *MaRHD3* into TA vector (pEASY®-T1)

Primers for *MaRHD3* (XM_009391195.2) were designed with flanking *Bgl*II sequence (forward primer) and *Spe*I sequence (reverse primer, without stop codon sequence) at the 5' end of each primer (Table S1, Appendix A). Polymerase chain reaction (PCR) using TransStart® FastPfu Fly DNA Polymerase (TransGene Biotech, China) was carried out in a total of 50 µL reaction volume as shown in Table 3.1. The thermal cycling condition was programmed as 95^{0}C for 5 min; 30 cycles of 95^{0}C for 1 min, 50^{0}C for 40 s and 72^{0}C for 1 min; and a final extension of 72^{0}C for 15 min. The amplicons were analysed on 1% agarose gel and visualized with a ChemiDoc™ Imaging System (Bio-Rad Laboratories Inc., USA). An amplicon of the expected size (2.4 kb) was gel excised and purified using FavorPrep GEL/PCR Purification Mini Kit (Favorgen, Taiwan) following the manufacturer's protocol. The PCR product was then used for "A-tailing" in a reaction mixture as shown in Table 3.2 and incubated for 20 min at 70^{0}C. Fresh "A"-tailed PCR product was then ligated with pEASY®-T1 in a total of 5 µL reaction, 4 µL of purified "A"-tailed PCR product and 1 µL of pEASY®-T1 Simple Cloning Vector. The reaction

mixture was gently mixed and incubated at room temperature for 30 min for ligation. Next, 5 µL of the ligated product was added into 50 µL of *Trans*1-T1 Phage Chemically Competent Cell (TransGene Biotech, China) following the manufacturer's protocol for transformation, with modification of 1 min at the heat-shock stage instead of 30 s. The cells were then plated on 25 mL LB agar plate with 20 µL X-gal (50 mg/mL, Promega) and 25 µL Ampicillin (100 mg/mL, Duchefa) for selection purposes.

Table 3.1: Master mix of TransStart®FastPfu DNA Polymerase PCR

Components	**Volume (µL)**	**Final Concentration**
cDNA Template	2	100 ng/µL
Forward Primer (10 µM)	1	0.2 µM
Reverse Primer (10 µM)	1	0.2 µM
5x TransStart®FastPfu Fly Buffer	10	1x
2.5 mM dNTPs	5	0.25 mM
TransStart®FastPfu Fly DNA Polymerase	1	2.5 units
ddH_20	30	-
Total volume	50	-

Table 3.2: Reaction mixture for "A-tailing" of purified PCR product

Components	**Volume (µL)**
Purified blunt-ended PCR product	4
Colourless GoTaq Reaction Buffer (5X)	2
dATP (1 mM)	2
$MgCl_2$ (25 mM)	0.6
GoTaq Flexi DNA polymerase (5 U/µL)	1
Total volume	10

3.4 Screening of transformed bacterial cells

Putatively transformed competent cells (*Trans*1-T1 Phage Chemically Competent Cell of *E. coli* and of *Agrobacterium tumefasciens LBA4404*) were screened using colony PCR. Single colonies were selected from LB agar plates, picked by a sterile toothpick and streaked onto a fresh LB agar plate with appropriate antibiotics (Table 3.3) to create a library of the potential recombinant clones. LB agar plates were incubated overnight at 37ºC for *E. coli Trans*1-T1 Phage Chemically Competent Cells or at 28ºC for Agrobacterium. Next, the same streaking toothpick was dabbed into 50 µL of sterile distilled water and boiled for 5 min. Five microliters from the boiled mixture was used as the PCR template. Colony PCR was carried out using GoTaq® Green Master Mix (Promega) with MaRHD3_Full_F and MaRHD3_Full_R primer (Table S1, Appendix A) and thermal cycling conditions programmed as 95^0C for 5 min; 30 cycles of 95^0C for 1 min, 50^0C for 30 s and 72^0C for 1 min; and a final extension of 72^0C for 10 min. The reaction mixture was set up as in Table 3.4.

Table 3.3: Antibiotics used for selection of bacterial colonies

	Antibiotics	**Final Concentration**
***E. coli Trans*1-T1 Phage Chemically Competent Cell**	Ampicillin	100 mg/L
Agrobacterium tumefasciens LBA4404	Rifampicin	10 mg/L
	Kanamycin	50 mg/L

Table 3.4: Colony PCR reaction setup

Components	Volume (µL)	Final Concentration
DNA	5	200 ng/µL
Forward Primer (10 µM)	1	0.2 µM
Reverse Primer (10 µM)	1	0.2 µM
GoTaq® Green Master Mix	12.5	1x
Distilled water	5	-
Total volume	25	-

3.5 Restriction enzyme digestion and ligation of *MaRHD*3 to pCAMBIA1304 vector

Recombinant plasmids of pEASY®-T1 harbouring *MaRHD*3 cDNA were confirmed by DNA sequencing using a service provided by First BASE Laboratories Sdn Bhd (Malaysia) with sequencing primers as listed in Table 3.5. pEASY®-T1 harbouring *MaRHD*3 cDNA and pCAMBIA1304 were digested with *Bgl*II and *Spe*I (New England Biolabs, USA), the reaction mixture was prepared as in Table 3.6, for 3 h at 37^{0}C. Digested products were separated by 0.7% agarose gel electrophoresis and excised from the gel followed by purification using FavorPrep GEL/PCR Purification Mini Kit (Favorgen, Taiwan) according to the manufacturer's protocol. Purified digested vector and insert were prepared as in Table 3.7 then ligated overnight at 4^{0}C using T4 DNA ligase (Promega, USA) following the manufacturer's protocol, to obtain a plant constitutive expression construct which was named as pCAMBIA1304*MaRHD3*.

Table 3.5: Primers used in sequencing for pEASY®-T1 harbouring *MaRHD*3

Primer Set	Sequence (5' to 3')	Annealing Temperature (^{0}C)
M13-pUC (-26)	CAG GAA ACA GCT ATG AC	55
T7 promoter	TAA TAC GAC TCA CTA TAG GG	55
Primer Walking_F	GAA GTA GTG GCT CTT TCA AGC	55
Primer Walking_R	GCT TGA AAG AGC CAC TAC TTC	55

Table 3.6: Digestion of pCAMBIA1304 and pEASY®-T1 harbouring *MaRHD3* cDNA

Components	Volume (µL)
Vector (pCAMBIA1304 and pEASY®-T1) (5µg)	10
*Bgl*II (NEB)	1.5
Buffer 3.1 (NEB)	5
Nuclease-Free water to final volume of	50
Digested vector from above	40
*Spe*I (NEB)	1.5
Buffer CutSmart (NEB)	5
Nuclease-Free water to final volume of	50

Table 3.7: Ligation mixture of digested pCAMBIA1304 and MaRHD3

Components	Volume (µl)
Digested pCAMBIA1304	1
Digested *MaRHD3* (*Bgl*II and *Spe*I)	5
Ligase 10X buffer	1
T4 DNA ligase (Weiss Units)	1
Nuclease-Free water to final volume of	10

3.6 Plant expression vector construction

MaRHD3 coding DNA sequence (2.4 kb) from recombinant pEASY®-T1 (full-length sequence, Figure S1, S2, S3, and S4, Appendix B) was cloned between *Bgl*II and *Spe*I sites of plant binary expression vector pCAMBIA1304 (CAMBIA, Australia) (12.3 kb) fused with mgfp-gus to form the recombinant plasmid. pCAMBIA1304*MaRHD3* (Figure 3.1A). Plasmid pCAMBIA1304MaRHD3 was introduced into Agrobacterium using a freeze-thaw transformation method (Holsters et al., 1978).

3.7 Subcellular localization of MaRHD3 protein in plant cells

Subcellular localization of MaRHD3-gfp fusion protein was determined using onion epidermal cells transformed with Agrobacterium harbouring either the pCAMBIA1304*MaRHD3* construct or empty vector (EV) pCAMBIA1304 (Figure 3.1B), according to the method of Sun et al. (2007) with modification, where the infection stage was in the presence of 100 µM of acetosyringone for 30 min at 28°C with shaking at 80 rpm. GFP fluorescence was detected under a confocal scale laser scanning microscope (Leica Tcs SP5 II, Germany).

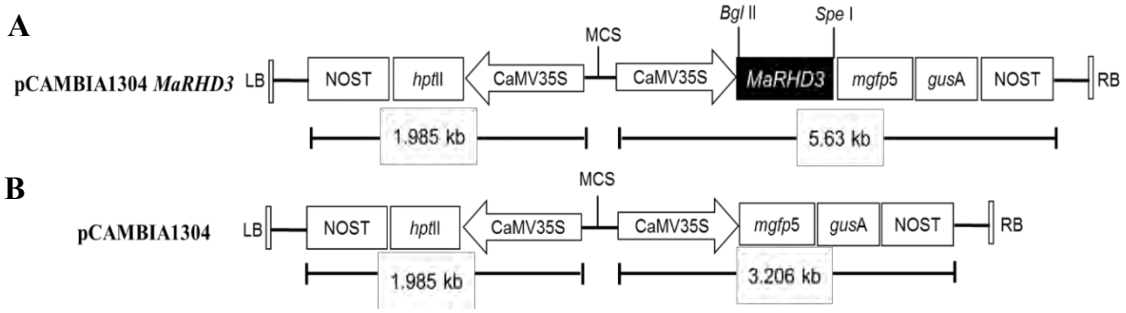

Figure 3.1: T-DNA region of binary vector pCAMBIA1304MaRHD3 and pCAMBIA1304. (A) T-DNA region (7615 bp) of binary vector pCAMBIA1304*MaRHD3*; *MaRHD3* (2424 bp) was cloned between *Bgl*II and *Spe*I sites. (B) T-DNA region (5191 bp) of binary vector pCAMBIA1304. RB: Right border; CaMV 35S: Cauliflower Mosaic Virus 35 Promoter; NOST: Nopaline synthase terminator; mgfp5:gusA: beta-glucuronidase and green fluorescence fusion gene; hptII: Hygromycin phosphotransferase.

3.8 Hygromycin, Polyethylene glycol – 8000 (PEG-8000) and Sodium chloride sensitivity test

Sensitivity tests for hygromycin, for PEG-8000 and for sodium chloride were performed on wild-type Arabidopsis seeds to determine the most effective threshold concentrations for each substance to use for the selection and challenge of transgenic seeds. In three separate sets of experiments, each run in triplicate (n=3) 100 stratified wild type Arabidopsis seeds were tested with 1. different concentrations of hygromycin (10 mg/L, 15 mg/L, 20 mg/L and 25 mg/L), 2. different concentrations of PEG-8000 (10 % (w/v), 15% (w/v), 20% (w/v) and 25% (w/v)) and 3. different concentrations of NaCl (50 mM, 100 mM, 150 mM and 200 mM of NaCl). For each experiment, seeds were screened by spreading evenly on each petri dish containing MS media supplemented with respective concentration of hygromycin, PEG-8000 or NaCl. All procedures were performed inside a laminar air flow cabinet and then the plates were placed on a culture rack at 22 ± 1ºC, 60 ± 5% relative humidity and 16-h/8-h light/dark in a controlled-

environment at growth room D, Plant Biotech Facility, CEBAR. The seed germination rate and seedling phenotypes were recorded for each concentration.

3.9 Plant transformation and screening of transgenic plants

A single colony of Agrobacterium in harbouring either the pCAMBIA1304*MaRHD3* or the empty vector (EV) was inoculated into 50 mL of liquid LB medium with 10 mg/L of rifampicin, and 50 mg/L of kanamycin, and grown overnight at 28°C to an OD600 of 0.7. The cells were harvested by centrifuging at 5000 rpm for 5 min and the pellet was resuspended in 5% sucrose solution containing 0.04% silwet L77 before use for the transformation of Arabidopsis *via* floral dip (Clough et al., 1998). Arabidopsis inflorescences were dipped in resuspended Agrobacterium inoculum. Excess inoculum from inflorescences was absorbed by sterile tissue paper. A black plastic bag sprayed with sterile distilled water was used to cover the plant for 24 h. After dark incubation, plants are uncovered and transferred to 22 ± 1°C with 60 ± 5% relative humidity and a 16-h/8-h light/dark in a controlled-environment at growth room D, Plant Biotech Facility, CEBAR. The transformation steps were repeated after 6 days for a second floral dip.

A total of 100 plants were transformed (5 independent transformation events with 20 plants for each event) for pCAMBIA1304*MaRHD3* and EV. Transgenic plants were screened on half strength MS agar medium supplemented with optimized threshold value 20 mg/L concentration of hygromycin. Randomly chosen surviving hemizygous plants were screened by PCR and DNA gel blot hybridization (section 3.12). Single copy transgene integrated lines were used for screening T_2 seeds (Table 4.3) to observe segregation patterns. Homozygous seedlings from the T_3 generation were selected *via*

progeny analysis using hygromycin and then those with transgene expression confirmed by RT-qPCR (section 3.13.4) were used for further analysis.

3.10 Genomic DNA isolation and PCR screening of putative transformed Arabidopsis

Genomic DNA was isolated using the FavorPrep™ Plant Genomic DNA Extraction Mini Kit (Favorgen, Taiwan) following the manufacturer's instructions. Internal gene-specific primers MaRHD3_SF and MaRHD3_SR (Table S1, Appendix A) were designed to amplify a 452 bp fragment specific to *MaRHD*3 sequence and distinct from the Arabidopsis native RHD3 sequence. This gene-specific primer along with GFP primers was used for screening of putative transformed Arabidopsis. The reaction setup was as shown in Table 3.8. The thermal cycling condition was programmed as 95^{0}C for 5 min; 30 cycles of 95^{0}C for 1 min, 50^{0}C for 30 s and 72^{0}C for 30 s; and a final extension of 72^{0}C for 10 min for *MaRHD3* primer. The thermal cycling condition was programmed as 95^{0}C for 5 min; 30 cycles of 95^{0}C for 1 min, 55^{0}C for 30 s and 72^{0}C for 30 s; and a final extension of 72^{0}C for 10 min for GFP primers. The amplicons were analysed on 1% agarose gel and visualized with a ChemiDoc^{TM} Imaging System (Bio-Rad Laboratories Inc., USA).

Table 3.8: Reaction mixture for PCR screening of transformed Arabidopsis

Components	Volume (µL)	Final Concentration
Genomic DNA	1	100 ng/µL
Forward Primer (10 µM)	1	0.2 µM
Reverse Primer (10 µM)	1	0.2 µM
GoTaq® Green Master Mix	12.5	1x
Sterile Distilled water	9.5	-
Total volume	25	-

3.11 Histochemical staining of GUS expression

To confirm successful transformation events, β-Glucuronidase (GUS) staining was carried out (Vitha et al., 1995). Transgenic and control leaves, flowers and roots were collected and soaked in X-gluc solution consisting of 0.1 M sodium phosphate (pH 7.0), 10 mM ethylenediaminetetraacetic acid, 0.5 mM potassium ferrocyanide, 0.5 mM potassium ferricyanide and 0.1% (w/v) X-gluc at 37^{0}C overnight. The stained plant materials were then bleached with 70% ethanol and viewed with a stereomicroscope (Olympus SZX7, Japan).

3.12 DNA gel blot hybridization of *MaRHD3*

DNA gel blot hybridization was performed to confirm the copy number of *MaRHD3* transgene in T_1 generation Arabidopsis. Fifteen micrograms of genomic DNA were digested with *SpeI* (NEB) at 24^{0}C overnight, electrophoresed on 0.8% agarose gel with 70V for 2 hours in 1X TBE buffer until the band was well separated. The digestion setup was as shown in Table 3.9. Next, the gel was agitated in 50 mL of denaturation solution (1.5 M of NaCl and 0.5 M of NaOH) for 45 min, this step is to denature double-stranded DNA into single stranded DNA which increases the efficiency of transferring DNA into

nylon membrane and subsequent hybridization to a labelled probe. Next, the denatured gel was rinsed with sterile distilled water twice and then agitated in neutralization solution (0.5 M Tris-HCl and 1.5 M NaCl) for 45 min prior to blotting. The neutralized gel was then equilibrated in 20X SSC (3 M NaCl, 300 mM Sodium Citrate; pH 7.0) for 15 min. The equilibrated gel was then blotted onto a positively charged nylon membrane (Roche Diagnostics, Mannheim, Germany) overnight. The nylon membrane edge was cut, to identify the side of the blotted DNA. The transfer assembly setup was as shown in Figure 3.2.

After blotting, the membrane was rinsed with 2X SSC and the transferred DNA was fixed to the nylon membrane by microwave irradiation at 900 W for 1 min. Next, the membrane was used for prehybridization. Prehybridization, hybridization, washing and immunological detection were carried out using DIG High Prime DNA Labeling and Detection Starter Kit I (Roche Diagnostics, Mannheim, Germany) according to the manufacturer's instructions. Prehybridization was carried out by adding 15 mL pre-warmed Dig Easy Hyb solution into container containing the membrane and incubated for 30 min at 46^0C under gentle agitation. In the meanwhile, the probe was a DIG-labelled 0.45 kb PCR product corresponding to the coding region of Hygromycin phosphotransferase II (hptII) (the primers for probe preparation are listed in Table S1, Appendix A). Probe labelling was performed using PCR DIG Probe Synthesis kit (Roche Diagnostics, Mannheim, Germany) following the manufacturer's protocol. DIG-labelled probe was denatured by boiling for 5 min and cooled rapidly on ice. The prehybridization solution was removed and 20 mL fresh pre-warmed DIG Easy Hyb solution was added to the membrane. Two micro litres of DIG-labelled probe (50 ng/mL) was mixed with fresh pre-warmed DIG Easy Hyb solution with gentle agitation and incubated at 46^0C for overnight. After hybridisation, the solution was discarded and the membrane was rinsed

twice with pre-warmed 2X SSC. Next, the membrane was washed with washing buffer (1X Maleic acid buffer with 0.3% Tween 20 (v/v), Roche Diagnostics, Mannheim, Germany) for 5 min at room temperature. The membrane was added with 30 mL of 1% blocking solution in 1X Maleic acid buffer followed by incubation for 1 hour at 37^0C. The solution was then discarded. Mixture of 5 µL anti-DIG-AP conjugate and 15 mL of 1% blocking solution was added to the membrane followed by incubation for 30 min at 37^0C. The membrane was washed twice with washing buffer, 15 min each washing. The membrane was then equilibrated in Detection buffer for 5 min at room temperature before incubated in the dark with freshly prepared colour substrate solution for 16-18 h. Hybridization bands were observed by the development of colour on the membrane. The membrane was rinsed with distilled water to stop the reaction and dry membrane was scanned using a DocuCentre-IV 2060 scanner (Fuji Xerox, Japan).

Table 3.9: Digestion of genomic DNA extracted from T_1 transgenic Arabidopsis expressing *MaRHD3* and from control plants

Components	**Volume (µL)**	**Final Concentration**
DNA	20	15 µg
*Spe*I (NEB)	2	-
10X CutSmart (NEB)	5	1X
Distilled water	23	-
Incubation time	overnight	-
Total volume	50	-

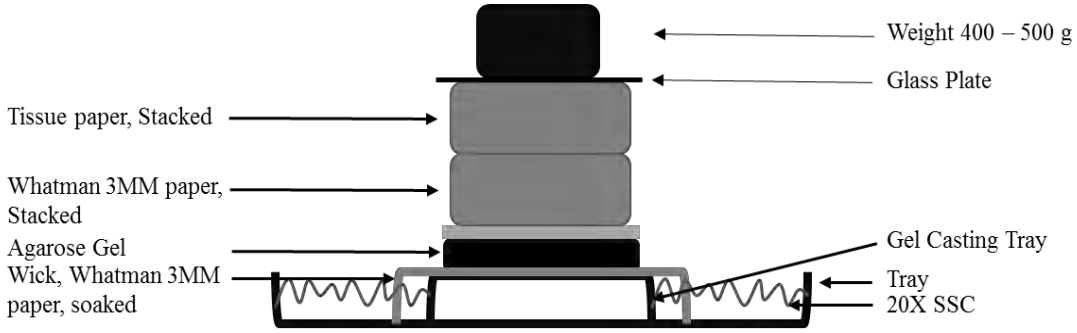

Figure 3.2: The blot assembly setup used in DNA gel blot hybridization. The diagram was adapted from DIG DNA labelling and detection Kit application manual (Roche Diagnostics, Mannheim, Germany)

3.13 Quantitative real-time reverse transcriptase PCR

3.13.1 Extraction of Total RNA

RNA extraction was done using a CTAB method (Kiefer et al., 2000). Banana roots and Arabidopsis leaf samples were ground into fine whitish powder using liquid nitrogen in pre-cooled mortar and pestle. Powdered samples were transferred into a 2 mL microcentrifuge tube and pre-heated at 65^{0}C of the 1 mL of CTAB buffer with 1% of beta-mercaptoethanol was added and the mixture vortexed. An equal amount of phenol, chloroform, isoamyl alcohol (PCI), pH 5.7, in the ratio of 25:24:1 was added, the sample mixed by vortex mixer then centrifuged for 15 min at 13000 rpm. Resulting aqueous phase of the centrifuged product was transferred into a new labelled 1.5 mL microcentrifuge tube. Cloroform isoamyl (CI) in the ratio of 24:1 were added into the clear aqueous phase and centrifuged for 15 min at 13000 rpm. Additional CI extraction steps were repeated 3 times. Next, two volumes of isopropanol were added to tubes, and labelled and stored at -80^{0}C overnight. The next day, tubes were removed from the freezer and centrifuged at 4^{0}C for 30 min at 10000 rpm. The supernatant was discarded and the pellet washed with 1 mL pre-chilled 70% ethanol, then, centrifuged at 4^{0}C for 15 min at 10000 rpm. Finally, the supernatant was discarded, the pellet dried at room temperature,

then 30 µL of DEPC treated water was added. RNA quality and quantity were checked by gel electrophoresis and spectrophotometry (see 3.13.2).

3.13.2 Determination of RNA quality and quantity

RNA quality was analysed on a 1% (w/v) agarose gel with 0.5% bleach according to the method (Aranda et al., 2012). Extracted RNA was quantified using a Nanodrop 2000/2000C spectrophotometer (Thermo Scientific) and purity was determined by measuring the UV absorbance of 260 nm, 280 nm, and 230 nm. Samples were measured in triplicate and the average value was taken. Only samples for which the absorbance ratio of A260nm/230nm ranged from 1.8 to 2.2 and A230nm/A260nm higher than 1 were used for cDNA synthesis.

3.13.3 cDNA synthesis by RT-PCR

Extracted RNA was converted into cDNA using QuantiTect® Reverse Transcription (Qiagen, Germany) according to the manufacturer's protocol. Genomic DNA removal was included in the kit with reaction setup as shown in Table 3.10. The reaction volume was set to 14 µL with RNA template standardized to 1 µg for each tube. The reaction mixture was incubated at 42^0C for 2 min and placed immediately on ice, to prevent RNA degradation.

Table 3.10: Genomic DNA removal reaction mixture

Components	**Volume (µL)**	**Final Concentration**
gDNA Wipeout Buffer (7X)	2	1x
RNA template	1	-
RNase-free water	Variable	-
Total volume	14	-

The total reaction (14 µL containing 1 µg of RNA) was then used as a template for cDNA synthesis by RT-PCR following manufacturer's protocol. The reaction mixture was set up as shown in Table 3.11 and incubated at 42^0C for 20 min followed by inactivation at 95^0C for 3 min. The cDNA samples were kept at -20^0C until further use.

Table 3.11: Reaction mixture of reverse-transcription

Components	**Volume (µL)**	**Final Concentration**
Quantiscript RT Buffer (5X)		1x
RT Primer Mix		
Quantiscript Reverse Transcriptase		
RNA template (Table 3.10)		-
Total volume		-

3.13.4 Quantitative real-time RT-PCR (RT-qPCR)

Primers for miRNA targets (mRNA), *MaRHD3*, *ABF-3,* and *RD29A*, were designed using the PrimeQuest IDT Tool (https://sg.idtdna.com/PrimerQuest/Home/Index) and were as listed in Table S1 (Appendix A). Stem-loop primers for miRNA were designed based on Kramer (2011) and were as listed in Table S2 and S3 (Appendix A). All real-time PCR was carried out in 20 µL reaction volumes using Power SYBR Master Mix (Life Technologies, USA). The reaction mixture was as shown in Table 3.12 and PCR performed using the QuantStudio™ 12K Flex system (Applied Biosystems, USA) with cycling conditions of 95ºC for 10 min, followed by 40 cycles of 95ºC for 15 s and 60ºC for 1 min. Dissociation curves for all selected genes were established at the end of the PCR cycle at 95ºC for 15 s, 60ºC for 1 min followed by 95ºC for 15 s (Figure S5, S6, and S7, Appendix c). All the real-time PCR analyses were normalized with U6 (Table S2, Appendix A, miRNAs, and miRNAs target; banana sample) and Actin (Table S1, Appendix A, *MaRHD3*, *ABF*-3, *RD29A*; Arabidopsis sample) which are standard internal controls, and run in technical triplicate for each of three biological replicates. Relative gene expression was determined from triplicate measurements using the $2^{-\Delta\Delta CT}$ method (Livak & Schmittgen, 2001).

Table 3.12: Reaction mixture for RT-qPCR

Components	**Volume (µL)**	**Final Concentration**
cDNA template	2	10 ng/µL
Forward Primer (10 µM)	1	0.5 µM
Reverse Primer (10 µM)	1	0.5 µM
Power SYBR Master Mix (5X)	10	1X
Sterile Distilled water	6	-
Total volume	20	-

3.13.5 Comparative analysis of RNAseq data with data from RT-qPCR

In order to validate RNAseq prediction data, comparative analysis was carried out between RNAseq prediction data and RT-qPCR expression data. RNAseq prediction data of miRNAs and their corresponding target of banana in response to salt stress was obtained from a study carried out by a research group at the University of Malaya (Lee et al., 2015). RT-qPCR expression data were generated using method as described in section 3.13.4). A total number of 12 selected miRNAs and 14 predicted targets were selected from the RNAseq prediction data based on their biological function which includes stress mechanism and defence, stress mechanism and root development (Appendix E). Histogram was plotted based on the fold changes on RNAseq prediction data and RT-qPCR expression data. Fold changes of RNAseq prediction data was obtained from Lee et al. (2015) and RT-qPCR expression data was calculated as described in section 3.13.4.

3.14 Germination assay and root phenotype examination

To estimate threshold values for sensitivity, 100 WT seeds were plated in triplicate on half strength MS solid medium, with increasing concentrations of either NaCl (0-200 mM) or PEG (0-25% (v/v)). Percentage of germination was scored after 14 d. The optimized threshold dosage of NaCl and PEG (Figure 4.15 and 4.17) were used for performing germination assays for seeds of homozygous Arabidopsis T_3 lines. One hundred seeds from each transgenic line, EV, and WT lines were plated in triplicate (n = 300) and incubated at 4˚C for 3 d to break seed dormancy, and then transferred to a plant growth chamber (22 ± 1°C with 60 ± 5% relative humidity (RH), 16 h light, 8 h dark) for 14 d. The percentages of seeds that had germinated and developed fully green expanded cotyledons were scored.

To record root phenotypes, 7 d old germinated seedlings grown in controlled conditions and seedlings which had no significant difference in primary root length (~0.7 cm) were transferred to half strength MS medium supplemented with either 100 mM NaCl or 20% (v/v) PEG and allowed to grow in a vertical position in a plant growth chamber (22 ± 1°C with 60 ± 5% RH, 16 h light, 8 h dark). After 14 d, primary root lengths were measured (20 replicates in each treatment, each treatment repeated three times). Roots were excised from seedlings after 14 d treatment with and without 20% PEG and were analysed with a stereomicroscope (Olympus SZX7, Japan). Root hairs were counted based on the region from the root tip to 1 cm along the root for each seedling.

3.15 Drought stress tolerance assay

A total of 30 seedlings from each transgenic line, EV and WT lines were grown in individual pots with well water conditions (water every day in the morning, 8.30 a.m.) for 10 weeks in a BSL-2 growth room at the Plant Biotech Facility, CEBAR, University of Malaya. For drought tolerance assay, plants were treated by withholding water for 7 d followed by 10 d of recovery and each experiment was repeated three times. Photographs were taken before drought and after the recovery period. The recovered plants were assessed for chlorophyll content, lipid peroxidation, ROS and ROS scavenging enzyme activity to determine the post effect of drought stress. Biomass accumulation was assessed by weighing fresh and dry weights of recovered plants.

3.16 Histochemical staining of ROS

Histochemical staining of H_2O_2 and $O_2^{\bullet-}$ radicals was performed according to the method described by Rangani et al. (2016). Leaves detached from drought-recovered plants were incubated in phosphate buffer containing either 3, 3'- diaminobenzidine tetrahydrochloride (DAB) solution (1 mg/mL, pH 7.6) or nitro blue tetrazolium (NBT) solution (1 mg/mL, pH 7.8) in the dark at ambient temperature until the appearance of dark spots (~8 h). The stained leaves were then bleached in methanol: acetic acid: glycerol (3:2:1) and photographed.

3.17 Estimation of chlorophyll content

Chlorophyll a (Chl a), chlorophyll b (Chl b) were estimated according to the method described by Inskeep and Bloom (1985) and carotenoid contents were estimated according to the method of Chamovitz et al. (1993). Leaves (100 mg) from drought recovered plants were homogenized in 2 mL of pre-chilled 100% N, N-dimethylformamide (DMF) in the dark and the homogenate was centrifuged at 13000 rpm for 10 min. The supernatant was collected and diluted fivefold and absorbance was measured at wavelengths of 664, 647, and 461 nm. Chlorophyll a, chlorophyll b and carotenoid concentration were calculated based on the formula listed in Appendix D.

3.18 Estimation of lipid peroxidation

The degree of lipid peroxidation was quantified by determining the concentration of malondialdehyde (MDA) produced by the thiobarbituric acid (TBA) reaction following the method described by Draper and Hardley (1990). Leaves (100 mg) were homogenized in 2 mL of 0.1% (w/v) trichloroacetic acid (TCA) solution. The homogenate was centrifuged at 13000 rpm for 15 min at 4°C, the supernatant was collected, and 500 µL of the supernatant was mixed with 2 mL of 0.5% (w/v) TBA prepared in 20% (w/v) TCA. The mixture was incubated at 95°C for 30 min, and the reaction was stopped by placing the tubes in ice. Samples were centrifuged at 10000 rpm for 5 min, and the absorbance of the supernatant was recorded at 532 nm. MDA concentration was calculated based on Lambert-Beer law with an extinction coefficient (ε^{M})= 155 $mM^{-1}cm^{-1}$. Results was presented as µmol MDA $g^{-1}FW$.

3.19 Estimation of ROS scavenging enzyme activity

3.19.1 Estimation of superoxide dismutase activity

Superoxide dismutase (SOD) activity was determined based on the inhibition of photochemical reduction of nitroblue tetrazolium (NBT) at 560 nm according to the method described by Sen Gupta et al. (1993). Leaf tissues (100 mg) were homogenized in 1 mL of 50 mM phosphate buffer (pH 7.8). The homogenate was centrifuged at 10000 rpm for 15 min at 4°C and 100 µL supernatant was added into a 3 mL reaction mixture (50 mM phosphate buffer (pH 7.8), 13 µM methionine, 63 µM NBT, 1.3 µM riboflavin). The reaction was started by exposing the solution under 30 W white fluorescent light and was stopped after 10 min by turning off the light. SOD concentration was calculated based on the formula listed in Appendix D.

3.19.2 Estimation of catalase activity

Catalase (CAT) activity was estimated based on the reduction in absorbance of H_2O_2 at 240 nm according to the method described by Aebi (1984). Leaf tissues (100 mg) were homogenized in 1 mL of 50 mM phosphate buffer (pH 7.8). The homogenate was centrifuged at 10000 rpm for 15 min at 4°C and 100 µL of supernatant was added into a 3 mL reaction mixture (3.2 mM H_2O_2 in 50 mM phosphate buffer (pH 7.0) and the resultant mixture was used for assessing absorbance. CAT concentration was calculated based on the formula listed in Appendix D.

3.19.3 Estimation of glutathione reductase activity

Glutathione reductase (GR) activity was determined by the oxidation of NAPDH at 340 nm according to the method described by Smith et al. (1989). Leaf tissues (100 mg) were homogenized in 1 mL of 50 mM phosphate buffer (pH 7.6). The homogenate was centrifuged at 10000 rpm for 15 min at 4°C and 50 µL was added into a 1 mL reaction mixture (1 mM oxidized glutathione, 2 mM NADPH) and used for assessing absorbance. GR concentration was calculated based on the formula listed in Appendix D.

3.19.4 Estimation of guaiacol peroxidase activity

Guaiacol peroxidase (POD) activity was determined by the rate of formation guaiacol dehydrogenation product at 436 nm according to the method described by Pütter (1974). Leaf tissues (100 mg) were homogenized in 1 mL of 100 mM phosphate buffer (pH 7.0). The homogenate was centrifuged at 10000 rpm for 15 min at 4°C and 100 µL was added into a 3 mL reaction mixture (20 mM Guaiacol solution, 12.3 mM H_2O_2) and used for

assessing absorbance. POD concentration was calculated based on the formula listed in Appendix D.

3.19.5 Estimation of ascorbate peroxidase activity

Ascorbate peroxidase (APX) activity was determined by the rate of oxidation of ascorbate at 290 nm according to the method described by Nakano and Asada (1981). Leaf tissues (100 mg) were homogenized in 1 mL of 100 mM phosphate buffer (pH 7.0). The homogenate was centrifuged at 10000 rpm for 15 min at 4°C and 600 µL was added into a 3 mL reaction mixture (5.0 mM Ascorbate, 0.5 mM H_2O_2) and used for assessing absorbance. APX concentration was calculated based on the formula listed in Appendix D.

3.20 Measurement of water loss rate and relative water content

The water loss rate of detached leaves was calculated by weighing freshly harvested leaves and then placing leaves abaxial side up and drying at a constant temperature of 22°C and RH 60%. The percentage of fresh weight loss was calculated after 30, 60, 90 and 120 min, following the method described by Tian et al. (2004). Relative leaf water content was determined according to the method Barrs and Weatherley (1962) by weighing leaf discs prepared from freshly harvested leaf tissue excised from 7 d drought stress-treated greenhouse-acclimatized plants. Leaf discs were placed in distilled water at 4ºC overnight and weighed the next morning to determine the turgid weight (TW). Following that, leaf discs were dried at 70ºC and the dry weight (DW) was determined. RWC was determined using the following formula:

$$RWC = (\text{fresh weight} - \text{dry weight}) \times (\text{turgid weight} - \text{dry weight})^{-1} \times 100.$$

3.21 Measurement of abscisic acid (ABA)

ABA content was measured according to the method described by Teh et al. (2013). Leaf tissues (100 mg) excised from 7 d drought stress-treated greenhouse-acclimatized plants were homogenized in a mixture of 1-propanol: H_2O: conc HCl (2:1:0.002, v/v; 500 µL). The homogenate was agitated at 4°C for 30 min and 1 mL of dichloromethane (CH_2Cl_2) was added, followed by agitation for another 30 min. The reaction mixture was then centrifuged at 14000 rpm for 5 min at 4 °C. Centrifugation separated the mixture into two phases with plant debris suspended between the layers. An aliquot of the lower layer (1 mL) was evaporated using a Genevac (Ipswich, United Kingdom) evaporator. The dry extracts were resolubilized in 300 µL methanol and ABA content was analysed in triplicate using a Waters Acquity (Massachusetts, United States) LC-MS. The separation was done using a reversed-phase C18 (1.8 µM, 2.1 × 100 mM; Waters) column set at 30 °C with corresponding solvent A (H_2O with 0.1% formic acid v/v), and solvent B (MeOH with 0.1% formic acid v/v); the flow rate was 0.3 mL/min. The gradient was as follows: 30% B (0−2 min), linearly increased to 100% B at 20 min. The autosampler temperature was set at 4 °C with a 3.0 µL injection volume. MS analysis was carried out on a Xevo TQs triple quadrupole mass spectrometer (Waters Corporation, Milford, MA). MS analysis was carried out in negative ion electrospray ionization modes of detection. The electrospray ionization capillary voltage on both modes was set at 2.5 kV, with the cone gas flow set at 150 L/ h, and desolvation temperature of 350 °C. The collision gas flow was set at 0.15 mL/min. The total acquisition duration for both UPLC and MS was set at 15 and 5 min, respectively.

3.22 Statistical analysis

All statistical analyses were performed using SPSS Version 24.0 for Windows (SPSS Inc., Chicago, IL, USA). The significant difference was analysed by two-tailed t-test. Multiple comparisons were performed with the Tukey HSD test (Tukey, 1949) ($P \leq 0.05$ was considered as significant).

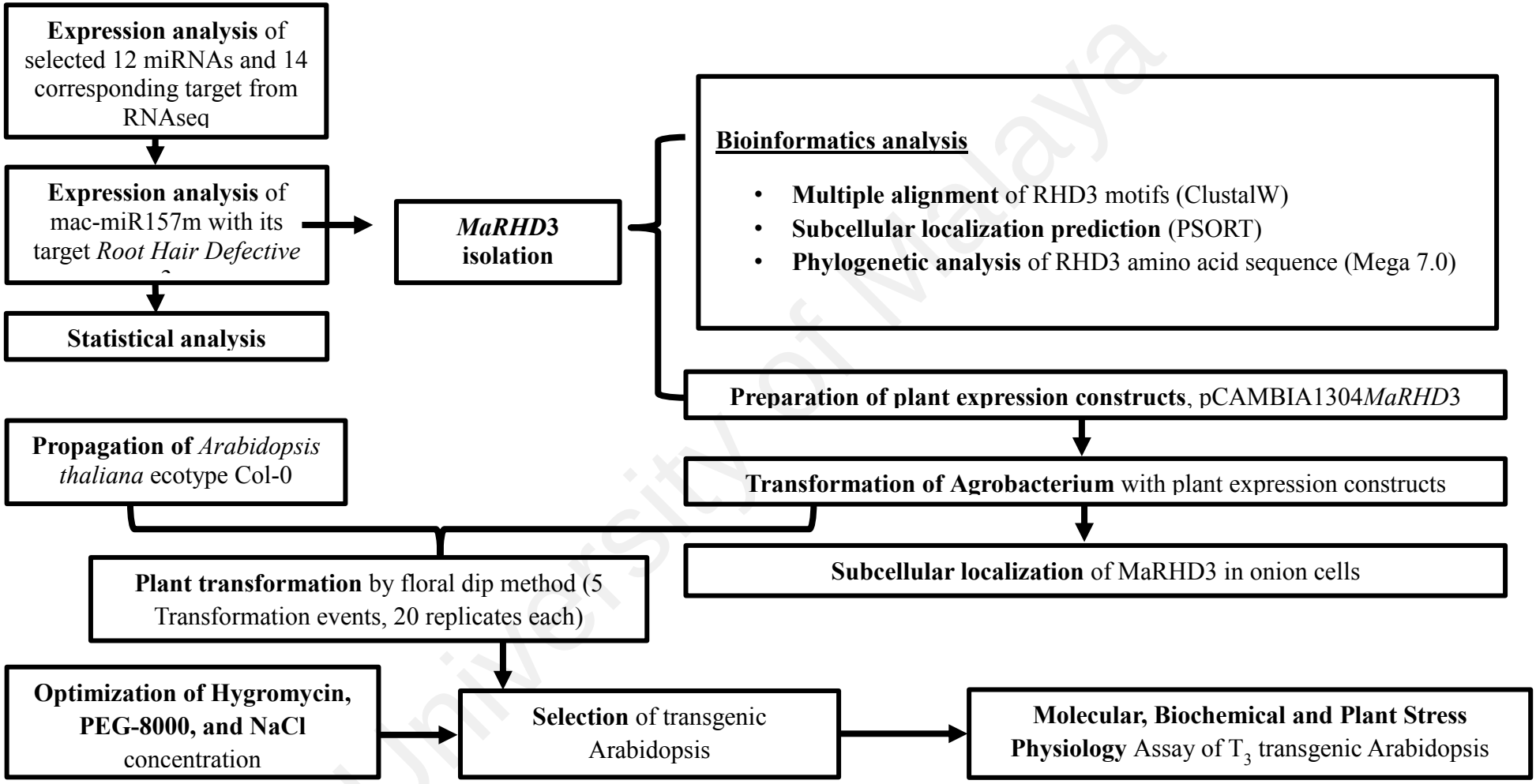

Figure 3.3: Summary of the experimental workflow of this study.

CHAPTER 4: RESULTS

4.1 Quantification of miRNAs and their predicted target mRNAs showed similar differential expression pattern in response to salt stress as predicted with RNAseq

A previous study by the research group at the University of Malaya, predicted differential expression of several banana miRNA and their corresponding target mRNA in response to salt stress, based on analysis of RNAseq transcriptome data (Lee et al., 2015). As part of this thesis study, the expression pattern of 12 selected miRNA and 14 predicted target mRNAs were determined using an RT-qPCR approach. The 12 miRNAs and 14 predicted target mRNAs are listed in Table S5 (Appendix G) and includes 6 plant orthologous miRNAs (mac-miR156, mac-miR157m, mac-miR159c, mac-miR159g, mac-miR162b.2, and mac-miR168) and 6 Musa-specific miRNAs (mac-miR6, mac-miR19, mac-miR37, mac-miR49, mac-miR62 and mac-miR66). RT-qPCR profiles showed that most of the miRNAs and their target mRNA showed similar fold changes in gene expression patterns to those determined from RNAseq data (Figure 4.1). For mac-miR157m, mac-miR159c, mac-miR159g, mac-miR162b.2m, mac-miR6, mac-miR19, mac-miR37, and mac-miR49 (Figure 4.1B, C, D, E, G, H, I and J) fold changes were in the same direction for both RNAseq data (Lee et al., 2015) and by RT-qPCR (current thesis and also reported in Lee et al., 2015) with only 2 out of 12 miRNAs (mac-miR168 and mac-miR62) and 5 of the miRNA-target (Avr9/Cf-9 rapidly, Tropine dehydrogenase, 1,2-oxophytodienoate reductase, protein IQ-domain 1-like and DEAD-like helicase) showing different expression patterns between PCR and RNAseq data (Fig 4.1A, F, K and L). Dissociation curves for all target genes are shown in Figure S5 and S6 (Appendix C). The remaining part of this thesis focused on the functional analysis of one of the candidate stress responsive mRNA, *MaRHD3,* a target of miRNA mac-miR157m.

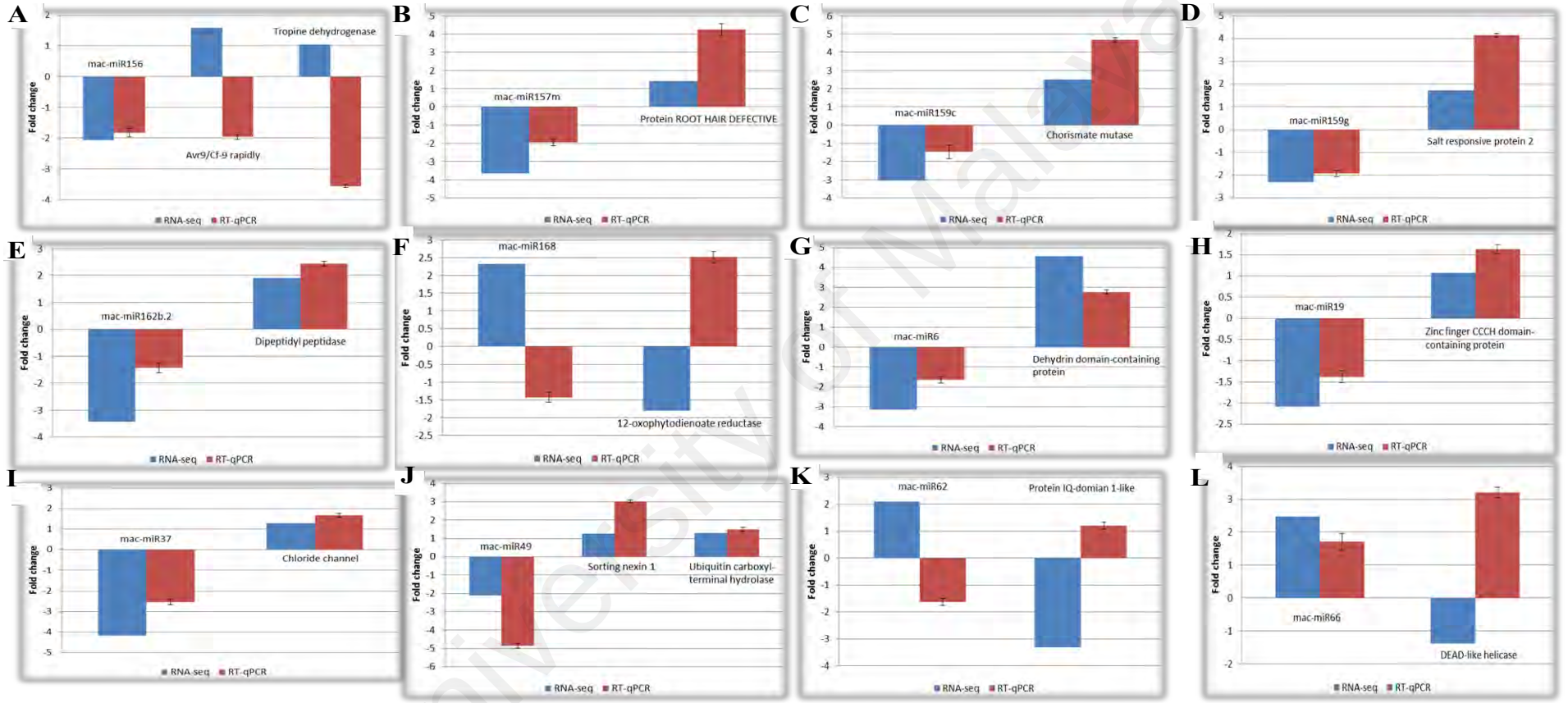

Figure 4.1: Change in expression of selected miRNAs and their corresponding target mRNA in banana roots following 300 mM NaCl treatment. MiRNAs and their predicted corresponding target mRNA were arranged in miRNA and miRNA target(mRNA) pairs for each panel, with panels (A)-(F) showing the plant orthologous miRNA and mRNA targets; and panels (G)-(L) showing *Musa* specific miRNA and mRNA targets. Fold changes in gene expression shown are relative to the expression in the non-stressed roots (control). RNAseq and RT-qPCR data are both shown in a linear scale. Errors bars indicate mean ± standard deviations obtained from three biological replicates for PCR data (shown in red). Blue bars represented RNAseq data (n=3). RT-qPCR results from this thesis were used to compared RNAseq data prediction done by previous PhD student and published in Lee et al. (2015).

4.2 Bioinformatics analysis of the MaRHD3 protein

Sequence analysis confirmed *MaRHD3* cDNA to be identical to the sequence reported from a salt treated transcriptome of *Musa acuminata* cv. Berangan (Sequence Read Archive, SRX535341, NCBI; Lee et al., 2015). *MaRHD3* cDNA showed 99% identity by alignment using ClusterW with the *RHD3* cDNA reported for another cultivar of *Musa acuminata* cv. Malaccensis (XP_009389470.1) as shown in Figure S8 (Appendix F). The predicted MaRHD3 protein has 807 amino acid residues with an estimated molecular mass of 89.7 kDa and an isoelectric point of 5.63. Amino acid alignment by MEGA 7.0 of the MaRHD3 with orthologues showed a closer evolutionary relationship with non-grass monocots oil palm and date palm compared to the grass monocots maize, foxtail millet, and wheat and to the dicots Arabidopsis and poplar (Figure 4.2). MaRHD3 protein was predicted by PSORT, to be cytoplasmic localized (89% reliability) with a lower likelihood of localisation to the endoplasmic reticulum (43.5%), mitochondria (34.8%), nucleus (17.4%) or vesicles (4.3%). No KDEL (ER retention motif), SKL (peroxisomal targeting signal) or VAC (possible vacuolar targeting motif) signal peptide sequences were observed in the C-terminus of the protein sequence (Table 4.1).

Multiple alignment analysis by ClusterW of the MaRHD3 protein sequence with orthologues confirmed MaRHD3 to contain five signatory G domains (G1–G5 motifs) essential for G protein-mediated signal transduction, consistent with other guanine nucleotide-binding proteins (G proteins) (Figure 4.3). These included the Walker A (G1) and B (G3) motifs (Walker et al., 1982); a T effector region (known as GTP binding region to initiate hydrolysis as reviewed in Wittinghofer and Vetter, 2011) (G2); the NKXD (NKDLDLP) motif known for conferring GTP binding specificity, predicted by Wang et al. (1997) as NKDLDLP motifs in Arabidopsis RHD3 protein due to structural resemblance (G4) and a weakly conserved SAK/L motif (G5) known for its stabilizing

function (Anand et al., 2006). Additionally, an RHD3 family specific conserved motif, FVIRD (Xu et al., 2012; Wang et al., 1997), with unknown function, was located at amino acids 167 to 171 (Figure 4.3).

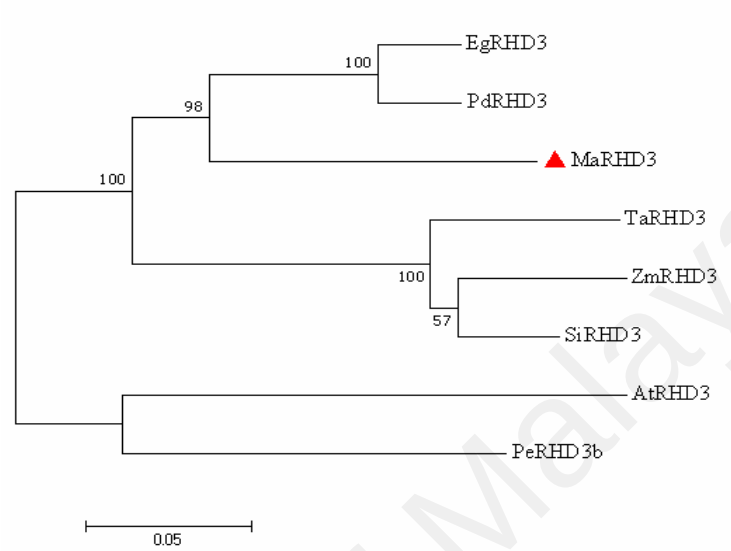

Figure 4.2: Phylogenetic relationship of full-length MaRHD3 proteins. Support values from a bootstrap analysis by MEGA 7.0 with 1000 replicates were used to ensure statistical reliability of each node. Alignment based on putative amino acid sequences of RHD3 from banana (XP_009389470.1), oil palm (XP_010925000.1), date palm (XP_008807967.1), maize (XP_008657782.1), wheat (AAS67855.2), foxtail millet (XP_012704194.1), Arabidopsis (NP_177439.2), and poplar (XP_002327435.1).

Table 4.1: Subcellular localization prediction of MaRHD3 protein by PSORT

Gene	Accession Number	Localization	Reliability (%)	ER membrane retention signals
AtRHD3	NP_177439.2	Cytoplasmic	76.7	SSKE
EgRHD3	XP_010925000.1	Cytoplasmic	76.7	-
MaRHD3	XP_009389470.1	Cytoplasmic	89	-
PdRHD3	XP_008807967.1	Cytoplasmic	76.7	-
PeRHD3b	XP_002327435.1	Nuclear	55.5	TLKD
SiRHD3	XP_012704194.1	Cytoplasmic	76.7	-
TaRHD3	AAS67855.2	Cytoplasmic	70.6	-
ZmRHD3	XP_008657782.1	Cytoplasmic	89	-

The RHD3 sequences were predicted based on https://www.genscript.com/psort.html

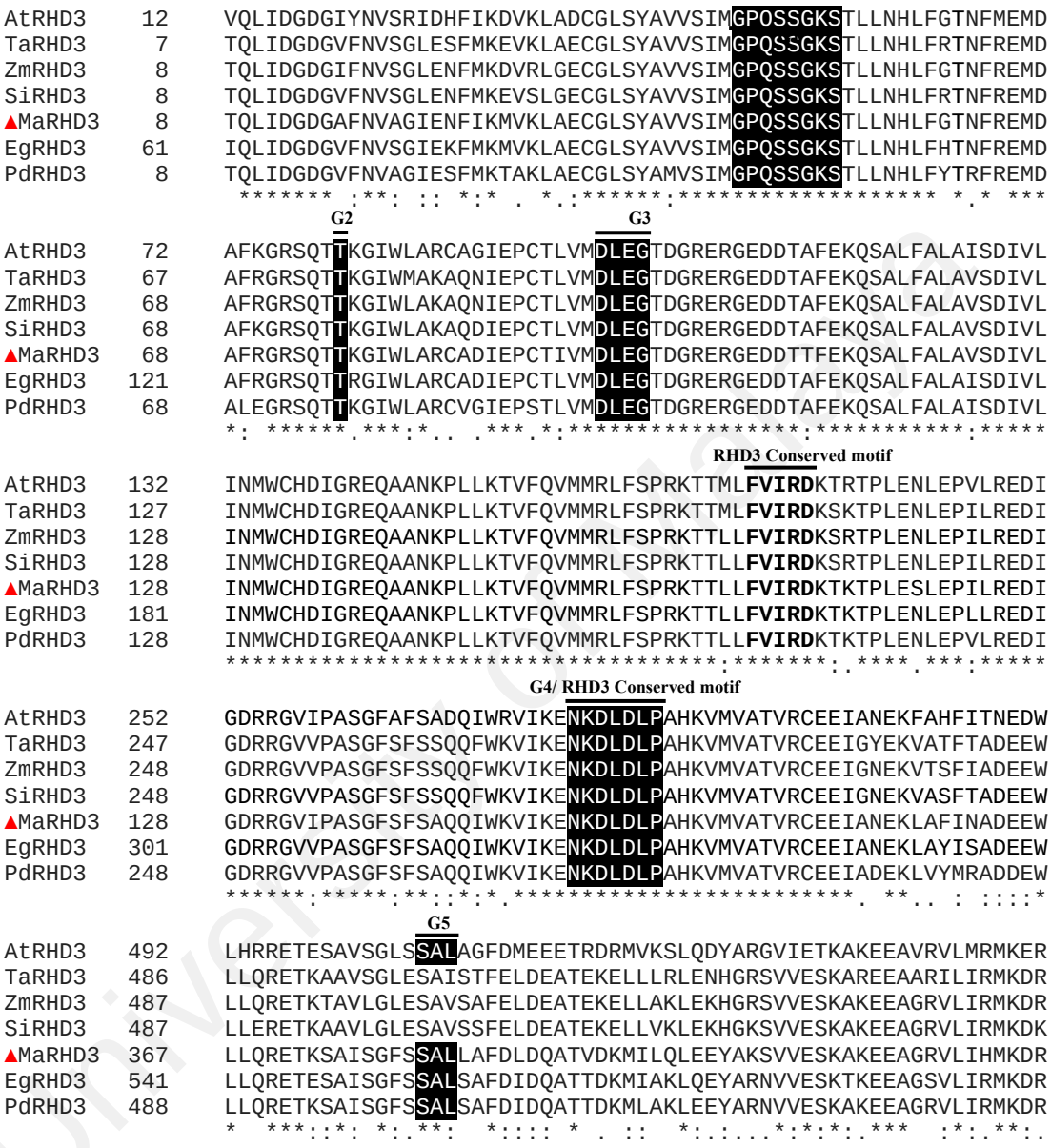

Figure 4.3: Multiple alignments of RHD3 amino acid sequences. MaRHD3 (XP_009389470.1) was aligned by ClusterW with the RHD3 annotated amino acid sequences of oil palm (XP_010925000.1), date palm (XP_008807967.1), maize (XP_008657782.1), wheat (AAS67855.2), foxtail millet (XP_012704194.1), and Arabidopsis (NP_177439.2). Five signatory G domains (G1-G5 motifs) are highlighted in black: G1:GXXXXGKS; G2:T; G3:DXXG; G4:NKDLDLP; G5: SAK/L and a unique conserved amino acid motif for RHD3 family (FVIRD) is highlighted in bold.

4.3 *MaRHD3* cDNA successfully cloned into pCAMBIA1304

4.3.1 Quality of RNA from 300 mM NaCl treated banana root tissues and *MaRHD3* cDNA isolation

RNA isolated from 300 mM treated banana roots showed a good quality of 28S rRNA and 18S rRNA bands on an agarose gel (Figure 4.4A). Full length of *MaRHD3* cDNA amplified from the RNA with *MaRHD*3 specific primers produced a product of the expected size of 2424 bp (Figure 4.4B). Colony PCR of the *MaRHD*3 cDNA (Figure 4.5A) ligated into pEASY®-T1 (TransGene Biotech, China) and transformed into *E. coli* produced bands of the expected size of 2424 bp (Figure 4.5C). Sequencing results showed 99.0% similarities in nucleotide sequences between the fragment cloned into the plasmid and the *MaRHD*3 sequence in Genbank database (XM_009397509.2) (Figure S1, S2, S3 and S4, Appendix B)

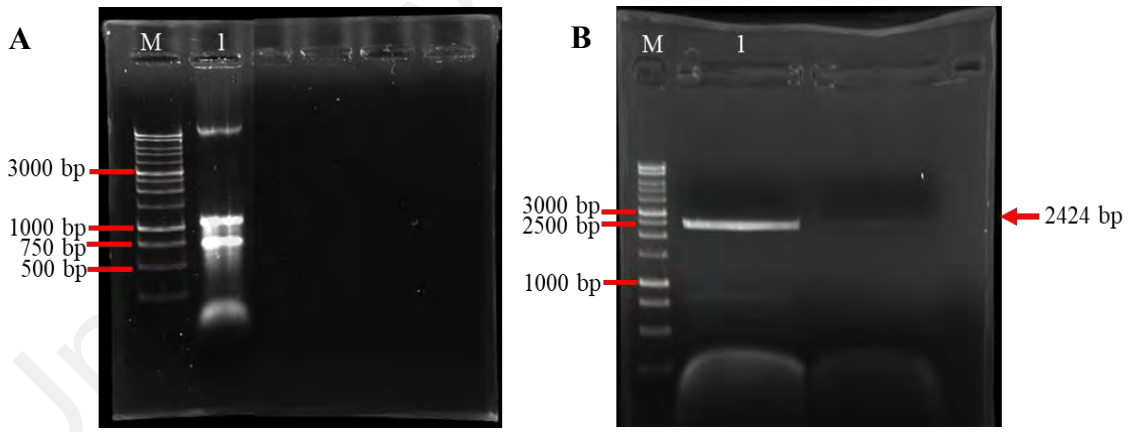

Figure 4.4: Agarose gel electrophoresis of total RNA and *MaRHD3* cDNA amplified from 300 mM NaCl treated banana root. (A) Total RNA extracted using CTAB method from 300 mM NaCl treated banana roots run on 0.7% agarose gel at 100 V for 30 min. Lane M: 1kb DNA ladder marker (Promega); Lane L1: Total RNA extracted from 300 mM NaCl treated banana root. (B) Agarose gel electrophoresis of full-length cDNA of *MaRHD3* (2424 bp) amplified from 300 mM salt-treated banana root tissues run on 0.7% agarose gel at 100 V for 30 min. Lane M: 1kb DNA ladder marker (Promega); Lane L1: *MaRHD3* cDNA amplified from 300 mM NaCl treated banana root.

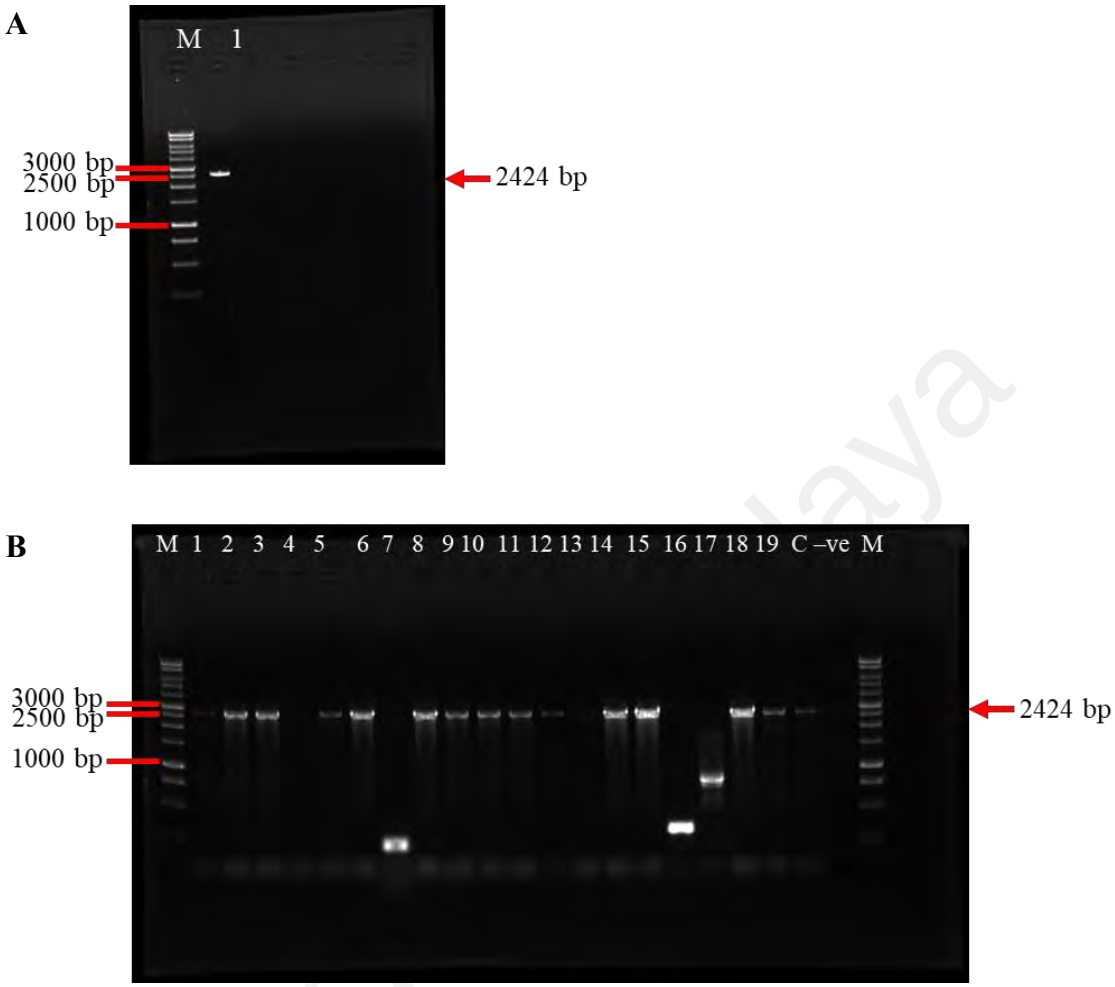

Figure 4.5: Agarose gel of purified *MaRHD3* cDNA, colony PCR of pEASY®-T1 harbouring *MaRHD3* cDNA, and plasmid DNA of pEASY®-T1 harbouring *MaRHD3* cDNA. (A) Purified *MaRHD3* cDNA (2424 bp) excised from PCR amplification of *MaRHD3* cDNA (Figure 4.4 B) on 0.7% agarose gel at 100 V for 30 min. Lane M: 1kb DNA ladder marker (Promega); Lane L1: Purified *MaRHD3* cDNA. (B) Colony PCR of pEASY®-T1 harbouring *MaRHD3* cDNA from transformed the *E. coli* competent cells. Lane M: 1kb DNA ladder marker (Promega); Lane L1-19: PCR of bacterial colonies with specific *MaRHD3* primers; Lane C: *MaRHD3* cDNA as positive control; Lane –ve; PCR without bacterial colony as negative control.

4.3.2 Cloning of *MaRHD3* cDNA into constitutive plant expression vector pCAMBIA1304

pEASY®-T1 vector harbouring *MaRHD3* and pCAMBIA1304 were double digested with *Bgl*II and *Spe*I (NEB, UK) and a band of the expected size of 2424 bp from pEASY®-T1 vector harbouring *MaRHD3* was observed on agarose gel (Figure 4.6A) while only single band was showed for pCAMBIA1304 (Figure 4.6B). The digested 2424 bp fragment of *MaRHD3* was purified and ligated into the *Bgl*II and *Spe*I-digested pCAMBIA1304. Putative *E. coli* competent cells harbouring recombinant clones were screened by colony PCR (Figure 4.6C) and positive recombinant clones of pCAMBIA1304*MaRHD3* were reconfirmed by digestion using *Bgl*II and *Spe*I, which produced a band of the expected size of 2424 bp on an agarose gel (Figure 4.7). pCAMBIA1304*MaRHD3* was mobilized in Agrobacterium and colony PCR with gene-specific forward primer and GFP reverse primer showed bands of the expected size of 3159 bp (Figure 4.7).

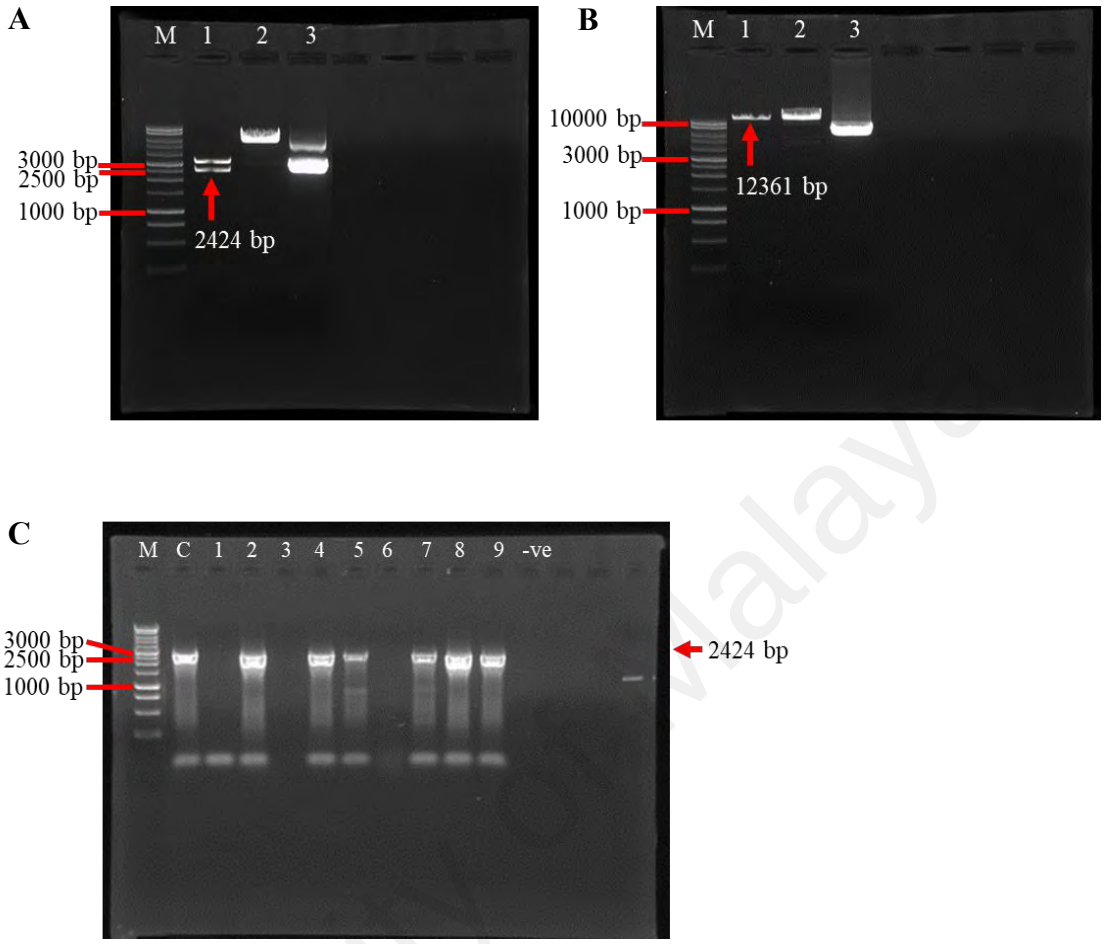

Figure 4.6: Agarose gel of plasmid DNA of *MaRHD3* in pCAMBIA1304. (A) Confirmation of pEASY®-T1_*MaRHD3* by double digestion using *Bgl*II and *Spe*I. Lane M: 1kb DNA Ladder (Promega); Lane1: Digestion of pEASY®-T1_*MaRHD3* with *Bgl*II and *Spe*I; Lane 2: Digestion of pEASY®-T1_*MaRHD3* with *Bgl*II; Lane 3: Uncut pEASY®-T1_*MaRHD3* as negative control. (B) Digestion of pCAMBIA1304 with *Bgl*II and *Spe*I. Lane M: 1Kb DNA Ladder (Promega); Lane 1: Digestion of pCAMBIA1304 with *Bgl*II and *Spe*I; Lane 2; Digestion of pCAMBIA1304 with *Bgl*II; Lane 3: Uncut pCAMBIA1304 as negative control. (C) Colony PCR of pCAMBIA1304 harbouring *MaRHD3* cDNA from transformed *E. coli* competent cells. Lane M: 1kb DNA ladder marker (Promega); Lane L1-9: PCR of bacterial colonies with specific *MaRHD3* primers; Lane C: *MaRHD3* cDNA as positive control; Lane –ve; PCR without bacterial colony as negative control.

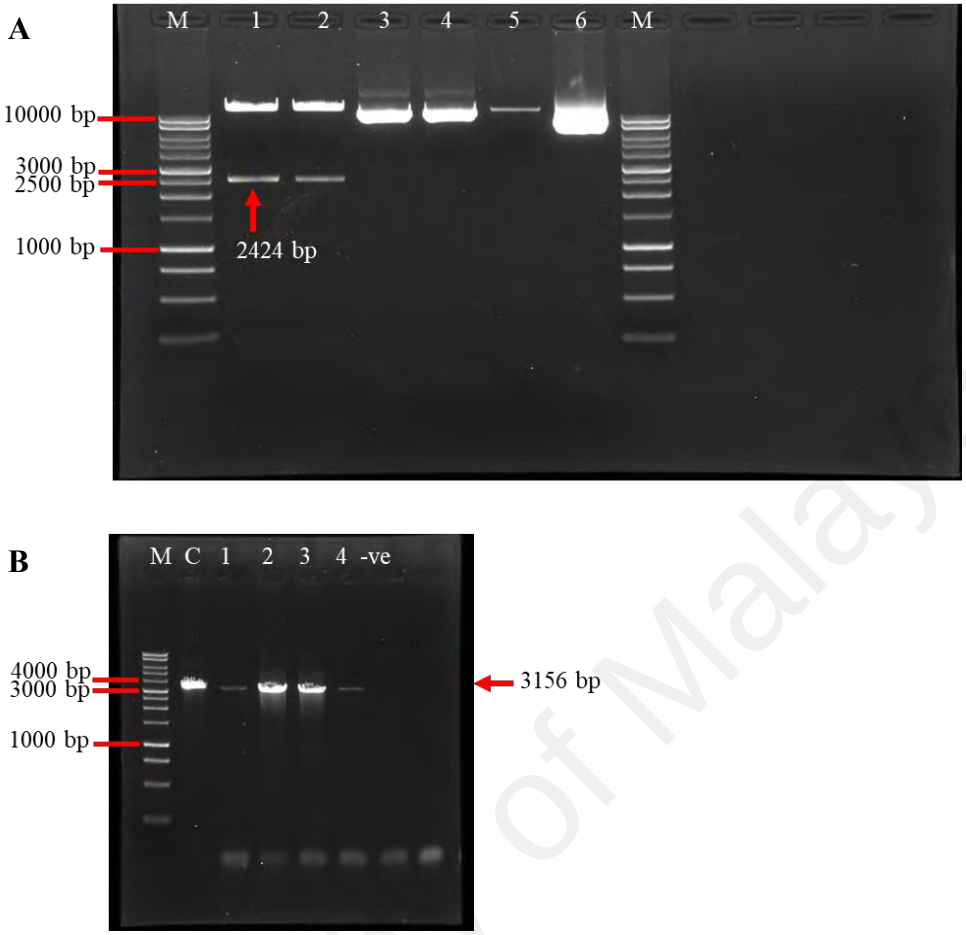

Figure 4.7: Confirmation of *MaRHD3* in pCAMBIA1304 and colony PCR of Agrobacterium transformed with pCAMBIA1304*MaRHD3*. (A) Confirmation of *MaRHD3* cDNA positive clones in pCAMBIA1304 by digestion of plasmid DNA of positively screened colony PCR by *Bgl*II and *Spe*I. Lane M: 1kb DNA Ladder (Promega); Lane1-2: Digested positive PCR colonies harbouring pCAMBIA1304*MaRHD3* plasmid DNA with *Bgl*II and *Spe*I; Lane 3-4: uncut pCAMBIA1304*MaRHD3* colony 1; Lane 5: Digestion of pCAMBIA1304 with *Bgl*II and *Spe*I; Lane 6: uncut pCAMBIA1304. (B) Colony PCR on Agrobacterium transformed with pCAMBIA1304*MaRHD3*. Lane M: 1kb DNA Ladder (Promega); Lane C: pCAMBIA1304 plasmid as positive control; Lane 2-4: PCR of bacterial colonies with specific *MaRHD3* forward primer and GFP reverse primer; Lane 6: PCR with pCAMBIA1304 as negative control.

4.4 Subcellular localization showed MaRHD3 protein localized in the cytoplasm

To identify the localization of MaRHD3 in plant cells, pCAMBIA1304*MaRHD3* was localized in onion epidermal cells. Confocal microscopy showed that the fluorescence signal of the fusion protein MaRHD3-GFP was only detected in the cytoplasm, while the positive control GFP was observed to be uniformly distributed throughout the cytoplasm and nucleus of the cell (Figure 4.8) in agreement with the subcellular localization prediction obtained from PSORT software (Table 4.1).

Construct	Fluorescence	Bright Field	Merge
pCAMBIA1304*MaRHD3*	(A) 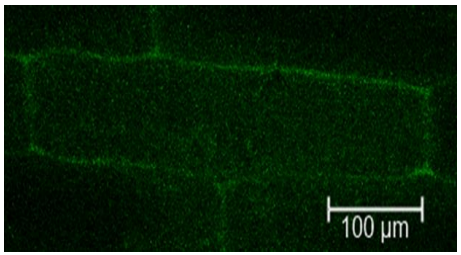	(B) 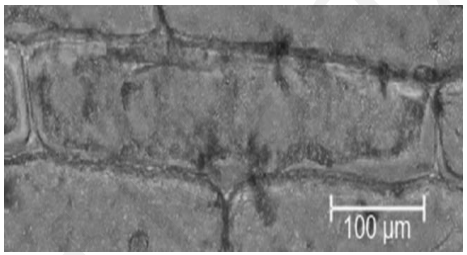	(C) 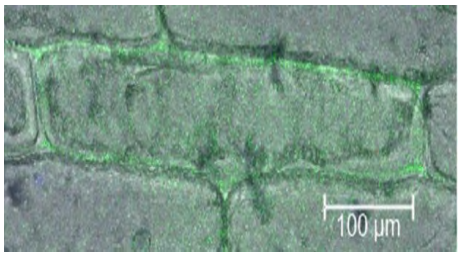
pCAMBIA1304	(D) 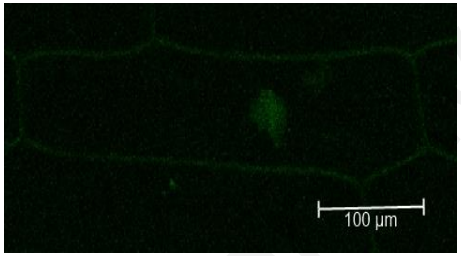	(E) 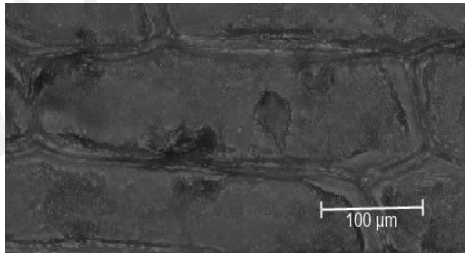	(F) 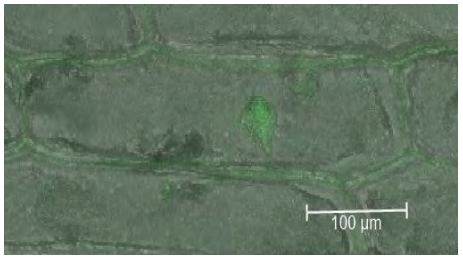

Figure 4.8: Subcellular localization of MaRHD3 in onion epidermal cell. The full-length coding region of *MaRHD3* fused with N-terminus GFP protein (pCAMBIA1304*MaRHD3*) and EV (pCAMBIA1304) were localized in onion epidermal cells. Localization of pCAMBIA1304*MaRHD3* (A-C); Localization of pCAMBIA1304 (positive control) (D-F); (A, D) in onion epidermal cell under 488 nm excitation light; (B, E) onion cell under bright field; (C, F) GFP in the onion cell of overlaid images; Scale bar = 100 µm.

4.5 Successful transformation of Arabidopsis with pCAMBIA1304*MaRHD3*

4.5.1 PCR, GUS expression and *MaRHD3* transcript analysis showed successful transformation of T_1 Arabidopsis with pCAMBIA1304*MaRHD3*

In order to investigate the biological role of *MaRHD3* in abiotic stress, the coding sequence of *MaRHD3* was placed under the control of a constitutive promoter (35SCaMV) into the Arabidopsis genome *via* Agrobacterium-mediated floral dip transformation. The T_1 seeds from nine transformed plants were screened in optimized hygromycin media (20 mg/L, Figure 4.9). A 0.2-2.4% transformation efficiency was observed (Table 4.2).

Nine PCR positive transgenic Arabidopsis T_1 lines (L1-9) (Figure 4.10A and B) randomly selected from the plants survived on hygromycin selective media, displayed strong and uniform GUS expression in leaf, flower and root tissues (Figure 4.11 I-III). No endogenous GUS expression was detected in WT tissues (Figure 4.11 IV-VI) ruling out the possibility of endogenous GUS expression. The accumulation of *MaRHD3* transcripts was confirmed in 5 randomly chosen PCR positive transgenic lines by reverse transcriptase-PCR analyses (Figure 4.12).

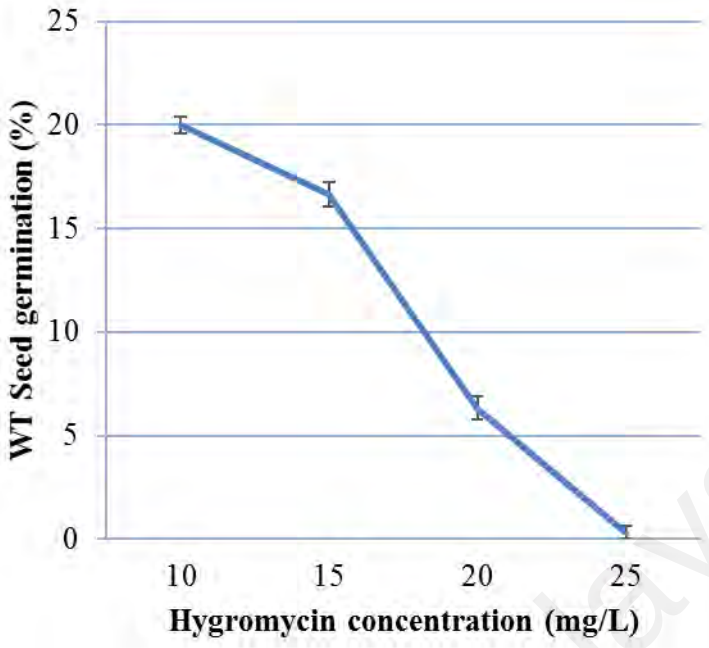

Figure 4.9: Sensitivity test of hygromycin for optimization of threshold value on wild type (WT) Arabidopsis seeds for 14 days. Sensitivity to hygromycin was tested at 10 mg/L, 15 mg/L, 20 mg/L and 25 mg/L. Data are means (±S.E.) of three replicates (each with 100 seeds).

Table 4.2: Hygromycin Screening of Arabidopsis seeds after floral dip transformation

*Lines	Number of plants surviving on hygromycin media	Transformation efficiency (%)
L1	15	1.5
L2	24	2.4
L3	10	1
L4	23	2.3
L5	21	2.1
L6	5	0.5
L7	2	0.2
L8	10	1
L9	9	0.9

*Each line produced 1000 seeds

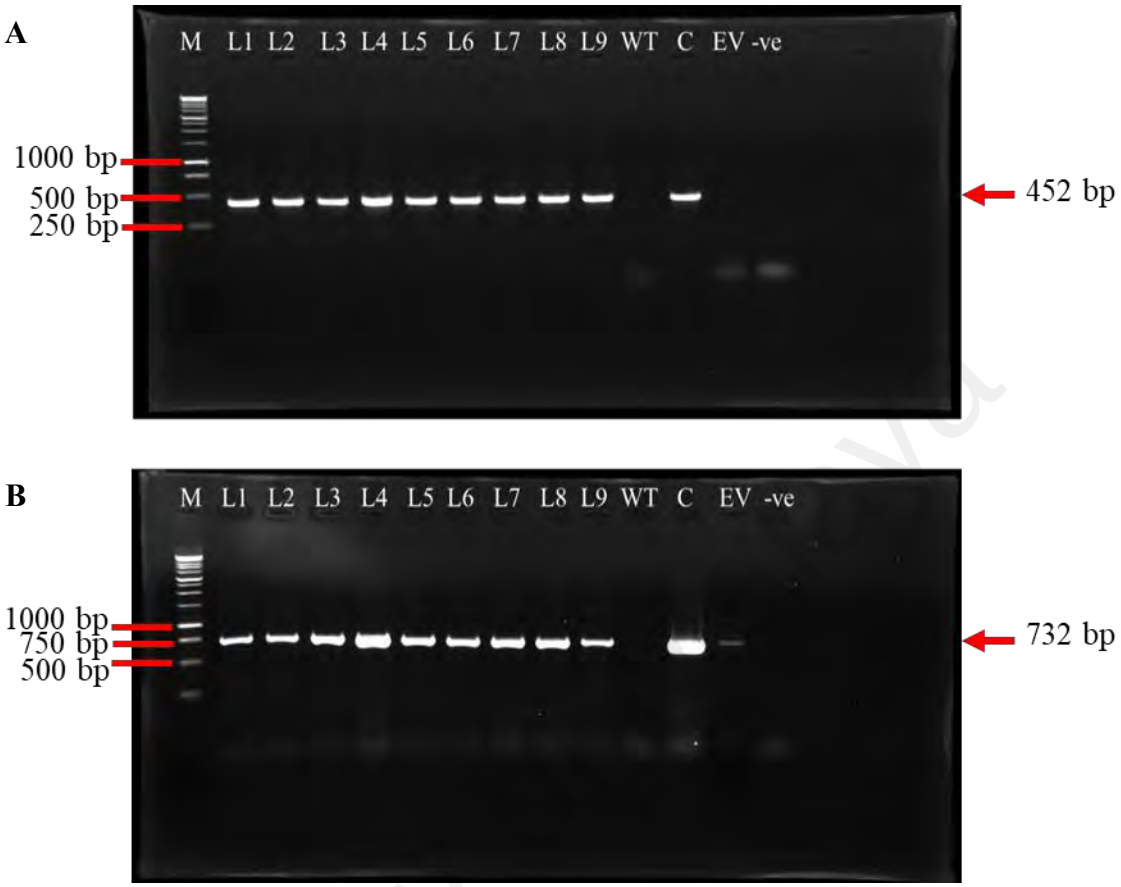

Figure 4.10: Agarose gel electrophoresis of T1 Arabidopsis lines transformed with *MaRHD3*. Agarose gel electrophoresis of PCR products using *MaRHD3* specific primer (A) and *GFP* primer (B); Lane M: 1kb DNA ladder marker (Promega); Lane L1-L9: genomic DNA from T_1 putative transgenic lines transformed with pCAMBIA1304*MaRHD3*, showing expected amplicon size of 452 bp (A, *MaRHD3*) and 732 bp (B, GFP); Lane WT: wild type plant negative control; Lane P: Plasmid DNA pCAMBIA1304*MaRHD3* amplification as positive control; Lane EV: pCAMBIA1304 transformed Arabidopsis; Lane -ve: PCR control (blank).

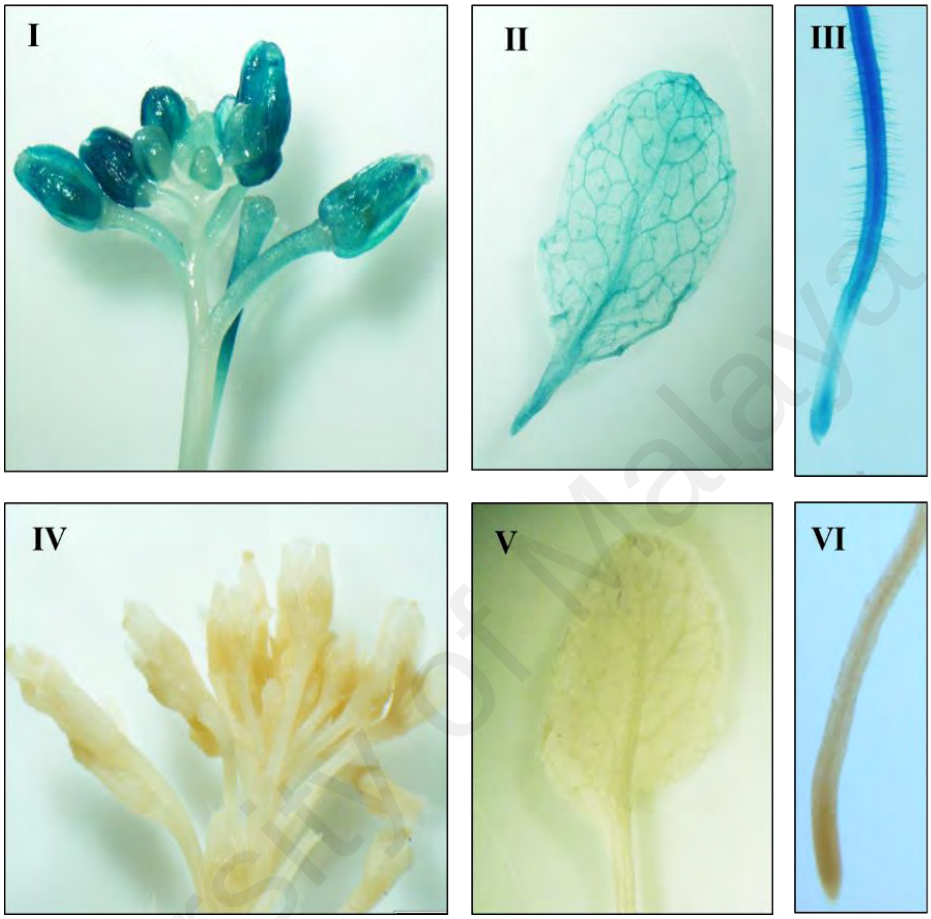

Figure 4.11: GUS Histochemical staining of tissues of T_1 transgenic Arabidopsis expressing *MaRHD3*. I, II and III: GUS activity in flower, leaf and root tissues of T_1 transgenic Arabidopsis expressing *MaRHD3*. IV, V, VI: GUS activity in flower, leaf and root tissues of wild-type Arabidopsis.

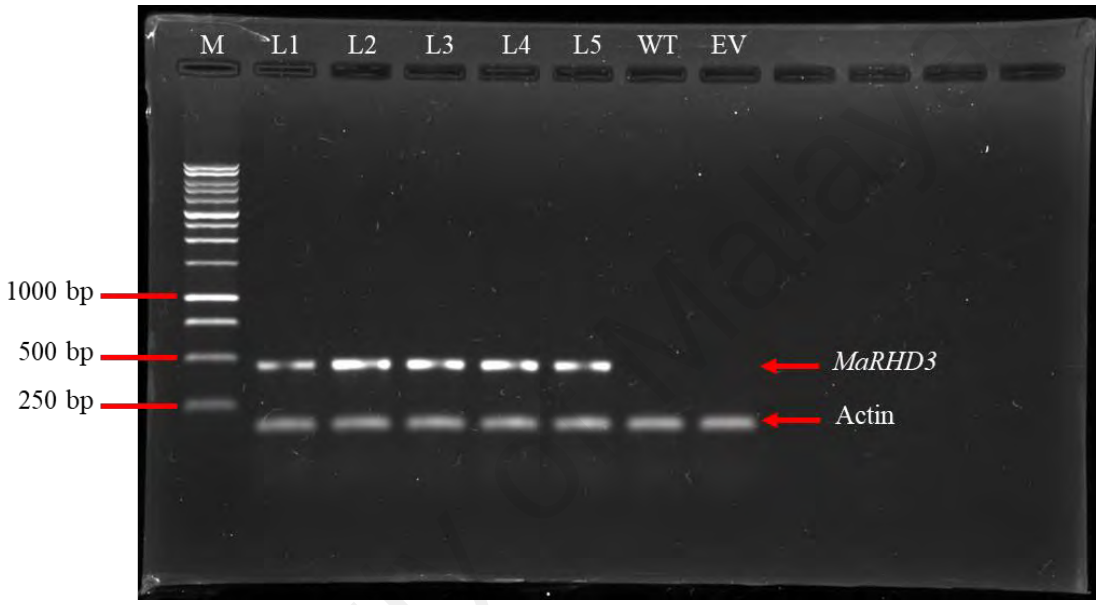

Figure 4.12: Transcript analysis of *MaRHD3* and reference gene Actin by reverse transcriptase PCR. Lane M: 1kb DNA ladder marker (Promega); Lane L1-L5: cDNA from PCR positive T_1 transgenic lines with expected size 452 bp for *MaRHD3* and 100 bp for Actin; Lane WT: wild-type (negative control); Lane: pCAMBIA1304 transformed Arabidopsis (negative control).

4.5.2 DNA gel blot hybridization showed single integration event of *MaRHD3* cDNA in T_1 transgenic Arabidopsis and PCR confirmed T_2 transgenic Arabidopsis harbouring *MaRHD3* cDNA

Examination of copy number of *MaRHD3* integrated into the Arabidopsis genome using DIG-labelled *hptII* probe showed differential integration patterns, confirming that the four lines examined, derived from independent transformation events (Figure 4.13) with three T_1 lines showing single integration events (L1, L3, and L4). No hybridization signal was detected for WT (Figure 4.13, lane WT). Hygromycin screening of T_2 seeds showed segregation followed a Mendelian ratio of 3:1 for the single integration events (Table 4.3). Seeds of nine randomly chosen PCR positive T_2 lines (Figure 4.14) were further screened in hygromycin to obtain T_3 lines. Three independent single integration T_3 lines (L1.11, L3.16, and L4.13) were randomly chosen from the four T_1 transgenic lines with single integration events were confirmed to show *MaRHD3* transcript expression by RT-qPCR (Figure 4.15) and homozygous seeds from T_3 lines were used for further stress challenge.

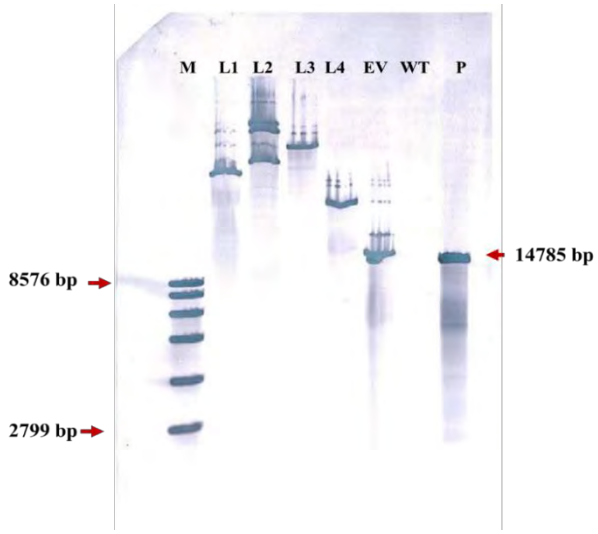

Figure 4.13: DNA gel blot hybridization of T_1 transgenic Arabidopsis. Four randomly selected T_1 lines were examined. Lane M: DIG-labelled DNA molecular weight marker VII (Roche Diagnostics, USA); Lane L1-L4: genomic DNA from PCR positive T_1 transgenic lines, Lane EV: pCAMBIA1304 transformed Arabidopsis, Lane WT: wild-type, Lane P: Plasmid DNA pCAMBIA1304*MaRHD3* control.

Table 4.3: Summary of hygromycin screening of T_2 transgenic Arabidopsis lines transformed with pCAMBIA1304*MaRHD3*

Line	Total of seeds used for hygromycin screening	Number of plants surviving on hygromycin media	Percentage of surviving (%)
L1.1	304	230	75
L1.2	294	212	72
L2.1	281	200	71
L3.1	296	225	76
L3.2	274	190	69
L3.3	299	211	71
L4.1	284	215	76
L4.2	296	204	69
L4.3	287	189	66

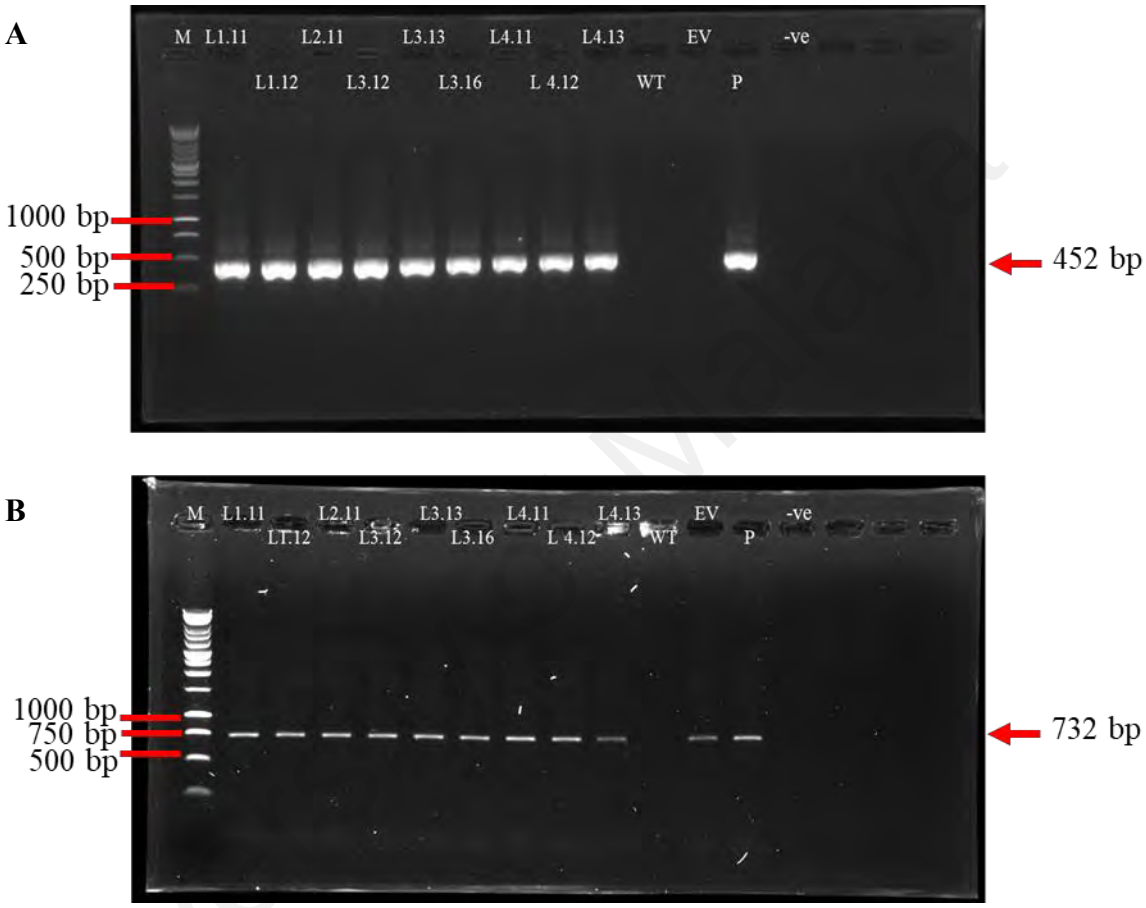

Figure 4.14: Agarose gel electrophoresis of T_2 Arabidopsis lines transformed with *MaRHD3*. Agarose gel electrophoresis of PCR products using *MaRHD3* specific primer (A) and *GFP* primer (B); Lane M: 1kb DNA ladder marker (Promega); Lane L1-L9: genomic DNA from T_2 Arabidopsis transgenic lines transformed with pCAMBIA1304*MaRHD3*, showing expected amplicon size of 452 bp (A, *MaRHD3*) and 732 bp (B, GFP); Lane WT: wild type plant negative control; Lane P: Plasmid DNA pCAMBIA1304*MaRHD3* amplification as positive control; Lane EV: pCAMBIA1304 transformed Arabidopsis; Lane -ve: PCR control (blank).

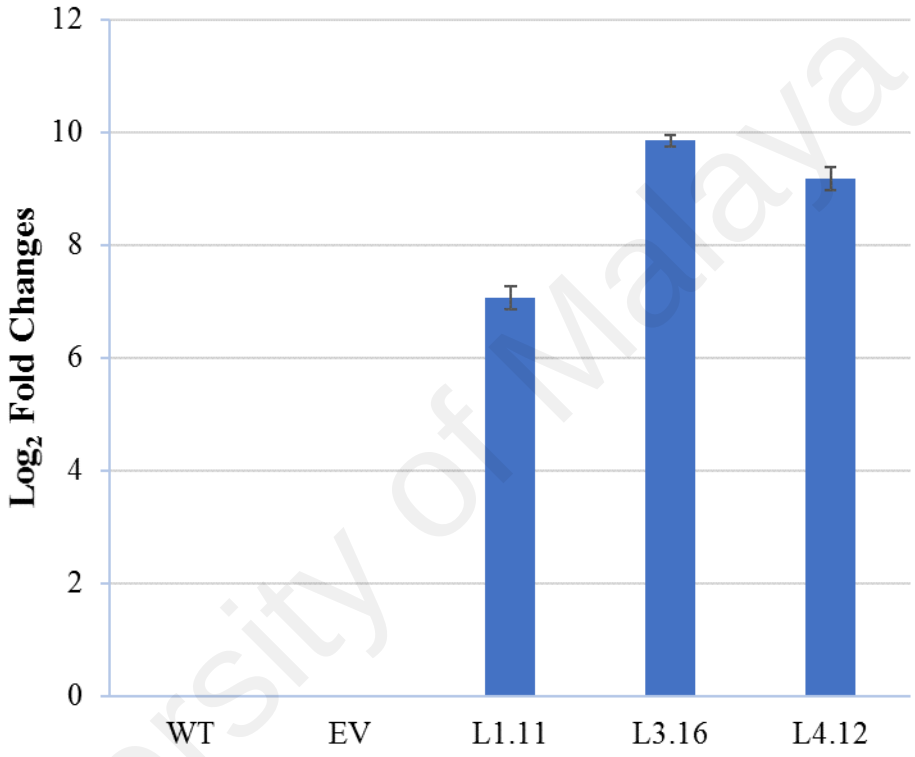

Figure 4.15: Quantification of *MaRHD3* in T_3 transgenic Arabidopsis by RT-qPCR. Expression levels of the *MaRHD3* in T_3 Arabidopsis lines (L1.11, L3.15, L4.12), as determined by RT-qPCR. The values are the means (± SE) of three replicates. Relative expression (Log_2 ratios) of *MaRHD3* was obtained by normalized C_T values of *Actin* (endogenous control), relative to the calibrator (WT; ration=0.0). Bars indicate standard error from amplification of the *MaRHD3* cDNA samples (n = 3).

4.6 Arabidopsis expressing *MaRHD3* do not show improvement in germination and survival rates under salt stress

4.6.1 Salt sensitivity test of wild type Arabidopsis seeds showed 150 mM of NaCl as an effective concentration for salt stress assay for transgenic Arabidopsis

In order to evaluate the threshold value of used for salt stress assay, NaCl concentration was optimized using wild-type Arabidopsis seeds for a period of 14 d (100 seeds from each line). Wild-type Arabidopsis seeds showed 83% germination rate in 50 mM of NaCl for 14 d. As the concentration increased to 100 mM and 150 mM of NaCl, germination rate of wild-type Arabidopsis was reduced to 53% and 10% respectively. At the highest concentration (200 mM of NaCl), wild-type Arabidopsis seeds showed 0% germination rate (Figure 4.16).

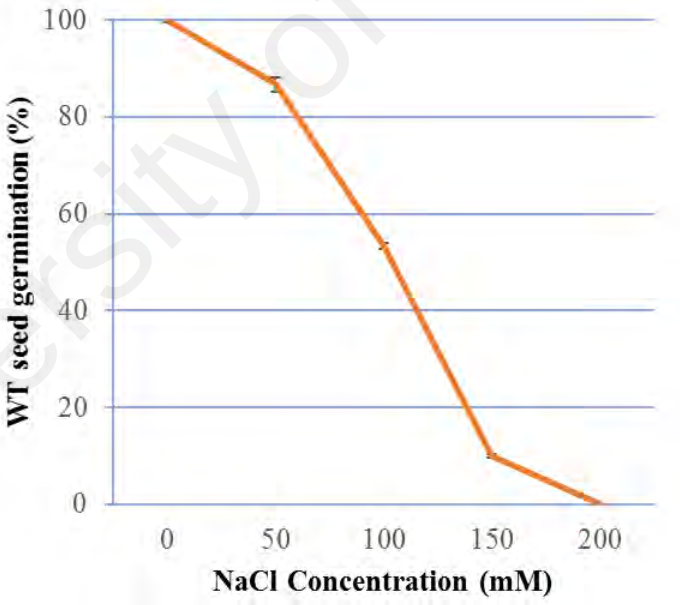

Figure 4.16: Sensitivity test of NaCl for optimization of threshold value on wild type (WT) Arabidopsis seeds for 14 days. Sensitivity test of NaCl was tested in four different concentrations which are 50 mM, 100 mM, 150 mM and 200 mM, 0 mM as control. Data are means (±S.E.) of three replicates (each with 100 seeds).

4.6.2 Germination rate of T_3 transgenic Arabidopsis seeds, Wild-type Arabidopsis seeds and pCAMBIA1304 transformed Arabidopsis seeds showed no significant improvement under 150 mM NaCl

To evaluate the function of *MaRHD3* expressing plants behaviour in response to abiotic stresses, *in vitro* germination assay of transgenic seeds was conducted with seeds from three T_3 transgenic lines (L1.11, L 3.16 and L4.13) along with EV and WT lines (100 seeds from each line) on MS solid media supplemented with effective concentration of NaCl (150 mM) for a period of 14 d after plating of seeds. Arabidopsis seedlings expressing *MaRHD3* had similar germination rates (8-10%) to WT and EV lines (Figure 4.17A) which consistent to the WT optimized result (Figure 4.16). After germination (7d post germination), seedlings from normal conditions were transferred to half strength MS medium with or without 100 mM NaCl and grown for 7 days. The growth of transgenic seedlings in control conditions did not show any significant differences in phenotype compared to EV and WT seedlings (Figure 4.17B) and transgenic seedlings subjected to salt stress also showed similar growth retardation and chlorosis as the EV and WT seedlings (Figure 4.17C), showing that *MaRHD3* expression had no beneficial effect under salt stress.

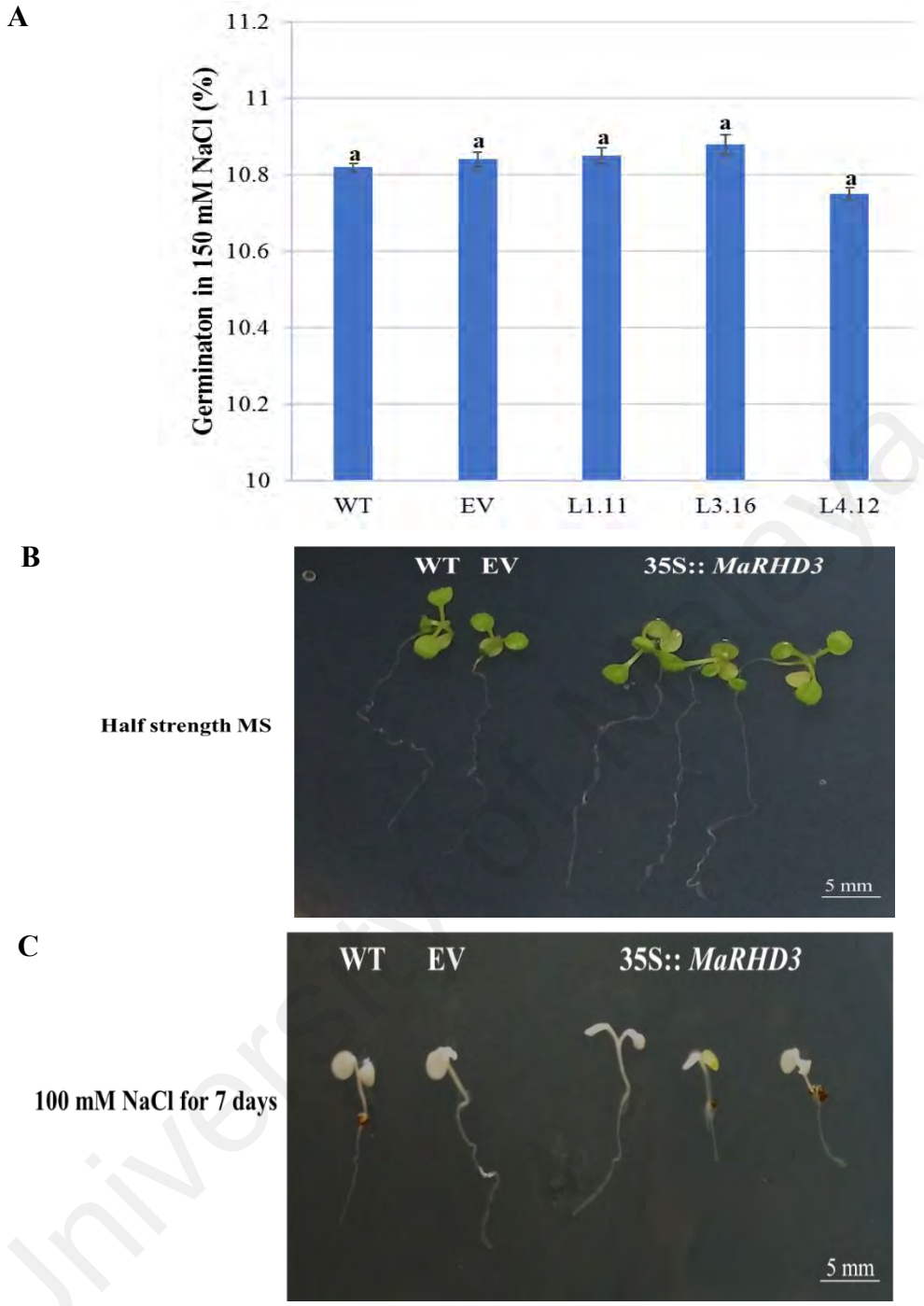

Figure 4.17: Salt sensitivity analysis in transgenic *MaRHD3* and control plants. (A) Seed germination assay of three homozygous transgenic lines (35S::*MaRHD3-1, 2, 3*), WT and EV on half strength of MS media supplemented with 150 mM NaCl at 14th d germination; data are means (±S.E.) of three replicates (100 seeds for each line) (B) 14 d old seedlings of three homozygous transgenic lines (35S::*MaRHD3-1, 2, 3*), WT and EV in half strength MS media. (C) 14 d old seedlings of three homozygous transgenic lines (35S::*MaRHD3-1, 2, 3*), WT and EV transferred in half strength MS media supplemented with 100 mM NaCl for 7 d. Differing letters (ie: a, b, c, d) indicate significant differences using two-tailed t-test followed by Tukey HSD multi-comparison analysis test (*P < 0.05).

4.7 Arabidopsis expressing *MaRHD3* showed improved germination and survival rates under drought stress

4.7.1 PEG-8000 sensitivity test of wild type Arabidopsis seeds showed 20% (w/v) of PEG-8000 as an effective concentration for drought stress assay for transgenic Arabidopsis

In order to evaluate the threshold value of used for drought stress assay, PEG-8000 concentration was optimized using wild-type Arabidopsis seeds for a period of 14 d (100 seeds from each line). Wild-type Arabidopsis seeds showed 13% germination rate in 10% (w/v) of PEG-8000 for 14 d. As the concentration increased to 15% (w/v) and 20% (w/v) of PEG-8000, germination rate of wild-type Arabidopsis was reduced to 10% and 5% respectively. As concentration reached 25% (w/v) of PEG-8000, wild-type Arabidopsis seeds showed 0% germination rate (Figure 4.18).

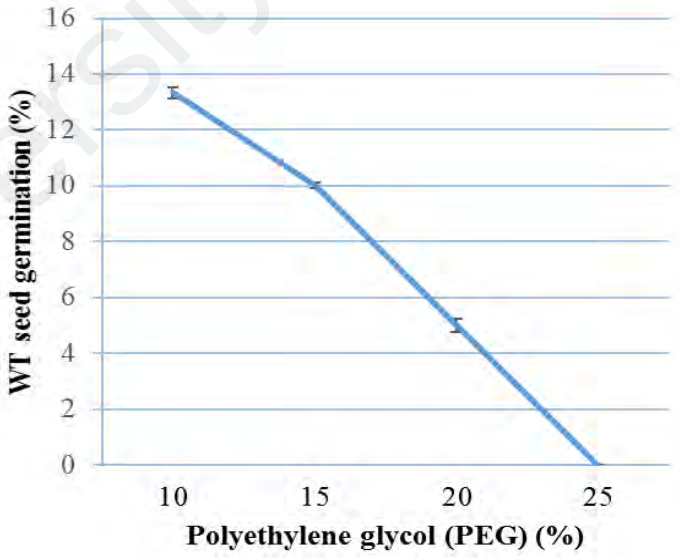

Figure 4.18: Sensitivity test of PEG-8000 for optimization of threshold value on wild type (WT) Arabidopsis seeds for 14 days. Sensitivity test of PEG-8000 was tested in four different concentrations which are 10% (w/v), 15% (w/v), 20% (w/v) and 25% (w/v). Data are means (±S.E.) of three replicates (each with 100 seeds).

4.7.2 Germination rate of T_3 transgenic Arabidopsis seeds, Wild-type Arabidopsis seeds and pCAMBIA1304 transformed Arabidopsis seeds showed significant improvement under 20% (w/v) PEG-8000

Salt and drought stress are always interconnected. Thus, further experiment was conducted *in vitro* germination assay of transgenic seeds in drought stress conditions. Seeds from three T_3 transgenic lines (L1.11, L 3.16 and L4.13) along with EV and WT lines (100 seeds from each line) were germinated on MS solid media supplemented with optimized concentrations of PEG-8000 (20%) (Figure 4.18) for a period of 14 d after plating of seeds. The germination assay in PEG-8000 (20%) media showed a notably higher percentage of germination of transgenic seeds (92-95%) compared to WT and EV seeds (17.5-20%) (Figure 4.19A and C). Furthermore, transgenic seedlings transferred to PEG for a period of 14 d had longer roots with enhanced branching (Figure 4.19B and D) and no sign of leaf chlorosis, compared to WT seedlings.

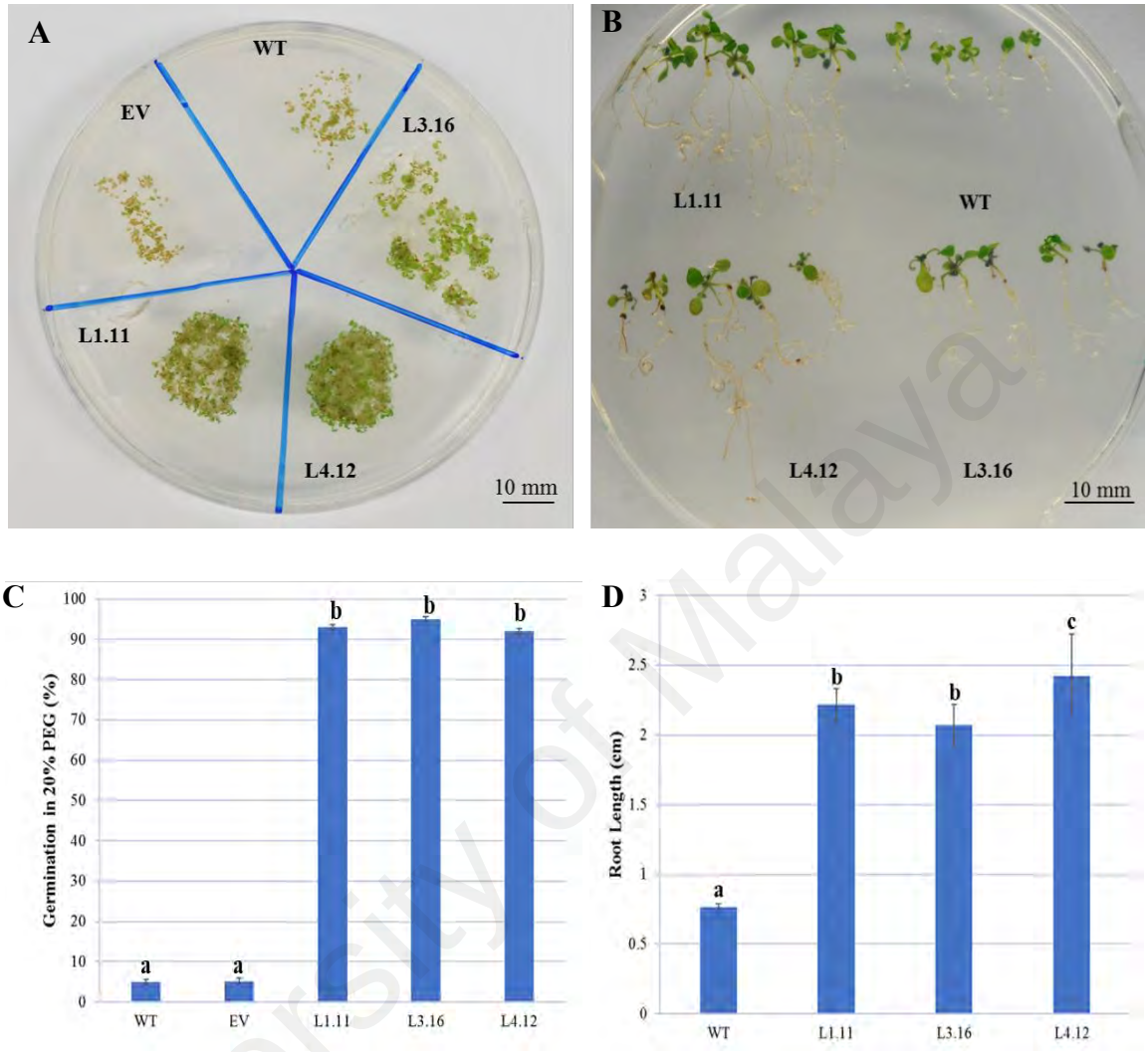

Figure 4.19: Drought sensitivity analysis of transgenic expressing *MaRHD3* and control plants. (A) Seed germination assay of 35S::*MaRHD3* (L1.11, L3.16, L4.12), WT and EV on half strength of MS media supplemented with 20% PEG-8000 (v/v) for 14 d after plating of seeds; Scale bar = 10 mm. (B) 21 d old seedlings of 35S::*MaRHD3* (L1.11, L3.16, L4.12) and WT on half-strength of MS media supplemented with 20% PEG (v/v); Scale bar = 10 mm. (C) Histogram showing percentage of seed germination of 35S::*MaRHD3* (L1.11, L3.16, L4.12), WT and EV on half strength of MS media supplemented with 20% PEG (v/v) at 14 d after plating of seeds; data are means (±S.E.) of three replicates (100 seeds for each line). (D) Histogram showing differences in root length of 35S::*MaRHD3* (L1.11, L3.16, L4.12) and WT at 14th d after the transferred of 7 d old germinated seedlings grown in half strength of MS media supplemented with 20% (v/v); data represent mean values (n=3) ±SE, n is the number of experimental replicates and SE denotes standard error. Differing letters (ie: a, b, c, d) indicate significant differences using two-tailed t-test followed by Tukey HSD multi-comparison analysis test (*$P < 0.05$).

4.8 Ectopic expression of *MaRHD3* enhanced lateral root branching and root hair density under drought stress

Owing to the altered root phenotype of transgenic lines under drought stress (Figure 4.19B), we examined root morphology of *MaRHD3* expressing seedlings under control as well as drought stress treatment to investigate possible structural differences between transgenic and WT plants. While there was no significant difference in root phenotype under control conditions (Figure 4.20A), under drought stress, transgenic plants displayed relatively longer roots (Figure 4.19D) with a higher number of lateral roots than WT plants (Figure 4.20B). Considering that root hairs have a major role in water absorption, we investigated whether *MaRHD3* expression has any effect on root hair numbers by quantifying root hair density in the root differentiation zone between the root tip and 10 mm above the root tip. A clear difference in the number of root hairs in the growing root hair zone was observed between drought exposed and control condition in WT plants (less root hairs under stress conditions: Figure 4.20A and C) and in *MaRHD3* expressing plants, which in contrast, showed a notably higher number of extended root hairs in drought stress compared to control conditions (Figure 4.20C).

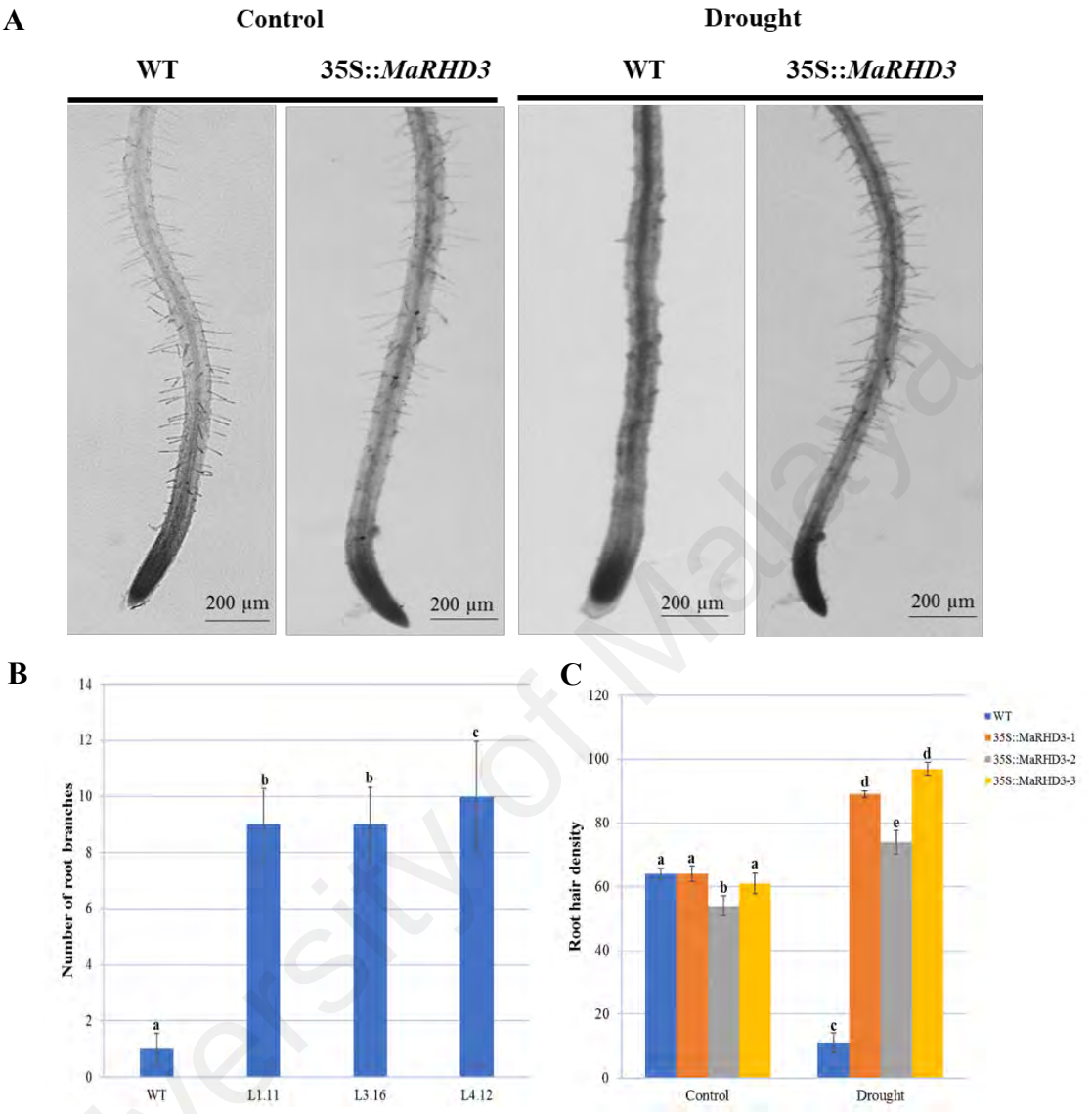

Figure 4.20: Root phenotype of transgenic expressing *MaRHD3* and control plants under drought conditions. (A) Typical root of three homozygous transgenic lines (35S::*MaRHD3-1, 2, 3*) and WT seedlings under control and drought conditions; Scale bar = 200 µm, magnification = 2X. (B) Number of root branches calculated at 14th d after the transfer of 7 d old germinated seedlings grown to half strength of MS media supplemented with 20% PEG (v/v); data are means (±S.E.) of three replicates (20 seedlings for each line). (C) Root hair density was calculated at 14th d after the transfer of 7 d old seedlings to half strength of MS media supplemented with 20% PEG (v/v); data are means (±S.E.) of three replicates. Differing letters (ie: a, b, c, d) indicate significant differences using two-tailed t-test followed by Tukey HSD multi-comparison analysis test (*$P < 0.05$).

4.9 Expression of *MaRHD3* enhances plant survival under drought stress

To investigate the response of transgenic plants in response to drought stress in greenhouse conditions, drought stress was simulated in soil grown transgenic plants along with control plants, by withholding water for a period of 10 d. Following drought stress, WT (82.2%) and EV (83.3%) plants showed severe wilting on the 10th d and only 20% plants were able to survive after re-watering (Figure 4.21 and Table 4.4). The transgenic lines arrested growth on the 10th d of drought stress (27.7%), however, most (86.7%) recovered and showed normal growth after re-watering. (Table 4.4).

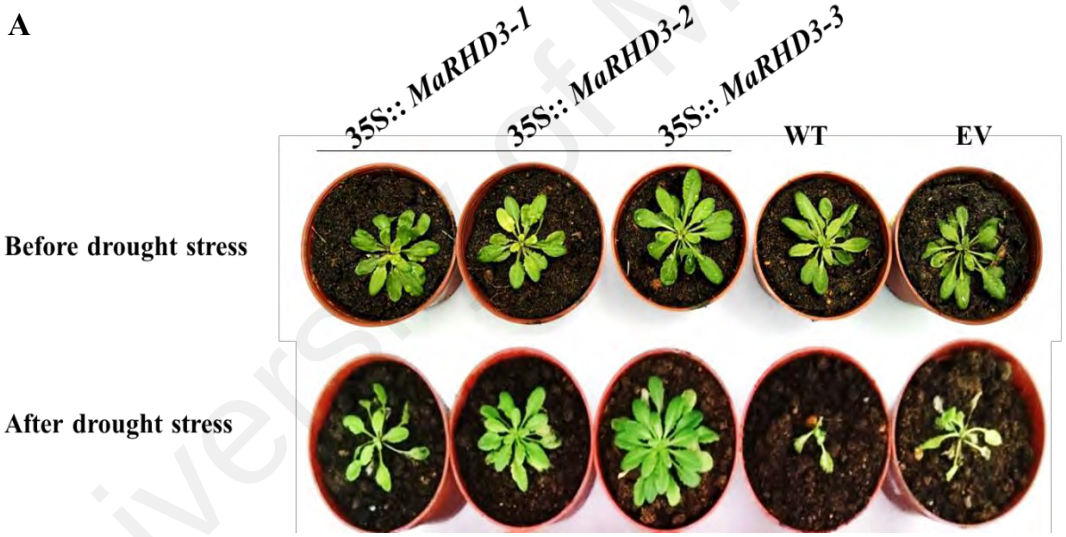

Figure 4.21: Drought tolerance assay of transgenic *MaRHD3* and control plants (WT and EV). Ten-week-old of three homozygous transgenic lines (35S::*MaRHD3-1, 2, 3*), WT and EV plants before and after (= 12.5 weeks old plants) drought stress.

Table 4.4: Survival rate of transgenic Arabidopsis lines (35S::*MaRHD3*) in exposure to drought stress

Lines	Experiment No	Total no of plant used	Number of plants showing severe wilting after 7 d of drought stress (symptom in more than three leaves)	No plants survived after recovery	Survival percentage
35S:: MaRHD3	1	30	8	26	86.7
	2	30	9	27	
	3	30	8	25	
EV	1	30	25	6	20
	2	30	24	7	
	3	30	25	5	
WT	1	30	26	6	20
	2	30	25	6	
	3	30	24	6	

4.10 Transgenic plants expressing *MaRHD3* showed lower photosynthetic damages under drought stress

Plants while following drought stress, the total chlorophyll content of control plants decreased to 58% of the initial value recorded before stress exposure (Figure 4.22). The level of reduction of chlorophyll b (66%) was higher than that for chlorophyll a (53%) and carotenoid (56.54%) in WT and EV plants following drought stress. The total chlorophyll content in the transgenic lines was 64-66% higher than that of control plants following drought stress treatment (Figure 4.22) indicating that the *MaRHD3* expressing transgenic plants had undergone less damage to their photosynthetic system.

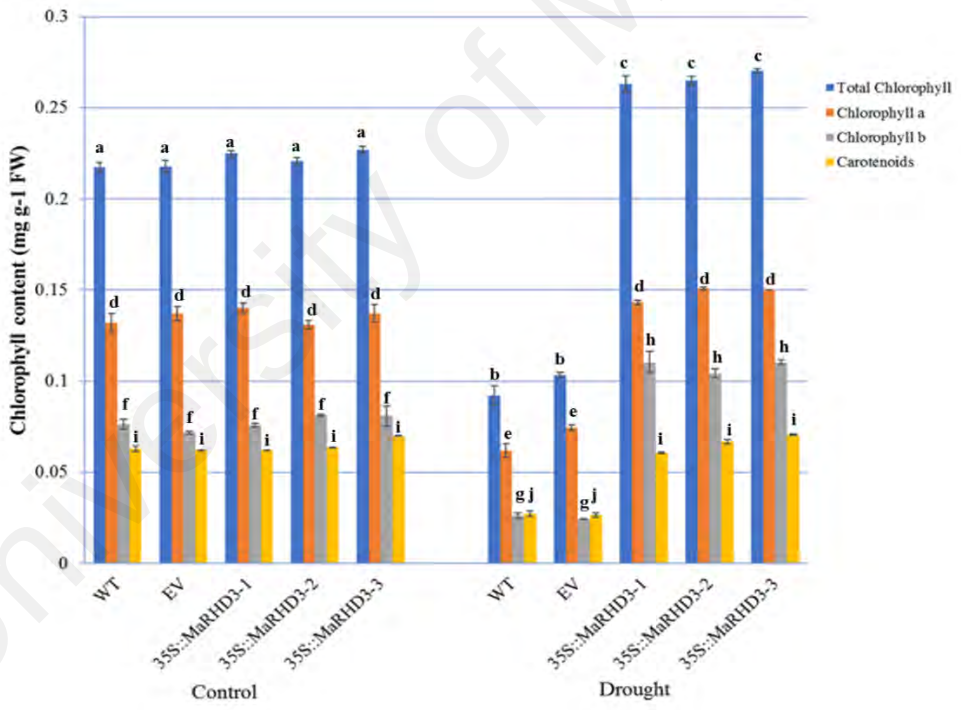

Figure 4.22: Comparison of chlorophyll content of three homozygous transgenic lines (35S::*MaRHD3-1, 2, 3*), and control plants (WT and EV) were estimated before and after drought stress. Data represent mean values (n=3) ±SE, n is the number of experimental replicates and SE denotes standard error. Differing letters (ie: a, b, c, d) indicate significant differences using two-tailed t-test followed by Tukey HSD multi-comparison analysis test (*P < 0.05).

4.11 Transgenic plants expressing *MaRHD3* showed lower lipid peroxidation under drought stress

An avoidance of oxidative damage in transgenic plants was supported by MDA content analysis, used as an indicator of membrane damage and membrane lipid peroxidation. Before drought stress exposure the levels of MDA in transgenic and control plants were very similar while following drought stress, MDA levels were significantly lower in transgenic plants compared to control plants (Figure 4.23).

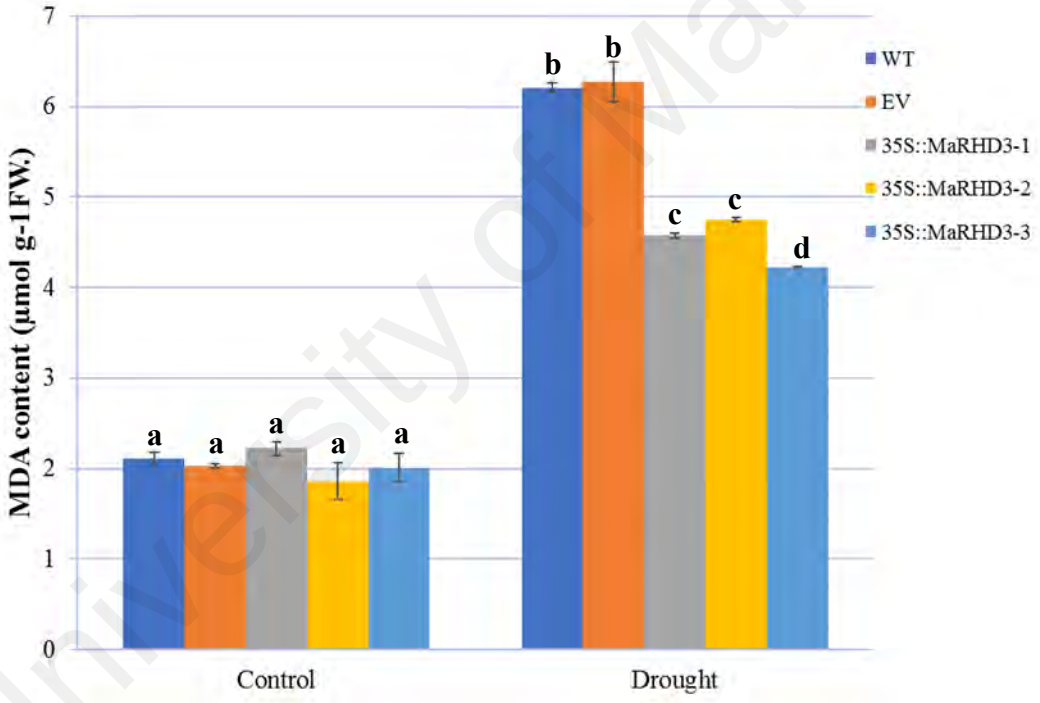

Figure 4.23: Comparison of lipid peroxidation level of three homozygous transgenic lines (35S::*MaRHD3-1, 2, 3)*, and control plants (WT and EV) were estimated before and after drought stress. Data represent mean values (n=3) ±SE, n is the number of experimental replicates and SE denotes standard error. Differing letters (ie: a, b, c, d) indicate significant differences using two-tailed t-test followed by Tukey HSD multi-comparison analysis test (*P < 0.05).

4.12 Transgenic plants expressing *MaRHD3* showed higher biomass accumulation and lower water loss rate under drought stress

The drought-induced physiological changes related to water stress in the transgenic plants was further assessed by measuring plant biomass and water loss rates. Fresh and dry biomass values of transgenic plants were similar to those of control plants under non-stress conditions (Table 4.5), but after drought stress, biomass accumulation was significantly higher in the transgenic lines. Water loss assay of detached rosette leaves showed the water loss percentage for drought-stressed transgenic plants was also significantly lower than that of the control plants (Figure 4.24) which corresponds with the higher relative water content in transgenic lines (40%) compared to control plants (Figure 4.25).

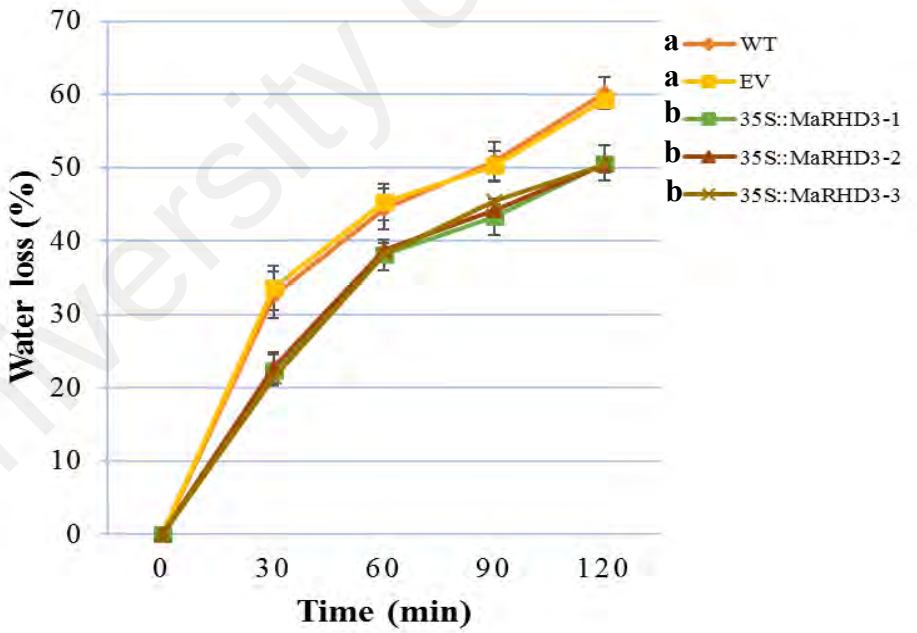

Figure 4.24: Water loss rate of three homozygous transgenic lines (35S::*MaRHD3-1, 2, 3*), and control plants (WT and EV) were estimated from detached leaves for a period up to 120 min. Data represent mean values (n=3) ±SE, n is the number of experimental replicates and SE denotes standard error. Differing letters (ie: a, b, c, d) indicate significant differences using two-tailed t-test followed by Tukey HSD multi-comparison analysis test (*P < 0.05).

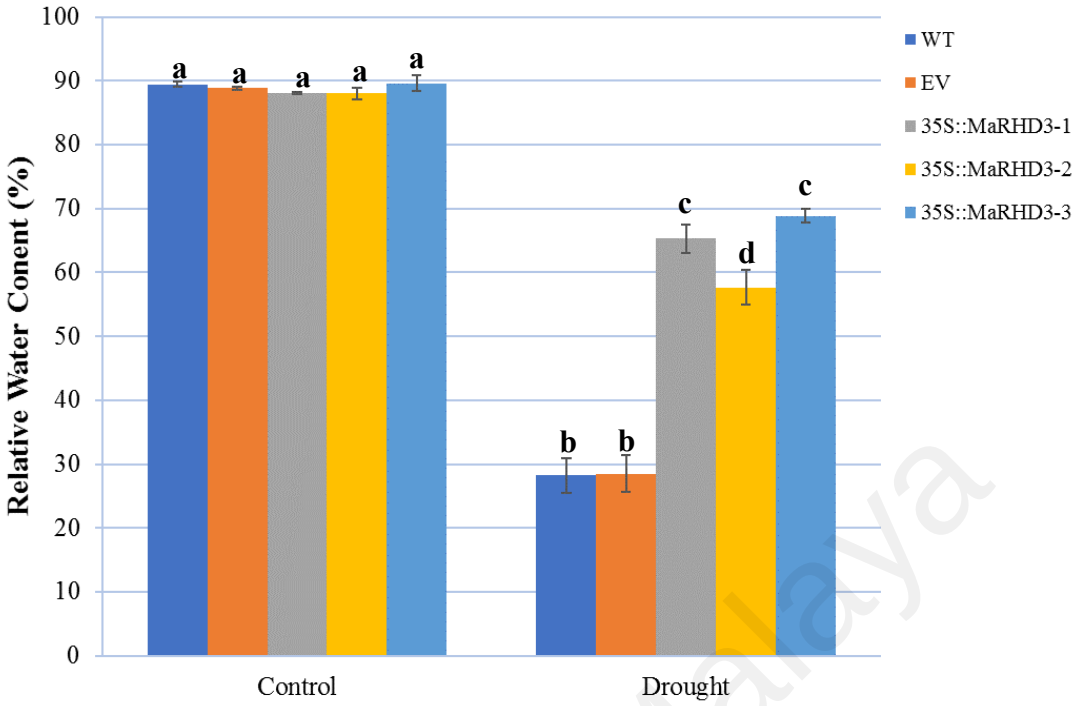

Figure 4.25: Comparison of the relative water content of three homozygous transgenic lines (35S::*MaRHD3-1, 2, 3*), and control plants (WT and EV) were measured from detached leaves before and on 7th d of drought stress. Data represent mean values (n=3) ±SE, n is the number of experimental replicates and SE denotes standard error. Differing letters (ie: a, b, c, d) indicate significant differences using two-tailed t-test followed by Tukey HSD multi-comparison analysis test (*P < 0.05).

Table 4.5: Plant biomass of control and transgenic plants before and after drought stress

Genotype	Control		After recovery from drought stress	
	Plant Fresh Weight (mg)	**Plant Dry Weight (mg)**	**Plant Fresh Weight (mg)**	**Plant Dry Weight (mg)**
WT	243.78±8.80^{a}	25.41±2.37^{b}	109.89±4.34^{c}	10.78±0.97^{e}
EV	240.11±4.48^{a}	22.56±2.24^{b}	116.11±1.62^{c}	10.44±1.33^{e}
L1.11	241.67±2.55^{a}	23.11±1.36^{b}	290±5.81^{d}	28.33±0.71^{b}
L3.16	243.67±2.06^{a}	25.56±2.19^{b}	314.22±4.41^{d}	27.89±1.26^{b}
L4.12	242.33±3.71^{a}	24±2.00^{b}	294.89±2.47^{d}	29.44±1.59^{b}

A total of 30 plants, germinated from control and three independent transgenic Arabidopsis lines were grown in control condition for a period of 10 weeks and then treated by withholding water for 7 d followed by 10 d of recovery. Data represent mean values (n=30) ±SE, n is the number of plants and SE denotes standard error. Differing Lletters (ie: a, b, c, d) indicate significant differences using two-tailed t-test followed by Tukey HSD multi-comparison analysis test (*$P < 0.05$).

4.13 Transgenic plants expressing *MaRHD3* showed up-regulation of *ABF-3* and down-regulation of *RD29A* under drought stress

A reduction in water loss is common in the ABA-mediated survival of plants during drought periods (Tuteja et al., 2007). Hence, to explore the molecular mechanism of *MaRHD3*, the expression was analysed with two marker genes, one from an ABA-dependent pathway (*ABF*-3) and another from an ABA-independent pathway (*RD29A*) in 7th d drought exposed transgenic and control plants. RT-qPCR results showed *ABF-3* expression was higher in the leaves of transgenic compared to control plants (Figure 4.26A), whereas, expression of *RD29A* was very much lower in the transgenic lines compared to that of the non-stressed control plants (Figure 4.26B). Hence, we quantified and compared the ABA content in leaves of 7th d drought stress treated transgenic and control plants using LC-MS, which showed higher ABA content (9-fold) in the transgenic lines compared to the stress control plants (Figure 4.26C). The higher and upregulation of an ABA pathway marker gene in the *MaRHD3* expressing plants supports the involvement of an ABA-dependent stress pathway in *MaRHD3* mediated drought regulation.

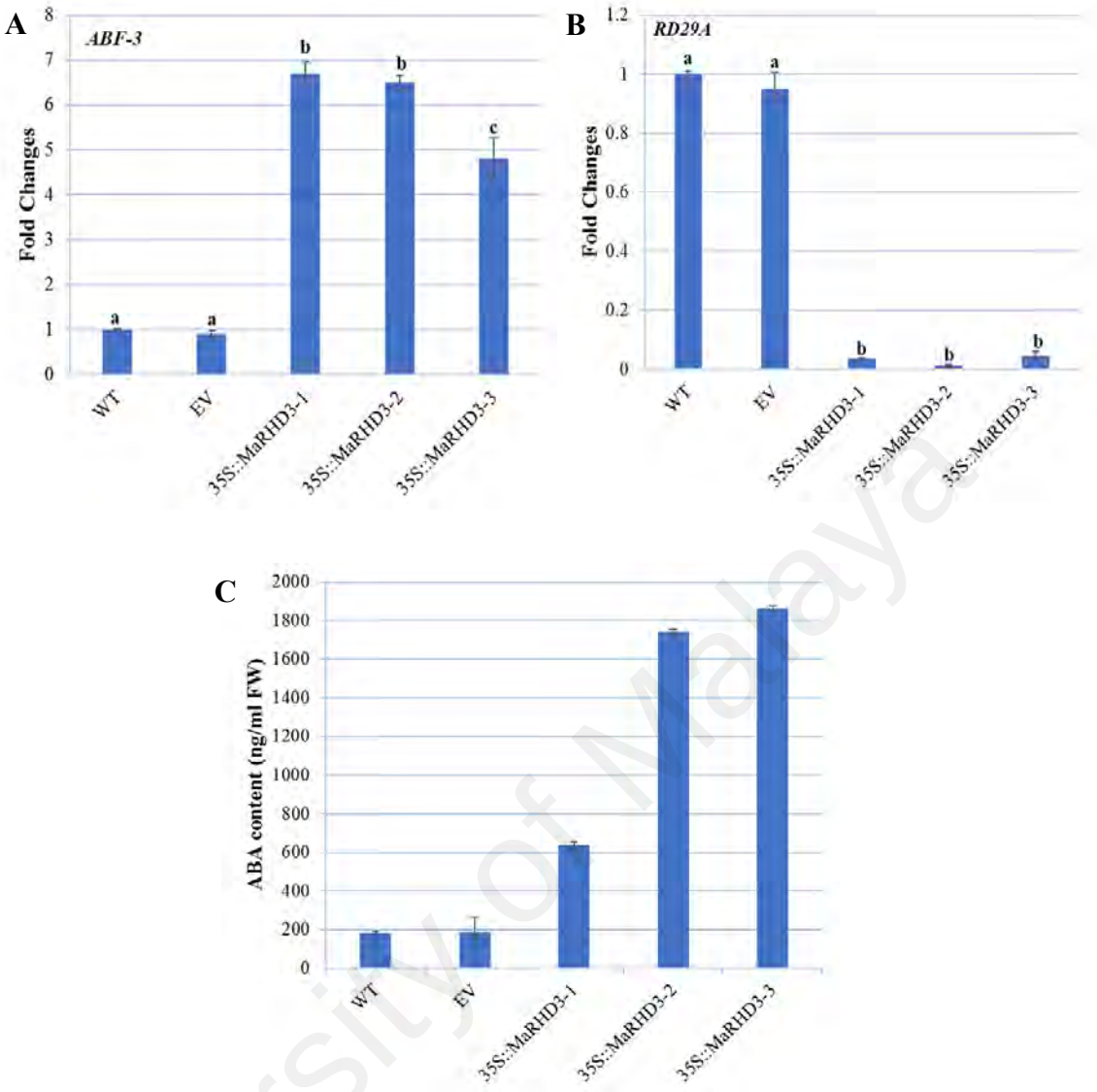

Figure 4.26: Quantitative PCR of ABA pathway genes and ABA quantification in transgenic *MaRHD3* and control plants during drought stress conditions (7th day). (A) RT-qPCR of *ABF-3* gene amplified from cDNA isolated from three homozygous transgenic lines (35S::*MaRHD3-1, 2, 3*), WT and EV plants. (B) RT-qPCR of *RD29A* gene amplified from cDNA isolated from three homozygous transgenic lines (35S::*MaRHD3-1, 2, 3*), WT and EV plants. The relative expression of *ABF-3* and *RD29A* cDNA was obtained by dividing the average number of *ABF-3* and *RD29A* transcript copies by the copy number of actin (endogenous control) for the same tissue. The lowest transcript level (*ABF-3* and *RD29A* cDNA in WT plants) was then set to a value of 1 and subsequently, expression levels are reported relative to this number. The values are the means (± SE) of three replicates. (C) ABA content of detached leaves from three homozygous transgenic lines (35S::*MaRHD3-1, 2, 3*), WT and EV at 7th day drought stress. Data represents mean values (n=3) ±SE, n is the number experimental replicates and SE denotes standard error. Differing letters (ie: a, b, c, d) indicate significant differences using two-tailed t-test followed by Tukey HSD multi-comparison analysis test (*P < 0.05). Data represent mean values (n=3) ±SE, n is the number of experimental replicates and SE denotes standard error. Letters indicate significant differences using two-tailed t-test followed by Tukey HSD multi-comparison analysis test (*P < 0.05).

4.14 Transgenic plants expressing *MaRHD3* have increased ROS scavenging ability under drought stress

As drought stress leads to oxidative damage due to the production of highly reactive ROS in plants, *MaRHD3* expressing plants was examined whether its expression changes ROS accumulation in detached leaves from transgenic plants following drought stress treatment. Before implementing of drought stress treatment, no noticeable differences were observed in DAB (for H_2O_2) and NBT (for $O_2^{\bullet-}$) staining between transgenic and control plants. However, following drought stress, DAB and NBT staining showed higher ROS (H_2O_2 and $O_2^{\bullet-}$) accumulation in leaves of control plants compared to transgenic plants, supporting a role of *MaRHD3* in enhancing ROS scavenging capability (Figure 4.22A). The activity of antioxidant enzymes superoxide dismutase (SOD), catalase (CAT), glutathione reductase (GR), peroxidase (POD) and ascorbate peroxidase (POX) were also not significantly different between transgenic and control plants in the absence of drought stress (Figure 4.22B-F). Following drought stress treatment both the transgenic and control plants showed higher SOD enzyme activity, with the highest levels in transgenic plants, with a maximum level of 1.6-fold in transgenic plants compared to control plants (Figure 4.22B). The transgenic *MaRHD3* expressing plants also displayed markedly higher levels of CAT (Figure 4.22C), GR (Figure 4.22D), POD (Figure 4.22E) and APX (Figure 4.22F) enzyme activity after drought stress treatment: The highest levels of CAT activity recorded among the transgenic plants was up to 2.7 to 3.1-fold higher than that of non-stressed transgenic plants (Figure 4.22D). GR enzyme activity was 3.5 to 3.6-fold higher in transgenic plants compared to non-stressed transgenic (Figure 4.22D). POD enzyme activity was 1.74 to 1.93-fold higher (Figure 4.22E) and APX enzyme was 1.87 to 1.91-fold higher activity (Figure 4.22F) in stressed transgenic plants compared to non-stressed transgenic plants.

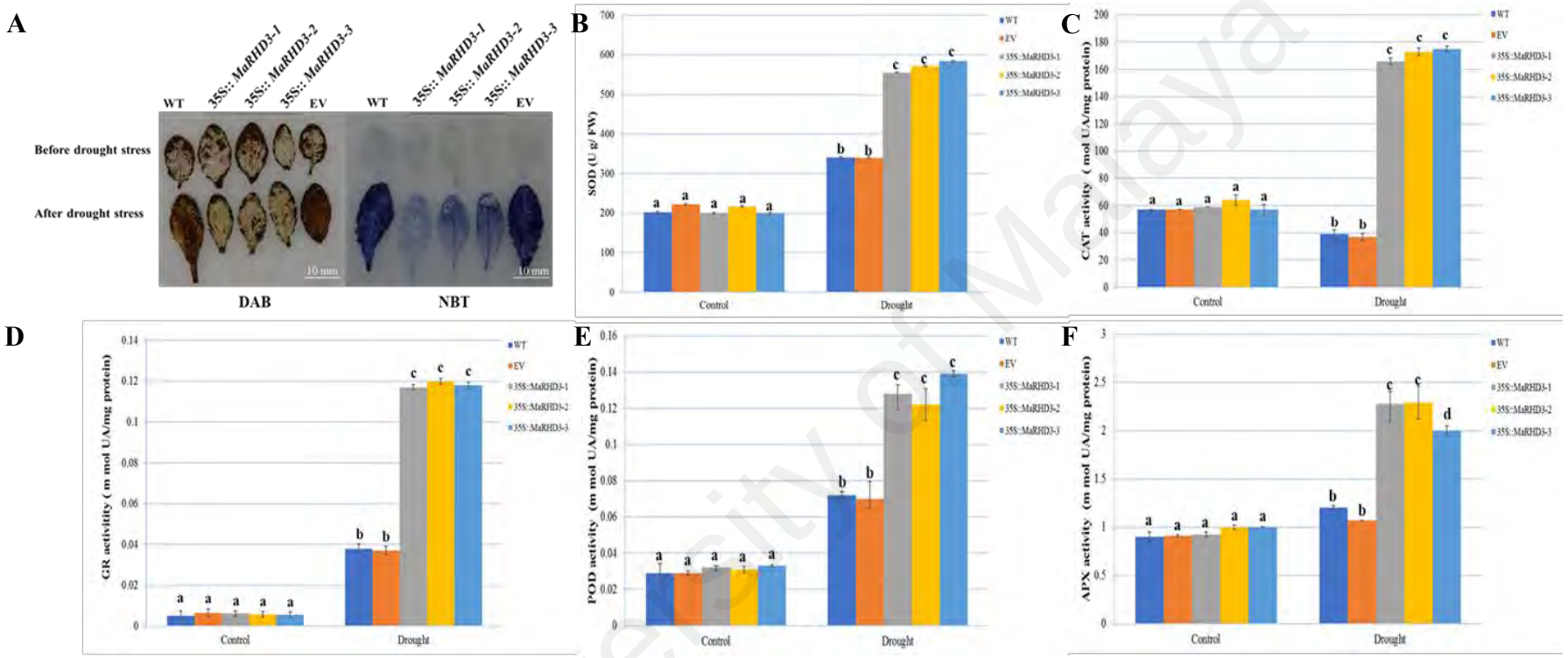

Figure 4.27: ROS histochemical staining of leaves of transgenic MaRHD3 and control plants before and after drought stress conditions. (A) Histochemical detection of oxygen radical (O2•-) and hydrogen peroxide radicle (H_2O_2) using NBT and DAB staining of detached leaves from 35S::MaRHD3 (transgenic), WT (wild-type) and EV (empty vector) plants before and after drought stress conditions. Representative examples taken from each of the three transgenic lines are shown. (B) Quantitation of ROS scavenging enzyme superoxide dismutase (SOD), (C) catalase (CAT), (D) glutathione reductase (GR), (E) guaiacol peroxidase (POD) and (F) ascorbate peroxidase (APX) in leaf tissues of 35S::MaRHD3, WT, and EV plants before and after exposure to drought stress. Data represent mean values (n=3) ±SE, n is the number of experimental replicates and SE denotes standard error. Differing letters (ie: a, b, c, d) indicate significant differences using two-tailed t-test followed by Tukey HSD multi-comparison analysis test (*$P < 0.05$).

CHAPTER 5: DISCUSSION

5.1 Expression analysis of miRNAs and their corresponding target

Plant miRNAs regulate gene expression by up-regulating stress responsive genes while down-regulating negative regulators (Ku et al., 2015) and this regulation is important in plants' adaptation in the response to abiotic stress conditions (Sunkar et al., 2012). To identify miRNAs in plants under salt stress, high throughput sequencing (RNAseq) and computational approaches were widely used Shriram et al. (2016). Thus, as part of the current thesis study, RT-qPCR validation of predictions made from RNAseq data was carried out. Most of the miRNA and their corresponding targets showed a similar inverse expression pattern as predicted from RNAseq data (Figure 4.1). This approach is supported by many studies such as RT-qPCR validation of RNAseq data in maize under Iranian mosaic virus infection (Gorbani et al., 2018) and in radish under high temperature stress (Mei et al., 2018).

In this study, RT-qPCR expression analysis of 8 miRNAs and their corresponding targets showed an inverse expression pattern in which miRNA was down-regulated and their corresponding target was up-regulated under salt stress in banana roots (Figure 4.1B, C, D, E, G, H, I and J). Up-regulation of corresponding miRNA targets permits an increased level of the respective proteins which are likely involved in plant adaptation during salt stress. In a study by Xu and Huang (2018), expression profiles of miRNA targets showed that several genes were up-regulated under heat and drought stress in *Agrostis stolonifera* which included *Linoleate 9S-lipoxygenase 1* (*LOX1*), *Patatin-like protein 2* (*PLP2*), *Delta-1-pyrroline-5-carboxylate synthase* (*P5CS*), *9-cis-epoxycarotenoid dioxygenase 1* (*NCED1*) and *3-ketoacyl-CoA synthase 11* (*KCS11*). In fact, these genes were functionally characterized to show involvement in abiotic stress, for example tomato plants overexpressing *TomLOXD* showed enhanced tolerance to high

temperature in (Hu et al., 2013); overexpression of *PuP5CS* conferred improved salt tolerance in switchgrass (Guan et al., 2018) and overexpression of *LeNCED1* improved drought tolerance in tomato (Tung et al., 2013). These examples of improved tolerance after up-regulation of miRNA-targets, support the active function of miRNA regulated genes in plant stress responses.

In this study, *protein root hair defective 3 (RHD3)* (Figure 4.1B), *chorismate mutase* (Figure 4.1C), *salt responsive protein 2* (Figure 4.1D), *dipeptidyl peptidase* (Figure 4.1 E), *dehydrin domain-containing protein* (Figure 4.1G), *zinc finger CCCH domain-containing protein* (Figure 4.1H), *chloride channel protein* (Figure 4.1I), *sorting nexin1* and *ubiquitin carboxyl-terminal hydrolase* (Figure 4.1J) were up-regulated under abiotic stress. These miRNA targets are probably transcripts or proteins expressed in the banana roots in response to salinity stress. Functional characterization of these genes can determine their suitability for enhancing tolerance to abiotic stresses that could be applied eventually to crop genetic improvement.

Orthologs of the banana RHD3, chorismate mutase, salt responsive protein 2, dipeptidyl peptidase, dehydrin domain-containing protein, zinc finger CCCH domain-containing protein, chloride channel protein, sorting nexin1 and ubiquitin carboxyl-terminal hydrolase have been reported to be functionally related to root development, stress mechanisms and defences under abiotic stress: Previous studies showed that *RHD3* was up-regulated under salinity stress in wheat (Shan et al., 2005), nutrient deficiency in Tea (Hajiboland et al., 2012), and drought stress in cotton (Ranjan & Sawant, 2015). *Chorismate mutase* was reported as positive regulator in salicylic acid biosynthesis which is protective as increased in salicylic acids enhance abiotic stress tolerance in plants, as reviewed in Khan et al., (2015). RT-qPCR of *Chorismate mutase* showed up-regulation

in banana and might be involved in salicylic acid biosynthesis as an adaptive response to salt stress. Proline is an osmoprotective molecule and reported to be involved in various abiotic stress by functioning as metal chelator, an antioxidative and signaling molecule as reviewed in Hayat et al., (2012). In order to catalyze the production of proline, dipeptidyl peptidase is needed in the process. Dipeptidyl peptidase was reported to degrade small proline-containing peptides in barley (Davy et al., 2000) and it is not surprising that up-regulation of *dipeptidyl peptidase* was observed in salt-stressed banana, as this would catalyze the production of proline for plant adaptation in response to salt stress. Dehydrin, which is induced in various plants by salinity, drought and cold stress, is a stress protein that stabilises membranes from dehydration under abiotic stress conditions, as reviewed in Hanin et al. (2011). *Dehydrin domain-containing protein* was up-regulated and probably functions in cellular protection from dehydration in banana in response to salt stress. In plants, CCCH has been reported to be involved in the regulation of ABA-regulated stress responses (Pradhan et al., 2017). ABA is known to be the central regulator for various abiotic stress responses (Vishwakarma et al., 2017). During salt stress, ABA was induced and *zinc finger CCCH domain-containing protein* up-regulation fits with involvement in an ABA regulatory pathway in response to salt stress in banana. Channel chloride protein is an anion channel which functionally involve in pH adjustment and chloride homeostasis in response to abiotic stress (Li et al., 2017). In fact, *chloride channel protein* mRNA also showed up-regulation during salt stress in maize (Wang et al., 2015) and the overexpression of *GmCLC1* in soybean gave plants with enhanced tolerance to salt stress (Wei et al., 2016). Thus, up-regulation of *chloride channel protein* may function in enhanced anion transport and homeostasis in response to salt stress in banana for plant adaptation. In Arabidopsis, *SORTING NEXIN1* was reported to be involved in high temperature stress (Hanzawa et al., 2013), iron deficiency stress (Ivanov

et al., 2014) and salt stress (Li et al., 2018). During salt stress conditions, nitric oxide (NO) accumulates in plant tissues by inducing NO synthase activity, which enhances plant tolerance to salt stress (Li et al., 2018a). Up-regulation of *SORTING NEXIN1* suggests it may be involved under salt stress in banana through regulation of NO synthase activity.

On the other hand, mac-miR156 with corresponding targets Avr9/Cf-9 rapidly and Tropine dehydrogenase (Figure 4.1A), mac-miR168 with corresponding target 12-oxophytodienoate reductase (Figure 4.1F), mac-miR62 with corresponding target Protein IQ-domain-1-like (Figure 4.1K) and mac-miR66 with corresponding target DEAD-like helicase (Figure 4.1L) did not show good agreement between RNAseq data prediction and RT-qPCR validation of expression. This may be due to biases during cDNA library construction and/or insufficient biological replicates (Auer & Doerge, 2010). Another possibility for different expression pattern between RT-qPCR validation expression profile with RNAseq data prediction is that in some cases, a miRNA-target is post-translationally inhibited but not cleaved (Rogers & Chen, 2013). It is also possible that the predicted mRNA target of a miRNA is not the true target of the miRNA: this can be determined by additional confirmation experiments such as degradome sequencing (also known as Parallel Analysis of RNA Ends). A degradome sequencing approach is now widely used for the identification of the target genes of known and novel miRNAs (Wang et al., 2016).

In this thesis, a miRNA target related to root hair development was chosen as the candidate for functional characterization, because root hairs constitute important parts of root systems. Root hair density (Leitner et al., 2010), extension (Tanaka et al., 2014; Miguel et al., 2015), and patterns (Grierson et al., 2014) are strongly influenced by environmental conditions and also root development determines the plant survivability in

response to abiotic stress conditions. The cDNA for the mac-miR157m target, *MaRHD3* was isolated (Figure 4.4B) and cloned into a constitutive plant expression vector for functional study. RHD3 has been associated with cell enlargement and root hair development in tomato as reported by Wang et al. (1997) and Poplar (Xu et al., 2012).

5.2 Optimization of hygromycin, NaCl and PEG-8000 concentration

The optimal concentration of selection agent is dependent upon the plant system and environment conditions. Thus, optimization of concentrations of hygromycin, PEG-8000 and NaCl was important for down-stream experiment to minimise the loss of transgenic Arabidopsis caused by hygromycin and maximise the effect of PEG-8000 and NaCl for introducing drought and salt stress respectively against transgenic Arabidopsis in this study.

5.2.1 Hygromycin

Hygromycin concentration is very crucial to screen stable transgenic from non-transformed Arabidopsis. Hygromycin sensitivity test showed that the effective concentration of hygromycin for transgenic Arabidopsis selection was 20 mg/L which showed 90% inhibition of wild-type Arabidopsis seedlings (Figure 4.9). Effective hygromycin concentration for transgenic Arabidopsis selection was reported to be in the range of 20-30 mg/L (Ee et al., 2014). In this study, 25 mg/L of hygromycin was not chosen to be used for transgenic Arabidopsis selection because of 100% inhibition was observed on wild-type Arabidopsis seedlings (Figure 4.9). This inhibition affects the grow of Arabidopsis seedlings by disturbing protein synthesis, this reduces the efficiency of selection process eventually leads to lower yield of transgenic Arabidopsis seed germination. In fact, higher concentrations of hygromycin used has been reported to restrain some protein synthesis, affects the safeguard functions by enlargement of intercellular space in the upper and lower epidermis of cotyledons, photosynthetic velocity and photosynthesis of Arabidopsis seedlings (Duan et al., 2011).

5.2.2 NaCl

NaCl is commonly used to induce salt stress to transgenic plants. In this study, the effective concentration of NaCl for determining stress survivability was 150 mM, which showed 10% germination rate of wild-type Arabidopsis (Figure 4.16). Effective NaCl concentration for transgenic Arabidopsis challenge was reported to be in the range of 50-150 mM (Shavrukov, 2012). Arabidopsis is salt stress sensitive (Jamil et al., 2011). Higher concentration of salt will cause inhibition of seed germination (Julkowska & Testerink, 2015), salt shock and plasmolysis to plant cells (Shavrukov, 2012), this consistent to 0% seed germination rate under 200 mM of salt in this study (Figure 4.16).

5.2.3 PEG-8000

PEG-8000 is commonly used to induce drought stress by reducing water potential for transgenic plants. In this study, PEG-8000 sensitivity test showed effective concentration of PEG-8000 for introducing drought stress to transgenic Arabidopsis was 20% (w/v) which showed 90% inhibition of wild-type Arabidopsis seedlings (Figure 4.18). This result consistent with other studies which 20% (w/v) of PEG-8000 was used to induce drought stress to transgenic Arabidopsis (Sharma et al., 2013; Shen et al., 2017). When PEG concentration increases, water deficit conditions reduce seed germination rate by restricting water availability to the weeds (Soltani et al., 2012). As concentration reached 25% (w/v) of PEG-8000, seed germination of wild-type Arabidopsis showed 0% (Figure 4.18), this may be due to PEG-8000 promoting higher water deficit stress causing degradation and inactivation of hydrolytic enzymes which are pivotal for seed germination (Pratap & Sharma, 2010).

5.3 Phylogenetic relation, predicted function and subcellular localization of MaRHD3, a GTP-binding protein

The multiple alignment analysis of RHD3 amino acid sequences showed the presence of five signatory domain of G proteins which are G1, G2, G3, G4 and G5 in the MaRHD3 amino acid sequence (Figure 4.3). Other studies have reported the presence of G protein domains in other G proteins such as GPA1 in Arabidopsis (Ma et al., 1990), TGA1 in Tomato (Hong et al., 1991) and SGA1 in Soybean (Kim et al., 1995). G1 domains are responsible for binding of α- and β-phosphate groups, G2 domains are responsible for Mg^{2+} binding, G3 domains provide residues for Mg^{2+} binding, G4 domains are responsible for nucleotide interacting whereas G5 domains act as recognition sites for guanine (Praduch et al., 2001). G proteins serve as molecular switches in plant stress signal transduction that plays an important function in regulating physiological and developmental processes (Pandey, 2017; Nitta et al., 2015). Numerous studies reported that G proteins were involved in plant adaptive responses including necrotrophic fungus defence in Arabidopsis (Suharsono et al., 2002), cell proliferation and root development in Arabidopsis (Ullah et al., 2001), and to direct the effects of ABA on stomatal opening and closure in Arabidopsis (Mishra et al., 2006). These studies suggest *MaRHD3* with conserved G protein domains may functionally respond in plant adaptive responses.

MaRHD3 showed high amino acid sequence similarity with the RHD3 sequences from other non-grass monocots, oil palm and date palm, and well conserved domains to the grass monocot maize, foxtail millet and wheat and to the dicots Arabidopsis and poplar in phylogram (Figure 4.2), supporting *MaRHD3* is a conserved G protein. Up to date, functional characterization of RHD3 gene was only reported in the dicot species Arabidopsis (Galway et al., 1997) and poplar (Xu et al., 2012) with no reports from non-

grass monocots oil palm and date palm. A study by Galway et al. (1997), demonstrated loss of function of *RHD3* in Arabidopsis resulted in a short and wavy root hair phenotype. A similar study demonstrated by Xu et al. (2012), overexpressing *PeRHD3* in poplar, showed longer and increased number of root hairs. These studies support that *MaRHD3* with conserved structure may share similar biological functions with the orthologs that are associated with root hair development.

The subcellular localization of MaRHD3 protein based on the green fluorescence signal in cytoplasm in an onion cell assay, confirmed the bioinformatics prediction (Table 4.1) that MaRHD3 is localized in the cytoplasm (Figure 4.8). Unlike the Arabidopsis RHD3, which has an endoplasmic reticulum (ER) membrane retention signal (SSKE), and was demonstrated by Chen et al. (2011) to be localized in the ER. The banana homolog, MaRHD3 protein, lacks ER and peroxisomal targeting signals when examined by bioinformatic predictive tools (Table 4.1), hence MaRHD3 protein is likely to function in the cytoplasm in banana root cells.

5.4 Arabidopsis expressing *MaRHD3* do not show improvement in germination and survival rates under salt stress

Early responses to salt and drought stress are similar as both produce osmotic stress to the plants. However, salt stress, not only involves reduction in osmotic potential but increases concentrations of ionic components (Na^+ and Cl^-) from the salt causing ionic toxicity, which inhibits cellular development and plant growth (Kumar et al., 2017). In this study, germination rate and phenotype of transgenic Arabidopsis showed no significant difference compared to control plants when treated with NaCl (Figure 4.17A, B, C). Seeds encapsulate all the essential elements for plant development. Water absorption is a necessity for seeds to germinate by activating the metabolic pathways needed for plant growth (Kaymakanova, 2009). Osmotic pressure caused by salt, limits the water entering seeds and allow ionic components to enter to the seeds, causing ionic toxicity thus affecting metabolic pathways that are required for plant development. No significant differences in term of phenotype was observed for transgenic plants compared to control plants in Figure 4.7B, suggesting that *MaRHD3* does not confer salt tolerance in the model plant system. In order to confirm if this is also the case in banana, the native host of this gene, future studies can be conducted involving over-expressing *MaRHD3* in banana.

As many cellular and metabolic responses to drought and salinity stress are shared and gene expression are overlapped (Chaves et al., 2009), this might explain why *MaRHD3* expression was observed under salt stress in the original study by Lee at al., (2015). Similar observations have been reported in other studies; expression of NAC transcription factor (*ATAF1*) was induced during high salinity and drought (Wu et al., 2009). However, overexpression of *ATAF1* in Arabidopsis showed enhanced tolerance to drought stress but sensitivity to salt stress (Wu et al., 2009). Arabidopsis *F-box E3 ubiquitin ligase-*

coding gene (*AtDIF1*) is expressed during salinity and drought stress (Gao et al., 2017). However, overexpression of *AtDIF1* in Arabidopsis plants showed sensitivity to drought stress but enhanced tolerance to salt stress (Gao et al., 2017). WRKY transcription factors are known to be key regulators in response to abiotic stress. Wei et al. (2018), demonstrated ectopic expression of woodland strawberry *FvWRKY42* in Arabidopsis to have enhanced osmotic resistance but hypersensitivity towards ABA. These studies show that genes identified as being associated with a specific abiotic stress may have antagonistic responses to the targeted abiotic stresses. *MaRHD3* might have different biological functions in different abiotic stress conditions, and in the current study drought stress challenge showed transgenic Arabidopsis expressing *MaRHD3* to have enhanced tolerance.

5.5 Arabidopsis expressing *MaRHD3* showed enhanced tolerance to drought stress

In plants, G proteins are involved in numerous cell signalling pathways, including ABA regulation of guard cell ion channels and stomatal aperture (Eckardt, 2004; Pandey et al., 2009; Zhao et al., 2010, Nitta et al., 2015). *MaRHD3* was identified as a G protein as discussed in section 5.3 and transgenic Arabidopsis overexpressing this protein showed enhanced drought tolerance (Figures 4.19, 4.20, 4.21, 4.22, 4.23, 4.24, 4.25, 4.26, 4.27; Table 4.4, 4.5). A study reported that GPA1 was identified with conserved GTP-binding domains in Arabidopsis (Ma et al., 1990), similar to multiple alignment analysis of *MaRHD3* in this study as discussed in section 5.3.A study reported that an Arabidopsis G protein, GPA1, is involved in ABA signalling in plant stress signal transduction (Assmann, 2002), consistent to the study demonstrated by Wang et al. (2001), loss of function of *GPA1* in Arabidopsis showed stomatal opening was insensitive to inhibition by exogenous ABA and water loss rate is significantly higher compared to wild type. A similar study demonstrated that Arabidopsis plants with loss of function of *GPA1* showed increased sensitivity to ABA treatment during seed germination and seedling development (Ullah et al., 2002). These studies show that the involvement of G proteins is important for signal transduction under drought conditions. A similar effect was observed from overexpression of *MaRHD3* in Arabidopsis, where water loss rate was significantly lower (Figure 4.24), seed germination rate was significantly higher (Figure 4.19A) and there was better seedling development in terms of root hairs (Figure 4.20) under drought conditions. ABA is known to be a central regulator and positively affected drought-stressed plants when exogenously applied or endogenously increased from overexpression of ABA related genes. A recent study by Li et al. (2017), showed application of ABA exogenously enhanced drought tolerance in creeping bentgrass, by

regulating stomatal conductance, leading to lower water loss rate. Another related study, in which ABA content was endogenously increased by overexpression of protein elicitors *MoHrip1* and *MoHrip2* from a pathogenic fungus, enhanced drought tolerance in transgenic rice by maintaining water retention (Wang et al., 2017). Consistent with those studies, *MaRHD3*-overexpressing transgenic Arabidopsis plants exposed to drought stress, showed higher ABA content (Figure 4.26C), lower water loss rate (Figure 4.24) and higher relative water content (Figure 4.25). These results support overexpression of *MaRHD3* promoting the increase in ABA content endogenously in transgenic Arabidopsis which can improve tolerance to drought stress by lowering water loss rate and maintaining a higher relative water content.

Roots serve as an interface between plant and soil. Increased root hair density and longer roots were reported as an adaptive feature for plants to maximize water and nutrient absorption in response to drought stress, as reviewed in Shahzad et al. (2018). In this thesis study, Arabidopsis expressing *MaRHD3* showed significantly higher germination rates (92-95%) (Figure 4.19A), extended root branching (Figure 4.19B), longer roots (Figure 4.19D) and a higher number of extended root hairs (Figure 4.20C) in response to drought stress compared to control plants. Changes in root hairs and sensitivity to water stress have been shown previously in Arabidopsis using the root hair-less mutant NR23 (*no root* hair line that expresses N23): This Arabidopsis mutant showed lack of root hairs resulting in 47% reduction in water absorption and the plants were highly susceptible to drought stress (Tanaka et al., 2014). A similar study reported that root-hairless mutants (knock down of *PLC5*) of Arabidopsis also showed high sensitivity to drought stress (Zhang et al., 2018). Another similar report in peanuts showed that enhanced in root formation was the key determinant for survivability during drought stress (Thangthong et al., 2018). These results show that root hair development and the

increase in root hair density and extension contribute to the enhanced plant tolerance in response to drought stress, similar to the effect of MaRHD3 overexpression in Arabidopsis where the roots were enhanced and drought stress survival was improved.

Photosynthetic pigments and biomass accumulation are key parameter that effect plant growth during water deficit conditions (Guo et al., 2015). Further investigation of Arabidopsis expressing *MaRHD3* showed the plants to have higher levels of photosynthetic pigments (Figure 4.22) and biomass accumulation (Table 4.5) under drought conditions compared to the same plants under non-stressed conditions, consistent with a role for RHD3 in drought stressed signal transduction. A study reported that photosynthetic pigments and biomass accumulation of two sympatric *Populus* species were significantly affected under water deficit conditions (Yin et al., 2005). A similar report showed that photosynthetic pigments and biomass accumulation of oilseed rape were suppressed under water deficit conditions (Liu et al., 2016). The growth of plant is highly dependent of its root formation. A study in common bean by Miguel et al. (2015) showed that a phenotype with long root hair had 89% higher biomass accumulation compared to phenotype with short root hair in response to phosphorous stress conditions. Photosynthetic pigments and carotenoid synthesis are highly dependent on mineral and nutrition from the soil (Daughtry et al., 2000). The roots have the sole responsibility to uptake and assimilate mineral and nutrition to the plants from soil (Sparks & Benfey, 2018). Higher photosynthetic pigment levels and biomass accumulation with longer root hair phenotype in Arabidopsis expressing *MaRHD3* were consistent with results from a study in which higher concentration of chlorophyll content and longer root hair phenotype were positively correlated in lentil under drought stress conditions (Kumar et al., 2012). Thus, healthy plant growth is often linked with better root phenotype, consistent with

longer root hair phenotype of Arabidopsis expressing *MaRHD3* under drought stress conditions.

The degree of oxidative damage caused by drought stress also is one of the key parameters that effect on plant growth (Hassan et al., 2017). To minimize the effect of oxidative damage to plants caused by ROS, plants produces ROS scavenging enzymes such as SOD, CAT, GR, POD, and APX as an adaptive response under abiotic stresses (Foyer & Noctor, 2005). Arabidopsis expressing *MaRHD3* showed lower levels of ROS (H_2O_2, $O_2^{\bullet-}$) in leaves (DAB and NBT staining, Figure 4.27A), higher levels of ROS-scavenging enzyme SOD (Figure 4.27B), CAT (Figure 4.27C), GR (Figure 4.27D), POD (Figure 4.27E), and APX (Figure 4.27F), suggesting effective antioxidant enzyme in scavenging ROS in response to drought stress. A study reported that RHD3 along with RHD2 and RHD4 involved in ROS production (Schiefelbein & Somerville, 1990). A similar study reported that *RHD2* is classified in the group of NADPH-oxidase (Carol & Dolan, 2006) and NADPH-oxidase was reported as a positive regulator in response to drought stress (He et al., 2017). In fact, loss of function of NADPH-oxidase in rice showed hypersensitive under drought stress conditions (Wang et al., 2016). The higher degree of ROS scavenging enzyme often correlated to drought tolerance, as observed in Arabidopsis expressing *MaRHD3*. A similar study reported that overexpression of *AnnSp2* in transgenic tomato showed higher degree of ROS scavenging enzyme (SOD, CAT and APX) which enhanced drought tolerance by elimination of ROS (Ijaz et al., 2017). Another important parameter to determine oxidative stress is the level of MDA, a reliable marker for the determination of lipid peroxidation (Del Rio et al., 1996). Plants MDA level also generally correlates to drought tolerance. Based on the study demonstrated by Li et al. (2018b), overexpression of *SoP5Cs* in transgenic sugarcane showed lower level of MDA along with higher expression of ROS-scavenging enzyme

(SOD) improved tolerance under drought stress, similar observation was observed in the current study in which Arabidopsis expressing *MaRHD3* showed lower level of MDA (Figure 4.23). The increase level of ROS scavenging enzyme along with lower level of lipid peroxidation, suggested that MaRHD3 was involved in ROS mediated cellular signalling in response to drought stress.

In drought stress, ABA has been reported as a central mediator which activates the response mechanism *via* ABA-responsive genes (Qin et al., 2011; Hubbard et al., 2010). In this study, Arabidopsis expressing *MaRHD3* showed 4-6-fold higher fold changes of *ABF-3* (Figure 4.26A), a responsive gene involved in ABA-dependent pathway, compared to the expression in control plants. The same conditions resulted in relatively low expression of *RD29A* (Figure 4.26B), a drought responsive gene from an ABA-independent pathway. Plant response to drought as an adaptive response has been widely shown to be mediated through an ABA-dependent pathway, while ABA-independent pathway was common in cold stress adaptive response (Agarwal & Jha, 2010). Overexpression of Arabidopsis *ABF-3* in creeping bentgrass showed enhanced tolerance to drought and heat stress (Choi et al., 2013) while *abf-3* mutants showed impaired downstream regulation of osmotic stress responsive genes involved in ABA signalling (Yoshida et al., 2015). A study showed that higher expression level of *ABF-3* was reported in Arabidopsis overexpressing *AtAIRP2* under drought conditions and positively involved in ABA-dependent drought stress responses (Cho et al., 2011). Similar observation was observed in this study, where there was higher expression of *ABF-3* in Arabidopsis overexpressing MaRHD3 under drought conditions. Taken together with data on a G protein (Figure 4.3), increased in ABA levels (Figure 4.26C) and higher expression of ABF-3 (Figure 4.26A), the data reported in this thesis support the hypothesis that *MaRHD3* is involved in stimulating G protein-mediated ABA signalling leading to better

tolerance of water deficit. The ABA signalling pathway response to abiotic stress is complex and involves multiple receptors and interactions, as reviewed in Nitta et al. (2015). In order to further characterise the pathway by which *MaRHD3* stimulates G protein-mediated ABA signalling, additional information on proteins interacting with *MaRHD3* is required which can be investigated by protein hybrid assays or tagging assays in the future.

CHAPTER 6: CONCLUSION

In conclusion, the three objectives of the study were achieved. Overexpression of *MaRHD3* in Arabidopsis significantly enhanced drought tolerance but not salt stress tolerance, which is supported by data from seed germination (Figure 4.19C), root length (Figure 4.19D), root branches (Figure 4.20B), root hair density (Figure 4.20C), total chlorophyll content (Figure 4.22), MDA content (Figure 4.23), water loss rate (Figure 4.24), relative water content (Figure 4.25), biomass accumulation (Table 4.5), level of endogenous ABA (Figure 4.26), up-regulation of *ABF-3* (Figure 4.26) and level of ROS enzyme (Figure 4.27). Future study is recommended involving overexpressing *MaRHD3* in banana to confirm if this is also the case in banana. Taken together with all the results, functional characterization of *MaRHD3* provide valuable information for crop improvement by generating stress tolerant varieties in the future.

In this study, quantification of expression of selected *Musa* specific miRNAs and their target mRNA in response to salinity were successfully validated by an RT-qPCR approach (Objective 1 was to quantify expression of selected *Musa* specific miRNAs and their target mRNA in response to salinity stress). This objective was supported with the result from Figure 4.1. A total of 12 miRNAs and 14 corresponding target mRNAs expression levels under stressed and non-stressed conditions were determined by RT-qPCR (Figure 4.1). By comparing RT-qPCR expression data with RNAseq expression data predictions, 8 miRNAs and their corresponding targets showed an inverse expression pattern in which miRNA was down-regulated and their corresponding target was up-regulated under 300 mM NaCl treatment in banana roots. Whereas, the remaining 4 miRNAs and their corresponding target based on RT-qPCR validation of expression showed disagreement to RNAseq data prediction in which different expression pattern was observed under 300 mM NaCl treatments in banana roots. These miRNA targets are

probably the transcripts and protein expressed involve in plant adaptive responses under salinity stress. In this thesis study, a mac-miR157m target protein*, root hair defective 3* was chosen for as a candidate for functional validation under abiotic stress. This candidate was based on the interest of biological function in root hair development functionally characterized in Arabidopsis under salinity and drought conditions. In future, other stress responsive up-regulated miRNAs targets including *chorismate mutase* (Figure 4.1C), *salt responsive protein 2* (Figure 4.1D), *dipeptidyl peptidase* (Figure 4.1 E), *dehydrin domain-containing protein* (Figure 4.1G), *zinc finger CCCH domain-containing protein* (Figure 4.1H), *chloride channel protein* (Figure 4.1I), *sorting nexin1* and *ubiquitin carboxyl-terminal hydrolase* (Figure 4.1J) are recommended for functional characterization in a plant system and may provide valuable information to crop genetic improvement in response to abiotic stress.

A miRNA mac-miR157m-target, *MaRHD3* was characterized by bioinformatics analysis (multiple alignment analysis (Figure 4.3), phylogenetic analysis (Figure 4.2), subcellular localization prediction (Table 4.1)) and was functionally tested in Arabidopsis under salinity and drought stress (Objective 2). Based on the multiple alignment analysis *MaRHD3* was identified as a G protein with signatory G protein domains (G1-G5, Figure 4.3) and showed high amino acid sequence similarity with homologs form other non-grass monocots oil palm and data palm and well conserved domain to the grass monocot maize, foxtail millet and wheat and to the dicots Arabidopsis and Poplar in phylogram (Figure 4.2). MaRHD3 was predicted to share a similar biological function associated in root hair development as reported in Arabidopsis (Galway et al., 1997) and Poplar (Xu et al., 2012) as discussed in section 5.3. Subcellular localization of MaRHD3 protein showed it to be different to Arabidopsis RHD3 protein as MaRHD3 was localized in the cytoplasm while Arabidopsis RHD3 has been reported to be localized in ER as discussed

in section 5.3. In summary for objective 2 (which was to characterize a selected miRNA mac-miR157m-target, *MaRHD*3, through bioinformatics and functional analysis), *MaRHD3* is a G protein with conserved domain to monocots and dicots plant and showed localization in cytoplasm in onion epidermal cells.

In this thesis, function of *MaRHD3* in Arabidopsis was tested in response to salinity and drought stress to meet Objective 3 (Objective 3 was to generate and characterise the phenotypes of transgenic Arabidopsis lines (T_3 generation) expressing *MaRHD3*). Transgenic Arabidopsis lines (T_3 generation) expressing MaRHD3 was successfully generated and their phenotypes in term of seed germination (Figure 4.19C), root length (Figure 4.19D), root branches (Figure 4.20B), root hair density (Figure 4.20C), with supporting data from physiological and biochemical analysis including total chlorophyll content (Figure 4.22), MDA content (Figure 4.23), water loss rate (Figure 4.24), relative water content (Figure 4.25), biomass accumulation (Table 4.5), level of ROS enzyme (Figure 4.27) were characterized (Objective 3). Although *MaRHD3* was up-regulated in salt stress, Arabidopsis overexpressing *MaRHD3* do not show significant improvement in term of germination rate and phenotype as compared to control plants (wild-type and empty vector) under salinity stress. Since transformed Arabidopsis plants constitutively expressing *MaRHD3* did not show improved tolerance to elevated salinity, Arabidopsis expressing *MaRHD3* was examined under drought stress. Interestingly, Arabidopsis expressing *MaRHD3* showed significant improvement under drought stress by altered root structure with enhanced branching and increased density of root hairs. These plants also had lower ROS levels along with higher concentration of ROS scavenging enzyme expression (SOD, CAT, GR, POD, and APX), higher relative water content along with reduced water loss rates, higher expression in fold changes of ABA marker (*ABF-3*) and higher ABA content, that support a relatedness to the ABA-mediated drought response

pathway. Future work is recommended on the protein-protein interaction of *MaRHD3* stimulated G protein-mediated ABA signalling pathway as discussed in section 5.5 as ABA signalling is a complex pathway involving multiple receptors and interactions (reviewed in Nitta et al., 2015).

REFERENCES

Acosta-Motos, J. R., Ortuño, M. F., Bernal-Vicente, A., Diaz-Vivancos, P., Sanchez-Blanco, M. J., & Hernandez, J. A. (2017). Plant responses to salt stress: Adaptive mechanisms. *Agronomy*, *7*(1), 18.

Aebi, H. (1984). Catalase in vitro. *Methods in Enzymology*, *105*, 121-126.

Agarwal, P. K., & Jha, B. (2010). Transcription factors in plants and ABA dependent and independent abiotic stress signalling. *Biologia Plantarum*, *54*(2), 201-212.

Agin, B., & Jegtvig, S. (2009). *Superfoods for dummies*. United States of America: John Wiley & Sons.

Anand, B., Verma, S. K., & Prakash, B. (2006). Structural stabilization of GTP-binding domains in circularly permuted GTPases: Implications for RNA binding. *Nucleic Acids Research*, *34*(8), 2196-2205.

Aranda, P. S., LaJoie, D. M., & Jorcyk, C. L. (2012). Bleach gel: A simple agarose gel for analyzing RNA quality. *Electrophoresis, 33*(2), 366-369.

Arbona, V., Manzi, M., Zandalinas, S. I., Vives-Peris, V., Pérez-Clemente, R. M., & Gómez-Cadenas, A. (2017). Physiological, metabolic, and molecular responses of plants to abiotic stress. In M. Sarwat, A. Ahmad, M. Abdin & M. Ibrahim (Eds.), *Stress signaling in plants: Genomics and proteomics perspective* (pp. 1-35). Springer, Cham.

Assaha, D. V. M., Ueda, A., Saneoka, H., Al-Yahyai, R., & Yaish, M. W. (2017). The role of Na^+ and K^+ transporters in salt stress adaptation in glycophytes. *Frontiers in Physiology*, *8*, 509.

Asseng, S., Ewert, F., Martre, P., Rötter, R. P., Lobell, D. B., Cammarano, D., ... Reynolds, M. P. (2015). Rising temperatures reduce global wheat production. *Nature Climate Change*, *5*(2), 143.

Assmann, S. M. (2002). Heterotrimeric and unconventional GTP binding proteins in plant cell signaling. *The Plant Cell*, *14*, S355-S373.

Bai, Q., Wang, X., Chen, X., Shi, G., Liu, Z., Guo, C., & Xiao, K. (2018). Wheat miRNA TaemiR408 acts as an essential mediator in plant tolerance to Pi deprivation and salt stress via modulating stress-associated physiological processes. *Frontiers in Plant Science*, *9*, 499.

Bakar, F. A., Yeo, C. C., & Harikrishna, J. A. (2015). Expression of the Streptococcus pneumoniae yoeB chromosomal toxin gene causes cell death in the model plant Arabidopsis thaliana. *BMC Biotechnology*, *15*(1), 26.

Barrs, H. D., & Weatherley, P. E. (1962). A re-examination of the relative turgidity technique for estimating water deficits in leaves. *Australian Journal of Biological Sciences*, *15*(3), 413-428.

Bartels, D., & Sunkar, R. (2005). Drought and salt tolerance in plants. *Critical Reviews in Plant Sciences*, *24*(1), 23-58.

Bielach, A., Hrtyan, M., & Tognetti, V. B. (2017). Plants under stress: Involvement of auxin and cytokinin. *International Journal of Molecular Sciences*, *18*(7), 1427.

Calanca, P. P. (2017). Effects of abiotic stress in crop production. In M. Ahmed & C.O. Stockle (Eds.), *Quantification of climate variability, adaptation and mitigation for agricultural sustainability* (pp. 165-180). Springer, Cham.

Calberto, G., Staver, C., & Siles, P. (2015). An assessment of global banana production and suitability under climate change scenarios. In A. Elbehri (Ed.), *Climate change and food systems: Global assessments and implications for food security and trade* (pp. 266-288). Rome: Food Agriculture Organization of the United Nations (FAO).

Carillo, P., Annunziata, M. G., Pontecorvo, G., Fuggi, A., & Woodrow, P. (2011). Salinity stress and salt tolerance. In A. Shanker & B. Venkateswarlu (Eds.), *Abiotic stress in plants-mechanisms and adaptations*. London, United Kingdom: InTechOpen.

Carol, R. J., & Dolan, L. (2006). The role of reactive oxygen species in cell growth: Lessons from root hairs. *Journal of Experimental Botany*, *57*(8), 1829-1834.

Chakravorty, D., Trusov, Y., Zhang, W., Acharya, B. R., Sheahan, M. B., McCurdy, D. W., ... Botella, J. R. (2011). An atypical heterotrimeric G‐protein γ‐subunit is involved in guard cell K+‐channel regulation and morphological development in Arabidopsis thaliana. *The Plant Journal*, *67*(5), 840-851.

Chamovitz, D., Sandmann, G., & Hirschberg, J. (1993). Molecular and biochemical characterization of herbicide-resistant mutants of cyanobacteria reveals that phytoene desaturation is a rate-limiting step in carotenoid biosynthesis. *Journal of Biological Chemistry*, *268*(23), 17348-17353.

Champion, J. (1967). *Notes et Documents sur les bananiers et leur culture*. Paris: Instituto Francais de Recherches Fruitieres Outre-Mer.

Chaves, M. M., Pereira, J. S., Maroco, J., Rodrigues, M. L., Ricardo, C. P. P., Osório, M. L., ... Pinheiro, C. (2002). How plants cope with water stress in the field? Photosynthesis and growth. *Annals of Botany*, *89*(7), 907-916.

Chen, J., Stefano, G., Brandizzi, F., & Zheng, H. (2011). Arabidopsis RHD3 mediates the generation of the tubular ER network and is required for Golgi distribution and motility in plant cells. *Journal of Cell Science*, 084624.

Cho, S. K., Ryu, M. Y., Seo, D. H., Kang, B. G., & Kim, W. T. (2011). The Arabidopsis RING E3 ubiquitin ligase AtAIRP2 plays combinatory roles with AtAIRP1 in ABA-mediated drought stress responses. *Plant Physiology*, 111.

Choi, Y. S., Kim, Y. M., Hwang, O. J., Han, Y. J., Kim, S. Y., & Kim, J. I. (2013). Overexpression of Arabidopsis ABF3 gene confers enhanced tolerance to drought and heat stress in creeping bentgrass. *Plant Biotechnology Reports*, *7*(2), 165-173.

Clough, S. J., & Bent, A. F. (1998). Floral dip: a simplified method for Agrobacterium‐mediated transformation of Arabidopsis thaliana. *The Plant Journal*, *16*(6), 735-743.

Cui, N., Sun, X., Sun, M., Jia, B., Duanmu, H., Lv, D., ... Zhu, Y. (2015). Overexpression of OsmiR156k leads to reduced tolerance to cold stress in rice (Oryza Sativa). *Molecular Breeding*, *35*(11), 214.

D'hont, A., Denoeud, F., Aury, J. M., Baurens, F. C., Carreel, F., Garsmeur, O., ... Da Silva, C. (2012). The banana (Musa acuminata) genome and the evolution of monocotyledonous plants. *Nature*, *488*(7410), 213.

Daryanto, S., Wang, L., & Jacinthe, P. A. (2016). Global synthesis of drought effects on maize and wheat production. *PLoS ONE*, *11*(5), e0156362.

Daughtry, C. S. T., Walthall, C. L., Kim, M. S., De Colstoun, E. B., & McMurtrey Iii, J. E. (2000). Estimating corn leaf chlorophyll concentration from leaf and canopy reflectance. *Remote Sensing of Environment*, *74*(2), 229-239.

Davis, A. M., Hall, A., Millar, A. J., Darrah, C., & Davis, S. J. (2009). Protocol: Streamlined sub-protocols for floral-dip transformation and selection of transformants in Arabidopsis thaliana. *Plant Methods*, *5*(1), 3.

Davy, A., Thomsen, K. K., Juliano, M. A., Alves, L. C., Svendsen, I., & Simpson, D. J. (2000). Purification and characterization of barley dipeptidyl peptidase IV. *Plant Physiology*, *122*(2), 425-432.

De Buck, S., & Swennen, R. (2016). Bananas, the green gold of the South. Retrieved on July 15, 2018 from http://ipbo.vib-ugent.be/publications/fact-series/bananas-the-green-gold-of-the-south

Del Rio, L. A., Palma, J. M., Sandalio, L. M., Corpas, F. J., Pastori, G. M., Bueno, P., & López-Huertas, E. (1996). Peroxisomes as a source of superoxide and hydrogen peroxide in stressed plants. *Biochemical Society Transactions, 24*(2), 434-438

Ding, Y., Ye, Y., Jiang, Z., Wang, Y., & Zhu, C. (2016). MicroRNA390 is involved in cadmium tolerance and accumulation in rice. *Frontiers in Plant Science*, *7*, 235.

Draper, H. H., & Hadley, M. (1990). Malondialdehyde determination as index of lipid Peroxidation. *Methods in Enzymology*, *186*, 421-431.

The Star Online. (2014). Dry, muddy, very windy: Malaysian weather goes extreme in 2014. Retrieved July 8, 2017 from https://www.thestar.com.my/lifestyle/features/2014/12/15/dry-muddy-and-very-windy-malaysian-weather-gets-extreme-in-2014/

Duan, H., Ding, X., Wei, Z., Zhou, C., & Zhou, Y. (2011). The influences of Hygromycin B on growth of Arabidopsis thaliana cotyledon and leaf. *African Journal of Biotechnology, 10*, 17742-17747.

Easterling, D. R., & Wehner, M. F. (2009). Is the climate warming or cooling?. *Geophysical Research Letters*, *36*(8).

Eckardt, N. A. (2004). Abscisic acid signal transduction: Function of G protein–coupled receptor 1 in Arabidopsis. *The Plant Cell*, *16*(6), 1353-1354.

Ee, S. F., Khairunnisa, M. B., Zeti-Azura, M. H., Noor Azmi, S., & Zamri, Z. (2014). Effective hygromycin concentration for selection of Agrobacterium-mediated transgenic Arabidopsis thaliana. *Malaysian Applied Biology, 43*(1), 119–123.

FAOSTAT. (2018). FAOSTAT. Retrieved Jun 10, 2018 from http://faostat.fao.org/

Farooq, M., Gogoi, N., Barthakur, S., Baroowa, B., Bharadwaj, N., Alghamdi, S. S., & Siddique, K. H. M. (2017). Drought stress in grain legumes during reproduction and grain filling. *Journal of Agronomy and Crop Science*, *203*(2), 81-102.

Fleischmann, A., Michael, T. P., Rivadavia, F., Sousa, A., Wang, W., Temsch, E. M., ... Heubl, G. (2014). Evolution of genome size and chromosome number in the carnivorous plant genus Genlisea (Lentibulariaceae), with a new estimate of the minimum genome size in angiosperms. *Annals of Botany*, *114*(8), 1651-1663.

Foyer, C. H., & Noctor, G. (2005). Oxidant and antioxidant signalling in plants: A re-evaluation of the concept of oxidative stress in a physiological context. *Plant, Cell & Environment*, *28*(8), 1056-1071.

Franco, J. A., Bañón, S., Vicente, M. J., Miralles, J., & Martínez-Sánchez, J. J. (2011). Root development in horticultural plants grown under abiotic stress conditions-a review. *The Journal of Horticultural Science and Biotechnology*, *86*(6), 543-556.

Galway, M. E., Heckman, J. W., & Schiefelbein, J. W. (1997). Growth and ultrastructure of Arabidopsis root hairs: The rhd3 mutation alters vacuole enlargement and tip growth. *Planta*, *201*(2), 209-218.

Gao, N., Qiang, X. M., Zhai, B. N., Min, J., & Shi, W. M. (2015). Transgenic tomato overexpressing ath-miR399d improves growth under abiotic stress conditions. *Russian Journal of Plant Physiology*, *62*(3), 360-366.

Gao, P., Bai, X., Yang, L., Lv, D., Li, Y., Cai, H., ... Zhu, Y. (2010). Over-expression of osa-MIR396c decreases salt and alkali stress tolerance. *Planta*, *231*(5), 991-1001.

Gao, S., Song, J. B., Wang, Y., & Yang, Z. M. (2017). An F-box E3 ubiquitin ligase-coding gene AtDIF1 is involved in Arabidopsis salt and drought stress responses in an abscisic acid-dependent manner. *Environmental and Experimental Botany*, *138*, 21-35.

Gao, S., Yang, L., Zeng, H. Q., Zhou, Z. S., Yang, Z. M., Li, H., ... Zhang, B. (2016). A cotton miRNA is involved in regulation of plant response to salt stress. *Scientific Reports*, *6*, 19736.

Gasster, M. (1963). The banana in geriatric and low-calorie diets. *Geriatrics*, *18*, 782-786.

Gasteiger, E., Hoogland, C., Gattiker, A., Wilkins, M. R., Appel, R. D., & Bairoch, A. (2005). Protein identification and analysis tools on the ExPASy server. In J.M. Walker (Ed.), *The proteomics protocols handbook* (pp. 571-607). Humana press.

Ghag, S. B., Shekhawat, U. K., & Ganapathi, T. R. (2015). Small RNA profiling of two important cultivars of banana and overexpression of miRNA156 in transgenic banana plants. *PLoS ONE*, *10*(5), e0127179.

Ghorbani, A., Izadpanah, K., & Dietzgen, R. G. (2018). Changes in maize transcriptome in response to maize Iranian mosaic virus infection. *PLoS ONE*, *13*(4), e0194592.

Goufo, P., Moutinho-Pereira, J. M., Jorge, T. F., Correia, C. M., Oliveira, M. R., Rosa, E. A., ... Trindade, H. (2017). Cowpea (Vigna unguiculata L. Walp.) metabolomics: Osmoprotection as a physiological strategy for drought stress resistance and improved yield. *Frontiers in Plant Science*, *8*, 586.

Grierson, C., Nielsen, E., Ketelaarc, T., & Schiefelbein, J. (2014). Root hairs. *The Arabidopsis Book*, *12,* e0172.

Guan, C., Huang, Y. H., Cui, X., Liu, S. J., Zhou, Y. Z., & Zhang, Y. W. (2018). Overexpression of gene encoding the key enzyme involved in proline-biosynthesis (PuP5CS) to improve salt tolerance in switchgrass (Panicum virgatum L.). *Plant Cell Reports*, 1-13.

Guan, Q., Lu, X., Zeng, H., Zhang, Y., & Zhu, J. (2013). Heat stress induction of mi R 398 triggers a regulatory loop that is critical for thermotolerance in Arabidopsis. *The Plant Journal*, *74*(5), 840-851.

Guo, M., Li, C., Facciotto, G., Bergante, S., Bhatia, R., Comolli, R., ... Murphy, R. (2015). Bioethanol from poplar clone Imola: an environmentally viable alternative to fossil fuel?. *Biotechnology for Biofuels*, *8*(1), 134.

Hajiboland, R., Farhanghi, F., & Aliasgharpour, M. (2012). Morphological and anatomical modifications in leaf, stem and roots of four plant species under boron deficiency conditions. *Anales de Biología*, *34*, 13-27.

Hajyzadeh, M., Turktas, M., Khawar, K. M., & Unver, T. (2015). MiR408 overexpression causes increased drought tolerance in chickpea. *Gene*, *555*(2), 186-193.

Hanin, M., Brini, F., Ebel, C., Toda, Y., Takeda, S., & Masmoudi, K. (2011). Plant dehydrins and stress tolerance: Versatile proteins for complex mechanisms. *Plant Signaling & Behavior*, *6*(10), 1503-1509.

Hanzawa, T., Shibasaki, K., Numata, T., Kawamura, Y., Gaude, T., & Rahman, A. (2013). Cellular auxin homeostasis under high temperature is regulated through a SORTING NEXIN1–dependent endosomal trafficking pathway. *The Plant Cell*, 113.

Hassan, W., Noreen, H., Rehman, S., Gul, S., Amjad Kamal, M., Paul Kamdem, J., ... BT da Rocha, J. (2017). Oxidative stress and antioxidant potential of one hundred medicinal plants. *Current Topics in Medicinal Chemistry*, *17*(12), 1336-1370.

Hayat, S., Hayat, Q., Alyemeni, M. N., Wani, A. S., Pichtel, J., & Ahmad, A. (2012). Role of proline under changing environments: A review. *Plant Signaling & Behavior*, *7*(11), 1456-1466.

He, H., Yan, J., Yu, X., Liang, Y., Fang, L., Scheller, H. V., & Zhang, A. (2017). The NADPH-oxidase AtRbohI plays a positive role in drought-stress response in Arabidopsis thaliana. *Biochemical and Biophysical Research Communications*, *491*(3), 834-839.

Holsters, M., De Waele, D., Depicker, A., Messens, E., Van Montagu, M., & Schell, J. (1978). Transfection and transformation of Agrobacterium tumefaciens. *Molecular and General Genetics MGG*, *163*(2), 181-187.

Hong, M., Qingjie, P., Lan, W., Zhenghong, L., Youming, W., & Xiuxian, L. (2011). Musella lasiocarpa var. rubribracteata (Musaceae), a new variety from Sichuan, China. *Novon: A Journal for Botanical Nomenclature*, *21*(3), 349-353.

Hong, M., Yanofsky, M. F., & Hai, H. (1991). Isolation and sequence analysis of TGA1 cDNAs encoding a tomato G protein α subunit. *Gene*, *107*(2), 189-195.

Hu, T., Zeng, H., Hu, Z., Qv, X., & Chen, G. (2013). Overexpression of the tomato 13-lipoxygenase gene TomloxD increases generation of endogenous jasmonic acid and resistance to Cladosporium fulvum and high temperature. *Plant Molecular Biology Reporter*, *31*(5), 1141-1149.

Hu, Y., Zhong, R., Morrison III, W. H., & Ye, Z. H. (2003). The Arabidopsis RHD3 gene is required for cell wall biosynthesis and actin organization. *Planta*, *217*(6), 912-921.

Huang, S. Q., Xiang, A. L., Che, L. L., Chen, S., Li, H., Song, J. B., & Yang, Z. M. (2010). A set of miRNAs from Brassica napus in response to sulphate deficiency and cadmium stress. *Plant Biotechnology Journal*, *8*(8), 887-899

Hubbard, K. E., Nishimura, N., Hitomi, K., Getzoff, E. D., & Schroeder, J. I. (2010). Early abscisic acid signal transduction mechanisms: Newly discovered components and newly emerging questions. *Genes & Development*, *24*(16), 1695-1708.

Huijser, P., & Schmid, M. (2011). The control of developmental phase transitions in plants. *Development*, *138*(19), 4117-4129.

Ijaz, R., Ejaz, J., Gao, S., Liu, T., Imtiaz, M., Ye, Z., & Wang, T. (2017). Overexpression of annexin gene AnnSp2, enhances drought and salt tolerance through modulation of ABA synthesis and scavenging ROS in tomato. *Scientific Reports*, *7*(1), 12087.

Inskeep, W. P., & Bloom, P. R. (1985). Extinction coefficients of chlorophyll a and b in N, N-dimethylformamide and 80% acetone. *Plant Physiology*, *77*(2), 483-485.

Ivanov, R., Brumbarova, T., Blum, A., Jantke, A. M., Fink-Straube, C., & Bauer, P. (2014). SORTING NEXIN1 is required for modulating the trafficking and stability of the Arabidopsis IRON-REGULATED TRANSPORTER1. *The Plant Cell*, 113.

Jamil, A., Riaz, S., Ashraf, M., & Foolad, M. R. (2011). Gene expression profiling of plants under salt stress. *Critical Reviews in Plant Sciences*, *30*(5), 435-458.

Janssens, S. B., Vandelook, F., De Langhe, E., Verstraete, B., Smets, E., Vandenhouwe, I., & Swennen, R. (2016). Evolutionary dynamics and biogeography of Musaceae reveal a correlation between the diversification of the banana family and the geological and climatic history of Southeast Asia. *New Phytologist*, *210*(4), 1453-1465.

Jeyabaskaran, K. J., Pandey, S. D., & Laxman, R. H. (2000). Studies on reclamation of saline sodic soil for banana (cv. Nendran). *Proceedings of the international conference on managing natural resources for sustainable agricultural production in the 21st century, 2*, 357-360.

Julkowska, M. M., & Testerink, C. (2015). Tuning plant signaling and growth to survive salt. *Trends in Plant Science*, *20*(9), 586-594.

Kaymakanova, M. (2009). Effect of salinity on germination and seed physiology in bean (Phaseolus vulgaris L.). *Biotechnology & Biotechnological Equipment*, *23*, 326-329.

Khan, M. I. R., Fatma, M., Per, T. S., Anjum, N. A., & Khan, N. A. (2015). Salicylic acid-induced abiotic stress tolerance and underlying mechanisms in plants. *Frontiers in Plant Science*, *6*, 462.

Khraiwesh, B., Zhu, J. K., & Zhu, J. (2012). Role of miRNAs and siRNAs in biotic and abiotic stress responses of plants. *Biochimica et Biophysica Acta (BBA)-Gene Regulatory Mechanisms*, *1819*(2), 137-148.

Kiefer, E., Heller, W., & Ernst, D. (2000). A simple and efficient protocol for isolation of functional RNA from plant tissues rich in secondary metabolites. *Plant Molecular Biology Reporter*, *18*(1), 33-39.

Kim, W. Y., Cheong, N. E., Lee, D. C., Je, D. Y., Bahk, J. D., Cho, M. J., & Lee, S. Y. (1995). Cloning and sequencing analysis of a full-length cDNA encoding a G protein alpha subunit, SGA1, from soybean. *Plant physiology*, *108*(3), 1315.

Koornneef, M., & Meinke, D. (2010). The development of Arabidopsis as a model plant. *The Plant Journal*, *61*(6), 909-921.

Koszler, V. (1959). Bananas for infantile diarrhoea. *Neue Osterreichische Zeitschrift fur Kinderheilkunde*, *4*, 212-214.

Ku, Y. S., Wong, J., Mui, Z., Liu, X., Hui, J., Chan, T. F., & Lam, H. M. (2015). Small RNAs in plant responses to abiotic stresses: regulatory roles and study methods. *International Journal of Molecular Sciences*, *16*(10), 24532-24554.

Kumar, D., Al Hassan, M., Naranjo, M. A., Agrawal, V., Boscaiu, M., & Vicente, O. (2017). Effects of salinity and drought on growth, ionic relations, compatible solutes and activation of antioxidant systems in oleander (Nerium oleander L.). *PLoS ONE*, *12*(9), e0185017.

Kumar, J., Basu, P. S., Srivastava, E., Chaturvedi, S. K., Nadarajan, N., & Kumar, S. (2012). Phenotyping of traits imparting drought tolerance in lentil. *Crop and Pasture Science*, *63*(6), 547-554.

Kumar, S., Stecher, G., & Tamura, K. (2016). MEGA7: Molecular evolutionary genetics analysis version 7.0 for bigger datasets. *Molecular Biology and Evolution*, *33*(7), 1870-1874.

Lamaoui, M., Jemo, M., Datla, R., & Bekkaoui, F. (2018). Heat and drought stresses in crops and approaches for their mitigation. *Frontiers in Chemistry*, *6*, 26.

Lan, P., Li, W., Lin, W. D., Santi, S., & Schmidt, W. (2013). Mapping gene activity of Arabidopsis root hairs. *Genome Biology*, *14*(6), 67.

Lata, C., & Prasad, M. (2011). Role of DREBs in regulation of abiotic stress responses in plants. *Journal of Experimental Botany*, *62*(14), 4731-4748.

Lee, W. S., Gudimella, R., Wong, G. R., Tammi, M. T., Khalid, N., & Harikrishna, J. A. (2015). Transcripts and microRNAs responding to salt stress in Musa acuminata Colla (AAA Group) cv. Berangan roots. *PLoS ONE*, *10*(5), e0127526.

Leitner, D., Klepsch, S., Ptashnyk, M., Marchant, A., Kirk, G. J. D., Schnepf, A., & Roose, T. (2010). A dynamic model of nutrient uptake by root hairs. *New Phytologist*, *185*(3), 792-802.

Leutwiler, L. S., Hough-Evans, B. R., & Meyerowitz, E. M. (1984). The DNA of Arabidopsis thaliana. *Molecular and General Genetics MGG*, *194*(1-2), 15-23.

Li T, Liu W, Wang F, Ma Q, Lu Y & Yuan T. (2018a) SORTING NEXIN 1 functions in plant salt stress tolerance through changes of NO accumulation by regulating NO synthase-like activity. *Frontier in Plant Science*, *9,* 1634.

Li, B., Tester, M., & Gilliham, M. (2017). Chloride on the move. *Trends in Plant Science*, *22*(3), 236-248.

Li, J., & Assmann, S. M. (1996). An abscisic acid-activated and calcium-independent protein kinase from guard cells of fava bean. *The Plant Cell*, *8*(12), 2359-2368.

Li, J., Phan, T. T., Li, Y. R., Xing, Y. X., & Yang, L. T. (2018b). Isolation, transformation and overexpression of sugarcane SoP5CS gene for drought tolerance improvement. *Sugar Tech*, *20*(4), 464-473.

Li, W., Wang, T., Zhang, Y., & Li, Y. (2015). Overexpression of soybean miR172c confers tolerance to water deficit and salt stress, but increases ABA sensitivity in transgenic Arabidopsis thaliana. *Journal of Experimental Botany*, *67*(1), 175-194.

Li, Z., Yu, J., Peng, Y., & Huang, B. (2017). Metabolic pathways regulated by abscisic acid, salicylic acid and γ-aminobutyric acid in association with improved drought tolerance in creeping bentgrass (Agrostis stolonifera). *Physiologia Plantarum*, *159*(1), 42-58.

Liu, D., Kong, D. D., Fu, X. K., Ali, B., Xu, L., & Zhou, W. J. (2016). Influence of exogenous 5-aminolevulinic acid on chlorophyll synthesis and related gene expression in oilseed rape de-etiolated cotyledons under water-deficit stress. *Photosynthetica*, *54*(3), 468-474.

Livak, K. J., & Schmittgen, T. D. (2001). Analysis of relative gene expression data using real-time quantitative PCR and the 2− ΔΔCT method. *Methods*, *25*(4), 402-408.

Ma, H., Yanofsky, M. F., & Meyerowitz, E. M. (1990). Molecular cloning and characterization of GPA1, a G protein alpha subunit gene from Arabidopsis thaliana. *Proceedings of the National Academy of Sciences*, *87*(10), 3821-3825.

Mallory, A. C., & Vaucheret, H. (2004). MicroRNAs: Something important between the genes. *Current Opinion in Plant Biology*, *7*(2), 120-125.

Martinuz, A., Zewdu, G., Ludwig, N., Grundler, F., Sikora, R. A., & Schouten, A. (2015). The application of Arabidopsis thaliana in studying tripartite interactions among plants, beneficial fungal endophytes and biotrophic plant-parasitic nematodes. *Planta*, *241*(4), 1015-1025.

Mei, Y., Guo, J., Ding, N., Liu, Y. F., Su, X. J., Zu, Y. X., ... Wang, W. W. (2018). Transcriptome profiles underlying the spermidine-elevated resistance to high temperature in the radish Raphanus sativus. *Acta Physiologiae Plantarum*, *40*(6), 109.

Meinke, D. W., Cherry, J. M., Dean, C., Rounsley, S. D., & Koornneef, M. (1998). Arabidopsis thaliana: A model plant for genome analysis. *Science*, *282*(5389), 662-682.

Miguel, M. A., Postma, J. A., & Lynch, J. (2015). Phene synergism between root hair length and basal root growth angle for phosphorus acquisition. *Plant Physiology*, 00145.

Mishra, G., Zhang, W., Deng, F., Zhao, J., & Wang, X. (2006). A bifurcating pathway directs abscisic acid effects on stomatal closure and opening in Arabidopsis. *Science*, *312*(5771), 264-266.

Munns, R., & Tester, M. (2008). Mechanisms of salinity tolerance. *Annual Review of Plant Biology*, *59*, 651-681.

Murashige, T., & Skoog, F. (1962). A revised medium for rapid growth and bio assays with tobacco tissue cultures. *Physiologia Plantarum*, *15*(3), 473-497.

Nakai, K., & Kanehisa, M. (1991). Expert system for predicting protein localization sites in gram-negative bacteria. *Proteins: Structure, Function, and Bioinformatics*, *11*(2), 95-110.

Nakano, Y., & Asada, K. (1981). Hydrogen peroxide is scavenged by ascorbate-specific peroxidase in spinach chloroplasts. *Plant and Cell Physiology*, *22*(5), 867-880.

Ni, Z., Hu, Z., Jiang, Q., & Zhang, H. (2012). Overexpression of gma-MIR394a confers tolerance to drought in transgenic Arabidopsis thaliana. *Biochemical and Biophysical Research Communications*, *427*(2), 330-335.

Nitta, Y., Ding, P., & Zhang, Y. (2015). Heterotrimeric G proteins in plant defense against pathogens and ABA signaling. *Environmental and Experimental Botany*, *114*, 153-158.

Nykiforuk, C. L., & Boothe, J. G. (2012). Transgenic expression of therapeutic proteins in Arabidopsis thaliana seed. In V. Voynov & C. Justin (Eds.), *Therapeutic proteins* (pp. 239-264). Humana Press.

Obaga, B. R., & Mwaura, F. O. (2018). Impact of farmers participation in banana value addition in household welfare in Kisii Central Sub-County. *International Academic Journal of Social Sciences and Education*, *2*(1), 25-46.

Olaoye, O. A., & Ade-Omowaye, B. I. (2011). Composite flours and breads: potential of local crops in developing countries. In V.R. Preedy., R.R. Watson & V.B. Patel (Eds.), *Flour and breads and their fortification in health and disease prevention* (pp. 183-192). San Diego: Academic Press.

Paduch, M., Jeleñ, F., & Otlewski, J. (2001). Structure of small G proteins and their regulators. *Acta Biochimica Polonica-English Edition*, *48*(4), 829-850.

Paez-Garcia, A., Motes, C. M., Scheible, W. R., Chen, R., Blancaflor, E. B., & Monteros, M. J. (2015). Root traits and phenotyping strategies for plant improvement. *Plants*, *4*(2), 334-355.

Pandey, S. (2017). Heterotrimeric G-protein regulatory circuits in plants: Conserved and novel mechanisms. *Plant Signaling & Behavior*, *12*(6), e1325983.

Pandey, S., Nelson, D. C., & Assmann, S. M. (2009). Two novel GPCR-type G proteins are abscisic acid receptors in Arabidopsis. *Cell*, *136*(1), 136-148.

Pandey, S., Zhang, W., & Assmann, S. M. (2007). Roles of ion channels and transporters in guard cell signal transduction. *FEBS letters*, *581*(12), 2325-2336.

Pradhan, S., Kant, C., Verma, S., & Bhatia, S. (2017). Genome-wide analysis of the CCCH zinc finger family identifies tissue specific and stress responsive candidates in chickpea (Cicer arietinum L.). *PLoS ONE*, *12*(7), e0180469.

Pratap, V., & Kumar Sharma, Y. (2010). Impact of osmotic stress on seed germination and seedling growth in black gram (Phaseolus mungo). *Journal of Environmental Biology*, *31*(5), 721.

Prince, L. M., & Kress, W. J. (2002). Zingiberales (Gingers and Bananas). In *Encyclopedia of life sciences*. Macmillan Publishers Ltd, Nature Publishing Group.

Pütter, J. (1974). Peroxidases. In H.U. Bergmeyer (Ed.), *Methods of Enzymatic Analysis* (pp. 685-690). Verlag Chemie: Weinhan.

Qadir, M., Quillérou, E., Nangia, V., Murtaza, G., Singh, M., Thomas, R. J., ... Noble, A. D. (2014). Economics of salt‐induced land degradation and restoration. In *Natural Resources Forum, 38*(4), 282-295.

Qin, F., Shinozaki, K., & Yamaguchi-Shinozaki, K. (2011). Achievements and challenges in understanding plant abiotic stress responses and tolerance. *Plant and Cell Physiology*, *52*(9), 1569-1582.

Rangani, J., Parida, A. K., Panda, A., & Kumari, A. (2016). Coordinated changes in antioxidative enzymes protect the photosynthetic machinery from salinity induced oxidative damage and confer salt tolerance in an extreme halophyte Salvadora persica L. *Frontiers in Plant Science*, *7*, 50.

Ranjan, A., & Sawant, S. (2015). Genome-wide transcriptomic comparison of cotton (Gossypium herbaceum) leaf and root under drought stress. *3 Biotech*, *5*(4), 585-596.

Ravi, I., & Vaganan, M. M. (2016). Abiotic Stress Tolerance in Banana. In N. Rao, K. Shivashankara & R. Laxman (Eds.), *Abiotic stress physiology of horticultural crops* (pp. 207-222). New Delhi: Springer.

Ravi, I., Uma, S., Vaganan, M. M., & Mustaffa, M. M. (2013). Phenotyping bananas for drought resistance. *Frontiers in Physiology*, *4*, 9.

Rogers, K., & Chen, X. (2013). Biogenesis, turnover, and mode of action of plant microRNAs. *The Plant Cell*, *25*(7), 2383-2399.

Saab, I. N., Sharp, R. E., Pritchard, J., & Voetberg, G. S. (1990). Increased endogenous abscisic acid maintains primary root growth and inhibits shoot growth of maize seedlings at low water potentials. *Plant Physiology*, *93*(4), 1329-1336.

Sah, S. K., Reddy, K. R., & Li, J. (2016). Abscisic acid and abiotic stress tolerance in crop plants. *Frontiers in Plant Science*, *7*, 571.

Samson, J. A. (1986). The minor tropical fruits. *Tropical fruits*. New York: Longman Inc.

Schiefelbein, J. W., & Somerville, C. (1990). Genetic control of root hair development in Arabidopsis thaliana. *The Plant Cell*, *2*(3), 235-243.

Seelig, M. S. (1969). Vitamin D and cardiovascular, renal, and brain damage in infancy and childhood. *Annals of the New York Academy of Sciences*, *147*(1), 539-582.

Sen Gupta, A. S. (1993). Overexpression of superoxide dismutase protects plants from oxidative stress. *Plant Physiology*, *103*, 1067-1073.

Shahzad, R., Harlina, P. W., Ayaad, M., Ewas, M., Nishawy, E., Fahad, S., ... Amar, M. H. (2018). Dynamic roles of microRNAs in nutrient acquisition and plant adaptation under nutrient stress: A review. *Plant Omics*, *11*(1), 58.

Shan, L., Zhao, S. Y., & Xia, G. M. (2005). Cloning of the full-length cDNA of the wheat involved in salt stress: Root hair defective 3 gene (RHD3). *Journal of Integrative Plant Biology*, *47*(7), 881-891.

Sharma, A., Li, X., & Lim, Y. P. (2014). Comparative genomics of Brassicaceae crops. *Breeding Science*, *64*(1), 3-13.

Sharma, N., Bender, Y., Boyle, K., & Fobert, P. R. (2013). High-level expression of sugar inducible gene2 (HSI2) is a negative regulator of drought stress tolerance in Arabidopsis. *BMC Plant Biology*, *13*(1), 170.

Shavrukov, Y. (2012). Salt stress or salt shock: which genes are we studying?. *Journal of Experimental Botany*, *64*(1), 119-127.

Shen, J., Lv, B., Luo, L., He, J., Mao, C., Xi, D., & Ming, F. (2017). The NAC-type transcription factor OsNAC2 regulates ABA-dependent genes and abiotic stress tolerance in rice. *Scientific Reports*, *7*, 40641.

Shriram, V., Kumar, V., Devarumath, R. M., Khare, T. S., & Wani, S. H. (2016). MicroRNAs as potential targets for abiotic stress tolerance in plants. *Frontiers in Plant Science*, *7*, 817.

Shrivastava, P., & Kumar, R. (2015). Soil salinity: A serious environmental issue and plant growth promoting bacteria as one of the tools for its alleviation. *Saudi Journal of Biological Sciences*, *22*(2), 123-131.

Sicher, R. C., Timlin, D., & Bailey, B. (2012). Responses of growth and primary metabolism of water-stressed barley roots to rehydration. *Journal of Plant Physiology*, *169*(7), 686-695.

Smith, I. K., Vierheller, T. L., & Thorne, C. A. (1989). Properties and functions of glutathione reductase in plants. *Physiologia Plantarum*, *77*(3), 449-456.

Soltani, A., Galeshi, S., Zeinali, E., & Latifi, N. (2002). Germination, seed reserve utilization and seedling growth of chickpea as affected by salinity and seed size. *Seed Science and Technology*, *30*(1), 51-60.

Somerville, C., & Koornneef, M. (2002). A fortunate choice: The history of Arabidopsis as a model plant. *Nature Reviews Genetics*, *3*(11), 883.

Song, J. B., Gao, S., Wang, Y., Li, B. W., Zhang, Y. L., & Yang, Z. M. (2016). miR394 and its target gene LCR are involved in cold stress response in Arabidopsis. *Plant Gene*, *5*, 56-64.

Sparks, E. E., & Benfey, P. N. (2018). The contribution of root systems to plant nutrient acquisition. In M.A. Hossain, T. Kamiya, D.J. Burritt, L.S.P. Tran, & T. Fujiwara (Eds.), *Plant macronutrient use efficiency* (pp. 83-92). London, United Kingdom: Academic Press.

Spollen, W. G., LeNoble, M. E., Samuels, T. D., Bernstein, N., & Sharp, R. E. (2000). Abscisic acid accumulation maintains maize primary root elongation at low water potentials by restricting ethylene production. *Plant Physiology*, *122*(3), 967-976.

Sreedharan, S., Shekhawat, U. K., & Ganapathi, T. R. (2013). Transgenic banana plants overexpressing a native plasma membrane aquaporin Musa PIP 1; 2 display high tolerance levels to different abiotic stresses. *Plant Biotechnology Journal*, *11*(8), 942-952.

Suharsono, U., Fujisawa, Y., Kawasaki, T., Iwasaki, Y., Satoh, H., & Shimamoto, K. (2002). The heterotrimeric G protein α subunit acts upstream of the small GTPase Rac in disease resistance of rice. *Proceedings of the National Academy of Sciences*, *99*(20), 13307-13312.

Sun, W., Cao, Z., Li, Y., Zhao, Y., & Zhang, H. (2007). A simple and effective method for protein subcellular localization using Agrobacterium-mediated transformation of onion epidermal cells. *Biologia*, *62*(5), 529-532.

Sunkar, R., Li, Y. F., & Jagadeeswaran, G. (2012). Functions of microRNAs in plant stress responses. *Trends in Plant Science*, *17*(4), 196-203.

Tanaka, N., Kato, M., Tomioka, R., Kurata, R., Fukao, Y., Aoyama, T., & Maeshima, M. (2014). Characteristics of a root hair-less line of Arabidopsis thaliana under physiological stresses. *Journal of Experimental Botany*, *65*(6), 1497-1512.

Teh, H. F., Neoh, B. K., Hong, M. P. L., Low, J. Y. S., Ng, T. L. M., Ithnin, N., ... & Kulaveerasingam, H. (2013). Differential metabolite profiles during fruit development in high-yielding oil palm mesocarp. *PLoS ONE*, *8*(4), e61344.

Thangthong, N., Jogloy, S., Jongrungklang, N., Kvien, C. K., Pensuk, V., Kesmala, T., & Vorasoot, N. (2018). Root distribution patterns of peanut genotypes with different drought resistance levels under early-season drought stress. *Journal of Agronomy and Crop Science*, *204*(2), 111-122.

Tian, L., DellaPenna, D., & Zeevaart, J. A. (2004). Effect of hydroxylated carotenoid deficiency on ABA accumulation in Arabidopsis. *Physiologia Plantarum*, *122*(3), 314-320.

Tung, S. A., Smeeton, R., White, C. A., Black, C. R., Taylor, I. B., Hilton, H. W., & Thompson, A. J. (2008). Over-expression of LeNCED1 in tomato (Solanum lycopersicum L.) with the rbcS3C promoter allows recovery of lines that accumulate very high levels of abscisic acid and exhibit severe phenotypes. *Plant, Cell & Environment*, *31*(7), 968-981.

Tuteja, N. (2007). Abscisic acid and abiotic stress signaling. *Plant Signaling & Behavior*, *2*(3), 135-138.

Ullah, H., Chen, J. G., Wang, S., & Jones, A. M. (2002). Role of a heterotrimeric G protein in regulation of Arabidopsis seed germination. *Plant Physiology*, *129*(2), 897-907.

Ullah, H., Chen, J. G., Young, J. C., Im, K. H., Sussman, M. R., & Jones, A. M. (2001). Modulation of cell proliferation by heterotrimeric G protein in Arabidopsis. *Science*, *292*(5524), 2066-2069.

United Nations. (2017). World population projected to reach 9.8 billion in 2050, and 11.2 billion in 2100. Retrieved July 8, 2017 from https://www.un.org/development/desa/en/news/population/world-population-prospects-2017.html

Valvekens, D., Van Montagu, M., & Van Lijsebettens, M. (1988). Agrobacterium tumefaciens-mediated transformation of Arabidopsis thaliana root explants by using kanamycin selection. *Proceedings of the National Academy of Sciences*, *85*(15), 5536-5540.

Vamerali, T., Saccomani, M., Bona, S., Mosca, G., Guarise, M., & Ganis, A. (2003). A comparison of root characteristics in relation to nutrient and water stress in two maize hybrids. In H. Lambers (Ed.), *Roots: The dynamic interface between plants and the earth* (pp. 157-167). Dordrecht: Springer.

Väre, H., & Häkkinen, M. (2011). Typification and check-list of Ensete Horan. names (Musaceae) with nomenclatural notes. *Adansonia*, *33*(2), 191-200.

Venkataramana, R. K., Sampangi-Ramaiah, M. H., Ajitha, R., Khadke, G. N., & Chellam, V. (2015). Insights into Musa balbisiana and Musa acuminata species divergence and development of genic microsatellites by transcriptomics approach. *Plant Gene*, *4*, 78-82.

Vinocur, B., & Altman, A. (2005). Recent advances in engineering plant tolerance to abiotic stress: achievements and limitations. *Current Opinion in Biotechnology*, *16*(2), 123-132.

Vishwakarma, K., Upadhyay, N., Kumar, N., Yadav, G., Singh, J., Mishra, R. K., ... Sharma, S. (2017). Abscisic acid signaling and abiotic stress tolerance in plants: A review on current knowledge and future prospects. *Frontiers in Plant Science*, *8*, Article#161.

Vitha, S., Bene, K., Phillips, J., & Gartland, K. (1995). Histochemical GUS analysis. *Methods of Molecular Biology, 44*, 185-193.

Walker, J. E., Saraste, M., Runswick, M. J., & Gay, N. J. (1982). Distantly related sequences in the alpha-and beta-subunits of ATP synthase, myosin, kinases and other ATP-requiring enzymes and a common nucleotide binding fold. *The EMBO Journal*, *1*(8), 945-951.

Wang, H., Lockwood, S. K., Hoeltzel, M. F., & Schiefelbein, J. W. (1997). The ROOT HAIR DEFECTIVE3 gene encodes an evolutionarily conserved protein with GTP-binding motifs and is required for regulated cell enlargement in Arabidopsis. *Genes & Development*, *11*(6), 799-811.

Wang, S., Su, S. Z., Wu, Y., Li, S. P., Shan, X. H., Liu, H. K., & Yuan, Y. P. (2015). Overexpression of maize chloride channel gene ZmCLC-d in Arabidopsis thaliana improved its stress resistance. *Biologia Plantarum*, *59*(1), 55-64.

Wang, X. Q., Ullah, H., Jones, A. M., & Assmann, S. M. (2001). G protein regulation of ion channels and abscisic acid signaling in Arabidopsis guard cells. *Science*, *292*(5524), 2070-2072.

Wang, X., Zhang, M. M., Wang, Y. J., Gao, Y. T., Li, R., Wang, G. F., ... & Chen, K. M. (2016). The plasma membrane NADPH oxidase OsRbohA plays a crucial role in developmental regulation and drought-stress response in rice. *Physiologia Plantarum*, *156*(4), 421-443.

Wang, Y., Li, L., Tang, S., Liu, J., Zhang, H., Zhi, H., ... Diao, X. (2016). Combined small RNA and degradome sequencing to identify miRNAs and their targets in response to drought in foxtail millet. *BMC Genetics*, *17*(1), 57.

Wang, Z., Han, Q., Zi, Q., Lv, S., Qiu, D., & Zeng, H. (2017). Enhanced disease resistance and drought tolerance in transgenic rice plants overexpressing protein elicitors from Magnaporthe oryzae. *PLoS ONE*, *12*(4), e0175734.

Wei, P., Wang, L., Liu, A., Yu, B., & Lam, H. M. (2016). GmCLC1 confers enhanced salt tolerance through regulating chloride accumulation in soybean. *Frontiers in Plant Science*, *7*, 1082.

Wei, W., Cui, M. Y., Hu, Y., Gao, K., Xie, Y. G., Jiang, Y., & Feng, J. Y. (2018). Ectopic expression of FvWRKY42, a WRKY transcription factor from the diploid woodland strawberry (Fragaria vesca), enhances resistance to powdery mildew, improves osmotic stress resistance, and increases abscisic acid sensitivity in Arabidopsis. *Plant Science*, *275*, 60-74.

Wittinghofer, A., & Vetter, I. R. (2011). Structure-function relationships of the G domain, a canonical switch motif. *Annual Review of Biochemistry*, *80*, 943-971.

Wu, T. L. (2000). Musaceae. *Fl. China*, *24*, 314-318.

Wu, Y., Deng, Z., Lai, J., Zhang, Y., Yang, C., Yin, B., ... Xie, Q. (2009). Dual function of Arabidopsis ATAF1 in abiotic and biotic stress responses. *Cell Research*, *19*(11), 1279.

Xia, K., Wang, R., Ou, X., Fang, Z., Tian, C., Duan, J., ... Zhang, M. (2012). OsTIR1 and OsAFB2 downregulation via OsmiR393 overexpression leads to more tillers, early flowering and less tolerance to salt and drought in rice. *PLoS ONE*, *7*(1), e30039.

Xie, R., Zhang, J., Ma, Y., Pan, X., Dong, C., Pang, S., ... Lv, Q. (2017). Combined analysis of mRNA and miRNA identifies dehydration and salinity responsive key molecular players in citrus roots. *Scientific Reports*, *7*, 42094.

Xu, M., Xie, W., & Huang, M. (2012). Overexpression of PeRHD3 alters the root architecture in Populus. *Biochemical and Biophysical Research Communications*, *424*(2), 239-244.

Xu, Y., & Huang, B. (2018). Comparative transcriptomic analysis reveals common molecular factors responsive to heat and drought stress in Agrostis stolonifera. *Scientific Reports*, *8*(1), 15181.

Xu, Y., Hu, W., Liu, J., Zhang, J., Jia, C., Miao, H., ... Jin, Z. (2014). A banana aquaporin gene, MaPIP1; 1, is involved in tolerance to drought and salt stresses. *BMC Plant Biology*, *14*(1), 59.

Yang, C., Li, D., Mao, D., Liu, X. U. E., Ji, C., Li, X., ... Zhu, L. (2013). Overexpression of micro RNA 319 impacts leaf morphogenesis and leads to enhanced cold tolerance in rice (O ryza sativa L.). *Plant, Cell & Environment*, *36*(12), 2207-2218.

Yin, C., Wang, X., Duan, B., Luo, J., & Li, C. (2005). Early growth, dry matter allocation and water use efficiency of two sympatric Populus species as affected by water stress. *Environmental and Experimental Botany*, *53*(3), 315-322.

Yoshida, T., Fujita, Y., Maruyama, K., Mogami, J., Todaka, D., Shinozaki, K., & Yamaguchi-Shinozaki, K. (2015). Four Arabidopsis AREB/ABF transcription factors function predominantly in gene expression downstream of SnRK2 kinases in abscisic acid signalling in response to osmotic stress. *Plant, Cell & Environment*, *38*(1), 35-49.

You, J., & Chan, Z. (2015). ROS regulation during abiotic stress responses in crop plants. *Frontiers in Plant Science*, *6*, 1092.

Yu, N., Cai, W. J., Wang, S., Shan, C. M., Wang, L. J., & Chen, X. Y. (2010). Temporal control of trichome distribution by microRNA156-targeted SPL genes in Arabidopsis thaliana. *The Plant Cell*, 109.

Zhang, B. (2015). MicroRNA: A new target for improving plant tolerance to abiotic stress. *Journal of Experimental Botany*, *66*(7), 1749-1761.

Zhang, Q., van Wijk, R., Zarza, X., Shahbaz, M., van Hooren, M., Guardia, A., ... Haring, M. A. (2018). Knock-down of Arabidopsis PLC5 reduces primary root growth and secondary root formation while overexpression improves drought tolerance and causes stunted root hair growth. *Plant and Cell Physiology*, *59*(10), 2004-2019.

Zhang, S., Yue, Y., Sheng, L., Wu, Y., Fan, G., Li, A., ... Wei, C. (2013). PASmiR: A literature-curated database for miRNA molecular regulation in plant response to abiotic stress. *BMC Plant Biology*, *13*(1), 33.

Zhang, W., He, S. Y., & Assmann, S. M. (2008). The plant innate immunity response in stomatal guard cells invokes G-protein-dependent ion channel regulation. *The Plant Journal*, *56*(6), 984-996.

Zhao, J., Yuan, S., Zhou, M., Yuan, N., Li, Z., Hu, Q., ... Luo, H. (2018). Transgenic creeping bentgrass overexpressing Osa-miR393a exhibits altered plant development and improved multiple stress tolerance. *Plant Biotechnology Journal, 17,* 233-251

Zhao, Z., Stanley, B. A., Zhang, W., & Assmann, S. M. (2010). ABA-regulated G protein signaling in Arabidopsis guard cells: a proteomic perspective. *Journal of Proteome Research*, *9*(4), 1637-1647.

Zheng, H., Kunst, L., Hawes, C., & Moore, I. (2004). A GFP-based assay reveals a role for RHD3 in transport between the endoplasmic reticulum and Golgi apparatus. *The Plant Journal*, *37*(3), 398-414.

Zhou, M., Li, D., Li, Z., Hu, Q., Yang, C., Zhu, L., & Luo, H. (2013). Constitutive expression of a miR319 gene alters plant development and enhances salt and drought tolerance in transgenic creeping bentgrass (Agrostis stolonifera L.). *Plant Physiology, 161*(3)*,* 1375-1391.

LIST OF PUBLICATIONS AND PAPERS PRESENTED

Journal Papers (ISI-cited)

1. Lee, W. S., Gudimella, R., **Wong, G. R**., Tammi, M. T., Khalid, N., & Harikrishna, J. A. (2015). Transcripts and MicroRNAs Responding to Salt Stress in *Musa acuminata* Colla (AAA Group) cv. Berangan Roots. *PLoS ONE, 10*(5), e0127526.

2. Gudimella, R., Singh, P., Mazumdar, P., **Wong, G. R**., Lau, S. E., & Harikrishna, J. A. (2018). Genome-wide regulatory network mapping of miRNA and transcription factors in banana roots. *Tropical Plant Biology*, *11*(3-4), 141-153.

3. **Wong, G. R**., Mazumdar, P., Lau, S. E., & Harikrishna, J. A. (2018). Ectopic expression of a Musa acuminata root hair defective 3 (MaRHD3) in Arabidopsis enhances drought tolerance. *Journal of Plant Physiology*, *231*, 219-233.

Conference Papers

1. International Conference on Molecular Biology and Biotechnology (ICMBB), 23rd MSMBB Scientific Meeting 9-11th March 2016, Connexion@Nexus, Kuala Lumpur Poster Presentation: Characterization and Molecular Cloning of Root Hair Defective 3 (RHD3): a Candidate Salt Responsive Gene in Banana (Musa acuminata cv Berangan) (**Poster presentation as presenter**)

2. ICGEB Workshop "Plant responses to light and stress: emerging issues in climate change" 10-12 October 2018, New Delhi, India, Oral Presentation: Improved stress tolerance from a stress-responsive microRNA-regulated gene from banana (**Oral paper as co-author, presented by Prof. Dr. Jennifer Ann Harikrishna**)

3. Collaboration Seminar of Chemistry and Industry (CoSCI), 2nd ISBMB Seminar 9-10th October 2018, Universitas Airlangga, Indonesia: Characterization of *Musa acuminate Root Hair Defective 3* (*MaRHD3*) in Arabidopsis (**Poster presentation as co-author, presented by Ms. Lau Su-Ee**)